ISSN: 2764-5886
e-ISSN: 2764-622X

Volume 6· N° 1 · March 2023

Journal of Bioengineering, Technologies and Health

An Official Publication of
SENAI CIMATEC

ISSN: 2764-5886 / e-ISSN 2764-622X

Volume 6 • Number 1 • March 2023

JOURNAL OF BIOENGINEERING TECHNOLOGIES AND HEALTH

An Official Publication of SENAI CIMATEC

EDITOR-IN-CHIEF
Leone Peter Andrade

PUBLISHED BY SENAI CIMATEC

March 2023
Printed in Brazil

JOURNAL OF BIOENGINEERING, TECHNOLOGIES AND HEALTH

An Official Publication of SENAI CIMATEC

JOURNAL OF BIOENGINEERING AND TECHNOLOGY APPLIED TO HEALTH

Volume 6 • Number 1 *March 2023*

SUMMARY

Original Articles

Statistical Study / Methods' Study

Systematic Review / Review Articles

The Journal of Bioengineering, Technologies and Health (JBTH) is an official publication of the SENAI CIMATEC (Serviço Nacional de Aprendizagem Industrial - Centro Integrado de Manufatura e Tecnologia). It is published quarterly (March - June - September - December) in English by SENAI CIMATEC. ISSN: 2764-5886 / e-ISSN 2764-622X. The editorial offices are at SENAI CIMATEC.

Editorial Office

Correspondence concerning subscriptions, advertisements, claims for missing issues, changes of address, and communications to the editors should be addressed to the Deputy Editor, Dr. Roberto Badaró, SENAI CIMATEC (Journal of Bioengineering, Technologies and Health – JBTH) – Avenida Orlando Gomes, 1845, Piatã, Zip code: 41650-010, Salvador-Bahia-Brazil; phone: (55 71) 3879-5501; or sent by e-mail: jbth@fieb.org.br / jbth.cimatec@gmail.com.

Permissions

COVER: Micrograph of the tape strip stretched with 10% $CaCO_3$ showing delamination (debonding) occurred during the stretching process. Influence of Calcium Carbonate Concentration on the Properties of Polypropylene Stretched Flat Tapes Used in Raffia Packaging. Joyce Batista Azevedo et al. J Bioeng. Tech. Health 2023;6(1):6.

Postmaster

Send address changes to JBTH, Avenida Orlando Gomes, 1845, Piatã, Zip Code: 41650-010, Salvador-Bahia-Brazil.

Information by JBTH-SENAI CIMATEC

Address: Avenida Orlando Gomes, 1845, Piatã, Zip Code: 41650-010, Salvador-Bahia-Brazil
Home-page: www.jbth.com.br
E-mail: jbth@fieb.org.br / jbth.cimatec@gmail.com
Phone: (55 71) 3879-5501 / 3879-5500 / 3879-9500

10.34178/jbth.v6i1

Influence of Calcium Carbonate Concentration on the Properties of Polypropylene Stretched Flat Tapes Used in Raffia Packaging

Joyce Batista Azevedo[1*], Benjamin Lazarus[2], Rosindo Pereira Lobo Junior[1], Willams Teles Barbosa[1], Luã Fonseca Seixas[1], Josiane Dantas Viana Barbosa[1]

[1]SENAI CIMATEC University Center; Salvador, Bahia, Brazil; [2]University of California; Materials Science and Engineering Program, San Diego, California, USA; [3]Federal University of Bahia; Institute of Science, Technology and Innovation, Camaçari, Bahia, Brazil

The production of stretched polypropylene (PP) tapes for packaging has recently led to advancements in raffia packaging, which has improved multiple technical characteristics. In addition to the beneficial economic impact, this packaging is more sustainable. The present work evaluated the properties of stretch tapes obtained with different concentrations of calcium carbonate ($CaCO_3$) to reduce the cost of production of raffia packaging. We produced the tapes in an industrial environment using a single-screw extruder with a flat die containing 3, 7, 10, 15, 17, and 20 wt % of $CaCO_3$. The tensile strength, elongation, and toughness of the tapes were evaluated. Tensile strength and toughness increase with the addition of $CaCO_3$ while the elongation decreases. Stearic acid ($CH_3(CH_2)16COOH$) in the filler contributed positively to the dispersion and distribution of the filler in the matrix, preserving the mechanical properties. The results showed that incorporating $CaCO_3$ in flat strips stretched from PP emerges as an alternative for cost reduction with raw material for raffia packaging.
Keywords: Polypropylene. Calcium Carbonate. Raffia. Stretched Tapes.

Introduction

In the 1980s, woven sacks made of natural fibers such as cotton or jute were the most widespread solutions in the packaging market for grain, sugar, seeds, and many other agricultural products. However, with the emergence of synthetic fibers called raffia, sack production began to transition away from these natural fibers. Thus, the packaging market saw the emergence of an economically more attractive alternative with characteristics of resistance, durability, and reuse [1].

Synthetic raffia packaging comprises several stretched tapes, and its manufacturing process consists of polymeric materials extrusion. Polypropylene (PP) and polyethylene (PE) are generally used in a single-screw extruder with a flat die. This process involves the extrusion of flat films and the cutting and drawing of the tapes. Initially, films are produced in a flat die extruder [2-4]. In this step, it is essential to control the crystallization of the polymer [5].

This work used an isotactic homopolymer PP with ~50%-80% crystallinity [6]. This property can be adjusted during production by changing the distance between the surface of the cooled water bath and the matrix, as well as the temperature of the bath water. These operational parameters directly interfere with the polymer crystallization process, defining the size and quantity of spherulites that form. Furthermore, the degree of crystallinity directly affects the tensile strength and elongation of the tapes [7].

After obtaining the film, it is cut into tapes. A cylinder with special blades and spacers pulls the film in tension for this operation. After cutting it, the ribbons are subjected to stretching [8]. The stretch is performed at different peripheral speeds between groups of cylinders positioned in sequence. It promotes the stretching of the raffia, resulting in a decrease in its width. This process is necessary to define the tape's final width and achieve the physical properties necessary for the optimal performance of the final product. However, as it is a physical and not a rheological process, stretching

Received on 18 November 2022; revised 31January 2023.
Address for correspondence: Joyce Batista Azevedo. Avenida Orlando Gomes, 1845, Piatã. Salvador, Bahia, Brazil. Zipcode: 41650-010. E-mail: joyce.azevedo@ufba.br. DOI 10.34178/jbth.v6i1.271.

J Bioeng. Tech. Health 2023;6(1):1-9

has limitations in the amount of stretching applied. It can negatively affect the product's mechanical properties if applied in excess or outside of pre-existing working standards used in the industry [8,9].

The stretching process creates a plastic deformation forcing the movement of the amorphous phase chains, as well as the reorientation of the crystals of the crystalline phase, increasing the mechanical strength due to the high orientation of the structures [10-12]. Therefore, it is necessary to apply a thermal treatment in the oriented film to avoid many problems in the process and the product, such as lousy formation and loss of raffia rolls, increase in production residue, rupture, and decrease of the nominal load capacity of the packages, in this case, the already stretched raffia. Therefore, the stretched tape goes through a heating process in cylinders with temperatures between 110ºC and 120 ºC for PP tapes. The temperature range must consider the temperature used during the stretching process. It must be lower to allow a partial relaxation of the oriented tape, generating a shrinkage that usually varies from 5% to 10%. Consequently, oriented raffia does not present relevant shrinkage problems in use or further processes. The main physical properties desired for raffia are tensile strength and elongation, which can vary depending on the degree of stretching to which it is subjected [13].

Raffia produced with PP and other polyolefins has significant advantages over natural fibers such as jute, cotton, and sisal [4], despite its difficulty to be recycled. It does not rot, is chemically resistant, lightweight, water resistant, and easy to handle. However, because of the growth in industrial production, there is also a necessity to improve the quality of the product and reduce manufacturing costs.

One of the alternatives for reducing manufacturing costs and improving the mechanical properties of the tapes is incorporating calcium carbonate ($CaCO_3$) as a filler. Its cost is ~20% lower than the virgin raw material used in raffia production [14]. Therefore, this study aims to evaluate the incorporation of different concentrations of $CaCO_3$ in the PP matrix. For this, $CaCO_3$ was treated with stearic acid ($CH_3(CH_2)16COOH$) to increase its degree of hydrophobicity. Since $CaCO_3$ is a polar substance with a high specific surface, it is incompatible with PP, which is non-polar, thus impairing its dispersion in the matrix [15]. Several studies have shown that when the mineral filler is surface treated with compounds such as fatty acids, silanes, or polymers, there is an improvement in the compatibility between the phases, minimizing the polar nature of the mineral filler [16-18]. The production of synthetic raffia is a topic that has received little attention in scientific literature. Therefore, there is a knowledge gap with countless possibilities for studies in the processing and fabrication of this product, as well as the raw material used, which can improve the production and mechanical properties of the tape. In this context, this study examines fillers' influence on PP tapes' properties as an avenue for cost reduction. It also provides an evaluation of process conditions and properties.

Materials and Methods

Materials

The tapes were obtained from stretched flat films using the PP homopolymer H503 HS manufactured by Braskem S.A. (Brazil). This polymer has a fluidity index of 3.5 g/10min and a density of 0.905 g/cm³ [6].

The $CaCO_3$ (80 wt %) used is a natural ground calcite with low plasticizer absorption, treated with 1.2 % stearic acid and granulometry ranging from 2.2 - 12 μm, supplied by Micron-Ita Ltda. (Brazil). The choice of the type of $CaCO_3$ is due to the greater ease of incorporation into mixtures because of its surface treatment with stearic acid.

Stretched Tapes

The PP tapes were manufactured with a Star EX 1600 flat die extruder by Star-linger Group (Austria), with a capacity of 650 kg/h and a final winding speed of up to 550 m/min. Table 1 describes the processing conditions. Concentrations of 3, 7, 10, 15, 17, and 20 w/w % of Ca-CO_3 were added to the PP matrix to obtain the tapes. For each formulation, 6 samples were obtained with a width of 4.9 mm and a thickness of 27.1 µm.

Characterizations

The selection of characterization techniques used in this work considers the mechanical stresses of tapes when used to produce sack-type packages.

The characterizations were performed according to BS 4611:1989, which defines test methods for polyolefin tapes [19]. Thus, in the tapes produced with $CaCO_3$, the tensile strength, elongation, and tenacity were determined. The results were compared to that presented by a PP tape without added carbonate provided by Group CATA Nordeste (Brazil). In addition, the fluidity index (IF) of the compounds was determined, and differential scanning calorimetry (DSC) and scanning electron microscopy (SEM) were performed to complement the mechanical characterization and elucidate the crystallinity and morphology of the PP tapes with and without the $CaCO_3$ filler.

Mechanical Properties

The mechanical evaluation of the tapes was carried out through an analysis of tensile strength, elongation, and tenacity. These tests were performed on a universal machine Emic model DL3000 in the test laboratory of the Group CATA, using a gripper distance of 250 mm and a constant speed of 250 mm/min. The test was performed on 6 samples of each composition. The samples were stored at a controlled temperature (25 °C) and humidity (55 %).

Fluidity Index (FI)

The FI analysis was performed using a DSM MI-1 plastometer, according to ASTM D-1238 [20], with a temperature of 230 °C, a load of 2.16 kg, a waiting time between samples of 20 seconds, and a material stabilization time of 100 seconds. In addition, the samples were dried for 3 hours at 100 ºC in an oven before the test.

Table 1. Process conditions for obtaining the strips stretched with $CaCO_3$ in a flat die extruder.

Parameter	**Value**
Feed zone temperature	55 °C
Temperature of heating zones (Z1-Z8)	245; 255; 265; 270; 270; 275; 275; 275 °C
Filter temperature	275 °C
Matrix temperature	275 °C
Temperature in the drafting oven	180 °C
Bath water temperature	35 °C
Screw speed	67 rpm
Speed 1st to 5th stretch	107; 513; 500; 485; 475 m/min
Stretch rate	5.6
Tower cylinder pressure	4 a 5 Bar
Filter pressure	90 a 150 Bar
Speed 1st to 5th stretch	55 °C

Differential Scanning Calorimetry (DSC)

The DSC evaluation was performed using a Q100 Universal V4.3A (TA Instruments) at the Technology and Innovation Center of Braskem S.A. (Brazil). The test was performed on PP flat tape samples (raffia) with 10 % $CaCO_3$ before and after stretching over a temperature range of – 20 ºC to 200 ºC with a reference rate of 10 ºC/min. The objective of this test was to verify the effect of stretching on the crystallinity of the product.

Morphology

The morphology of the stretched tapes was analyzed using a Jeol JSM-6510 LV scanning electron microscope (SEM). In addition, the samples underwent a carbon deposition process on the surface using a Denton Vacuum Desk V model.

Results and Discussion

Figure 1 shows the tensile strength results of the tapes with and without the incorporation of $CaCO_3$. Tapes with $CaCO_3$ presented higher tensile strength than the tape without $CaCO_3$. The incorporation of the filler resulted in an increase in tensile strength between 16% and 19%. However, there was minimal variation in tensile strength with different concentrations of $CaCO_3$.

The mechanical behavior of polymers is closely related to their morphology. For example, in the stretching process, there is an orientation of the polymer chains, which results in the formation of crystals that increase the material's mechanical strength [10,21]. In this process, the molecular chains begin to orient in the stretching direction when the polymer is between its Tg (glass transition temperature) and Tm (crystalline melting temperature). Thus, the spherulites (polymeric crystalline structures) become anisotropic, and the highest applied stress is concentrated in the amorphous regions due to this alignment [22].

The molecular chains in the amorphous regions are randomly distributed, and because they are entangled, they can interact with multiple crystals simultaneously. Furthermore, the oriented molecules that connect to more than one crystal form a three-dimensional network since they form fixed bridges interconnecting the crystals, allowing for the uniformity of the flow of molecular chains during the stretching process, generating a film of constant thickness [22].

Adding solid particles to the semicrystalline polymer influences the molecular orientation process. The resultant toughening mechanism of this

Figure 1. Tensile strength of tapes stretched with different concentrations of $CaCO_3$.

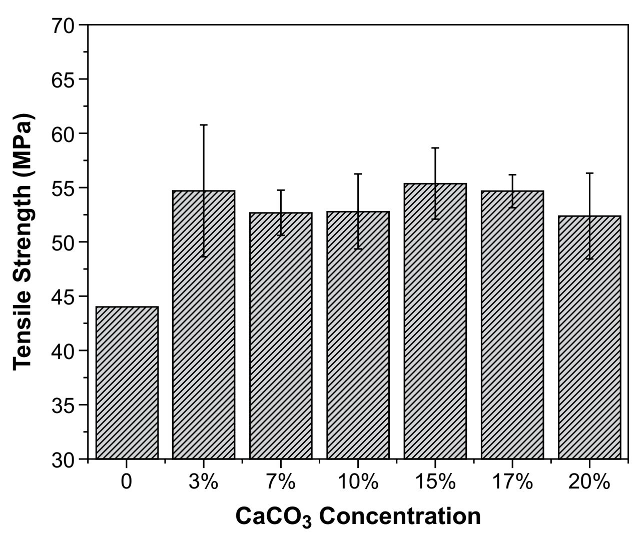

addition has been widely discussed in the literature. This mechanism involves changes in the polymer/charger interface, stress concentrations, and the formation of shear bands during loading [23-26].

Figure 2 shows a schematic of the debonding phenomenon that occurs during the stretching process of tapes that contain solid particles. At the beginning of the deformation, the filler acts as a stress concentrator in the matrix due to the difference between the elastic behavior of the phases (Phase I). As a result, a stress concentration is generated, and a triaxial stress state forms around the particle, referred to in the literature as delamination (Phase II). In the delamination phase, there is a displacement at the particle-polymer interface during flow. Finally, shear bands are created, leading to higher energy absorption during deformation (Phase III) [23,24].

Figure 2. Phases of the debonding phenomenon during the stretching process of tapes with the incorporation of solid particles.

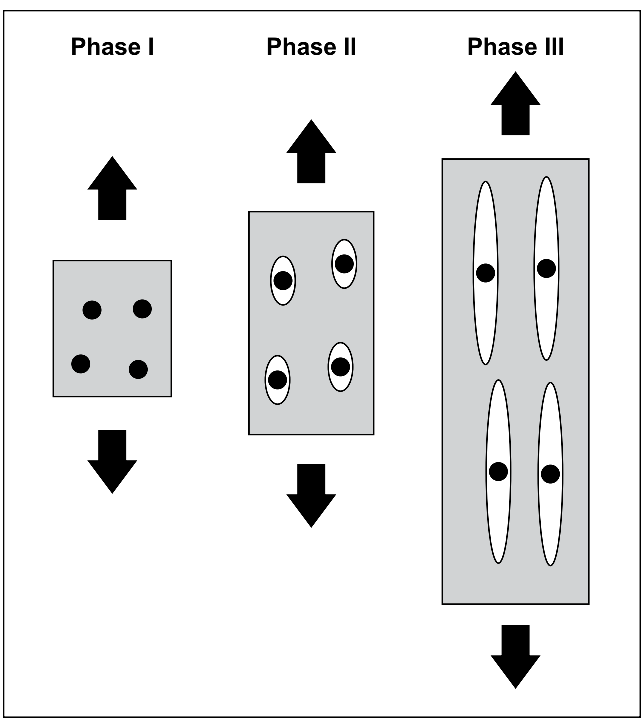

Source: Adapted from Eirasa and colleagues and Zuiderduin and colleagues [23,24].

Figure 3 shows a micrograph of the surface of the stretched flat tape with 10 % $CaCO_3$ incorporation. We also observe that the debonding phenomenon (orange arrows) is possible.

As for the $CaCO_3$ content in the samples (Figure 1), there is no trend or significant variation in the results obtained for tensile strength. However, using a greater volume of filler without significant loss of mechanical properties implies a cost reduction and economic gain in manufacturing products made from the tapes.

Figure 4 presents the morphology of the extruded films before the stretching process. These scans verify that the surface treatment of stearic acid applied to $CaCO_3$ allowed the dispersion and homogeneous distribution of the matrix particles without forming agglomerates, which also benefits the material's tensile strength [17,18]. This behavior corroborates the results obtained for the fluidity index of the samples (Figure 5).

MFI results in Figure 5 presented a variation in the fluidity index between the sample. The highest values were obtained for the tapes with 10% $CaCO_3$ incorporation, compared to pure PP.

The flow index increased due to the mineral fillers behaving as a lubricant for the molten polymer. According to Guillet [26], viscosity reduction also occurs since, after treatment, the filler adsorbs the polymer more entirely and quickly due to the decrease in surface tension, increasing its dispersion and reducing the viscosity. Therefore, the filler particle size and surface treatment are required for the application studied. Since the mineral filler particle usually has a surface tension higher than the surface tension of the polymer. If there is no proper surface treatment, the particles tend to agglomerate and not disperse because the particle-particle interaction force can be greater than the particle-polymer force [18,24,27,28].Therefore, equalizing the surface tension of the $CaCO_3$ particles provided by the surface treatment may have contributed to better dispersion (reduced agglomerates) and increased polymer-particle interaction, with a substantial increase in the flow index.

Figure 6 shows the elongation results of the stretched tapes. The elongation tends to decrease

Figure 3. Micrograph of the tape strip stretched with 10% $CaCO_3$ showing delamination (debonding) occurred during the stretching process.

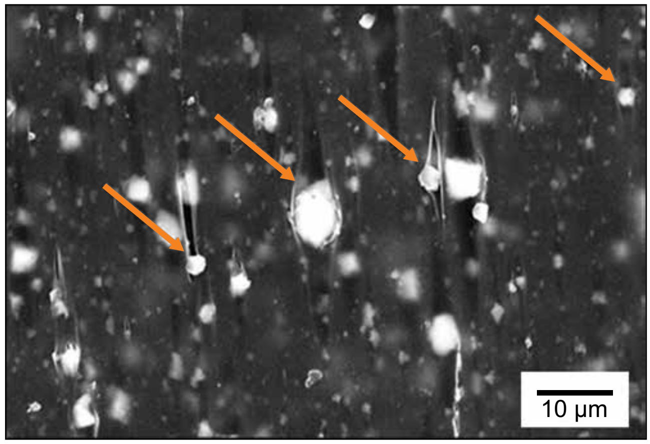

Figure 4. Micrographs of the surface of the flat tapes before stretching: (a) Tape with 10 % $CaCO_3$, and (b) Tape with 15% $CaCO_3$.

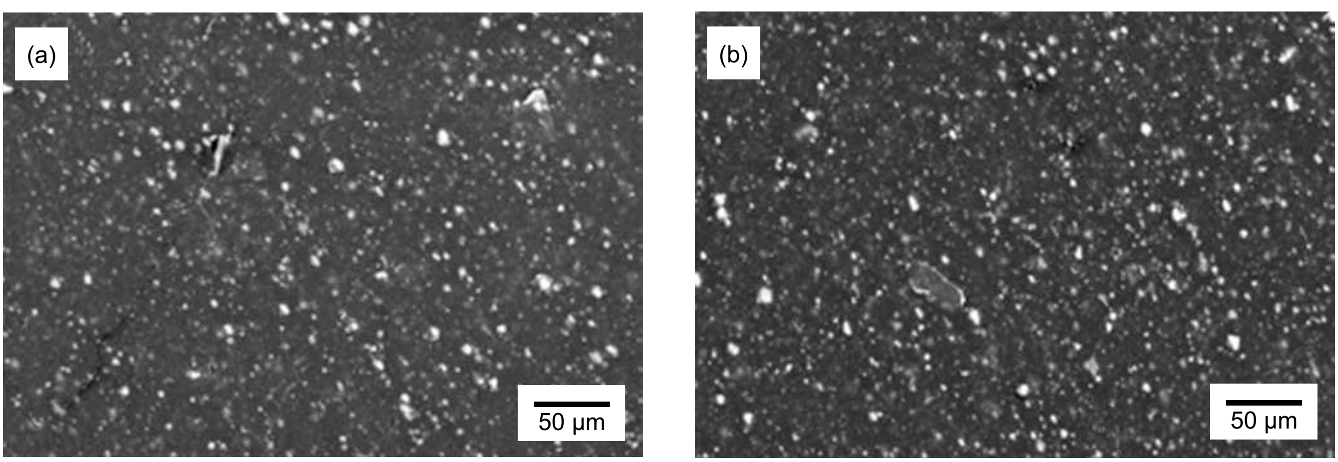

Figure 5. Melt flow index (MFI) of tapes stretched with different concentrations of $CaCO_3$.

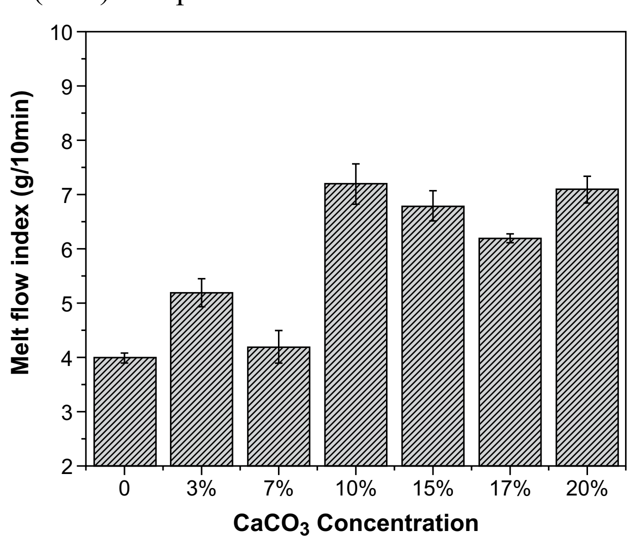

Figure 6. Elongation of stretched tapes.

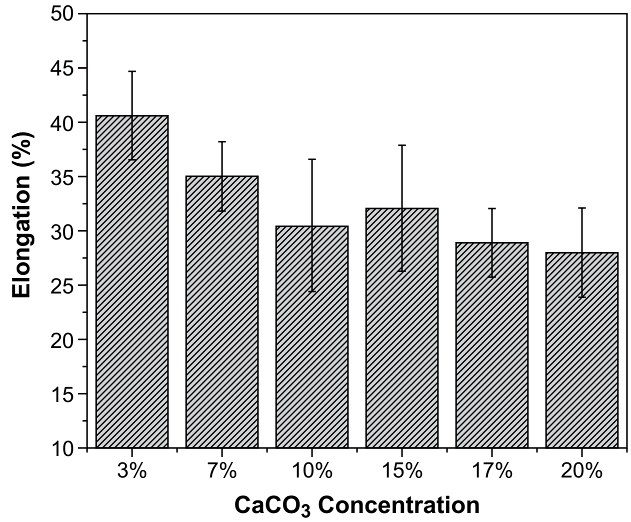

with increasing concentrations of $CaCO_3$. The reduction in elongation may be related to the formation of agglomerates due to the higher concentration of $CaCO_3$ particles in the matrix, accentuating the delamination phenomenon. With the formation of agglomerates, there is an increase in fracture points, which reduces the elongation capacity of the tapes [24,29,30].

Another condition to consider is that the molecules in the amorphous region are very close when aligned, which can lead to stretch-induced crystallization during testing [22]. Ordered groups of molecules are formed, where the surface energy is similar to the energy of a crystal nucleus. Thus, a stretched film acquires a higher degree of crystallinity at the end of the orientation process [31].

Table 2 presents the results of the DSC analysis of the tapes with the incorporation of 10 % of $CaCO_3$ without styrel and after stretching. The crystalline melting temperature (Tm) and crystallization temperature (Tc) were close for both tapes. However, there was an increase in crystallinity for the tape after the stretching process, with a crystallization rate of 57.23 %, higher than the tape without stretching (54.05 %).

In an industrial scale process, it is also possible to control the degree of longitudinal alignment of the chains by keeping the tape stretching process under control. Consequently, the degree of crystallization can be controlled to guarantee that the final material has the desired tensile strength without sacrificing elongation [11]. This effect can be realized by controlling the film cooling steps before cutting the tapes, thus providing control over forced crystallization by cooling and/or controlling the stretch rate, forcing stretch-induced crystallization [13]. In addition, these process parameters can be controlled and worked individually or together during extrusion to obtain products with crystallization suitable to the required mechanical properties [7].

Figure 7 shows the toughness results for the stretched tapes. Again, there were no significant variations in the toughness of the tapes with the increase in the concentration of $CaCO_3$. However, the toughness values were higher than the minimum

Table 2. DSC analysis of tape with 10 % $CaCO_3$ before and after stretching.

Sample	TC (°C)	TM (°C)	Crystallization Rate
No stretching	118.12	163.73	54.05
After stretching	118.31	163.50	57.23

Figure 7. Toughness (gf/Denier) of the stretched tapes.

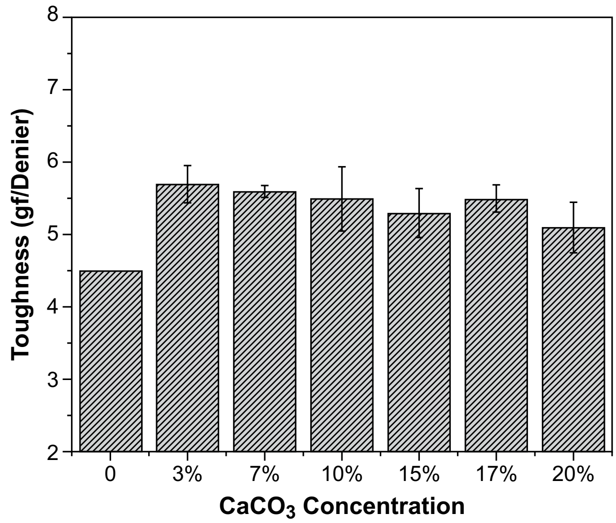

standard of 4.5 gf/Denier used by the raffia industry for this type of product [32].

During processing, there was an increase in dust generation during drawing as the concentration of $CaCO_3$ increased, most notably in concentrations above 15 %. It indicates that at high concentrations, the delamination phenomenon generated filler loss. It is important to emphasize that the addition of mineral filler to the polymeric matrix can lead to a reduction in the cost of the raw materials. It also brings improvement in some of the main mechanical properties of raffia.

Conclusions

It is possible to obtain flat-stretched PP raffia tape using $CaCO_3$ as a filler. The concentrations in this study did not alter the tensile strength and toughness properties considered standard for the raffia packaging industry. However, the elongation of the tapes was influenced by increasing the concentration of $CaCO_3$ and the crystallization obtained during the stretching of the tapes. Using $CaCO_3$ treated with stearic acid contributed to obtaining a better dispersion and distribution of the filler in the matrix, preserving the mechanical properties, and positioning itself as an alternative to reduce the cost of raw material for packaging with raffia.

Acknowledgment

The authors thank Group Cata Nordeste and SENAI CIMATEC for supporting the research.

References

1. Lobo Junior R. Influence of adding calcium carbonate on mechanical properties of flat raffia tape stretches produced by the flat die process. Ph.D. Dissertation, SENAI CIMATEC, 2017.
2. Camacho-Ferre F. Técnicas de producción en cultivos protegidos. Caja Rural Intermediterránea - Caja Rural, Almeria, Spain, 2003.
3. Duque-Acevedo M, Belmonte-Ureña LJ, Toresano-Sánchez F, Camacho-Ferre F. Biodegradable raffia as a sustainable and cost-effective alternative to improve the management of agricultural waste biomass. Agronomy 2020;10:1261. https://doi.org/10.3390/agronomy10091261.
4. López-Marín J, Gálvez A, del Amor FM et al. The cost-benefits and risks of using raffia made of biodegradable polymers: The case of pepper and tomato production in greenhouses. Horticulturae 2022;8:133.
5. Vlachopoulos J, Müller P, Polychronopoulos N, Tanifuji S-I. Flat Film and Sheet Dies. In: Carneiro O, Nobrega JM (eds) Design of Extrusion Forming Tools, 1 st. Smithers Rapra, London, UK, 2012, 113–140.
6. Brasken. Data Sheet Polypropylene H503. 2017:1–1.
7. Maier C, Calafut T. Polypropylene, The definitive user's guide and databook, 1st. Elservier, Amsterdam, Netherlands, 1998.
8. Galeski A, Kryszewski M, Kowalewski T. High orientation of toughened chalk-filled isotactic

polypropylene: Preparation and properties. Polym Eng Sci 1992;32:1217–1227. https://doi.org/10.1002/pen.760321707.
9. Sadeghi F, Carreau PJ. Properties of uniaxially stretched polypropylene films. Can J Chem Eng 2008;86:1103–1110. https://doi.org/10.1002/cjce.20109.
10. Abraham TN, Wanjale SD, Bárány T, Karger-Kocsis J. Tensile mechanical and perforation impact behavior of all-PP composites containing random PP copolymer as matrix and stretched PP homopolymer as reinforcement: Effect of β nucleation of the matrix. Compos Part A Appl Sci Manuf 2009;40:662–668. https://doi.org/10.1016/j.compositesa.2009.03.001.
11. Zhou YG, Turng LS, Shen CY. Morphological evolution and orientation development of stretched iPP Films: Influence of draw ratio. J Polym Sci Part B Polym Phys 2010;48:1223–1234. https://doi.org/10.1002/polb.22013.
12. Amornsakchai T, Bassett DC, Olley RH et al. On morphologies developed during two-dimensional compaction of woven polypropylene tapes. J Appl Polym Sci 2000;78:787–793. https://doi.org/10.1002/1097-4628(20001024)78:4<787::AID-APP110>3.0.CO;2-A.
13. Tabatabaei SH, Carreau PJ, Ajji A.Effect of processing on the crystalline orientation, morphology, and mechanical properties of polypropylene cast films and microporous membrane formation. Polymer (Guildf) 2009;50:4228–4240. https://doi.org/10.1016/j.polymer.2009.06.071.
14. Ersoy O, Köse H. Comparison of the effect of reactive and nonreactive treatments on the dispersion characteristics of a calcium carbonate (calcite) filler in a polypropylene matrix composite. Polym Compos 2020;41:3483–3490. https://doi.org/10.1002/pc.25634.
15. Rahmani M, Ghasemi FA, Payganeh G.Effect of surface modification of calcium carbonate nanoparticles on their dispersion in the polypropylene matrix using stearic acid. Mech Ind 2014;15:63–67. https://doi.org/10.1051/meca/2014009.
16. Özen I, Şimşek S. Effect of stretching temperature on breathability and waterproofness properties of polyethylene films containing different calcium carbonates. J Plast Film Sheeting 2016;32:380–401. https://doi.org/10.1177/8756087915597025.
17. Wan W, Yu D, Xie Y et al. Effects of nanoparticle treatment on the crystallization behavior and mechanical properties of polypropylene/calcium carbonate nanocomposites. J Appl Polym Sci 2006;102:3480–3488. https://doi.org/10.1002/app.24561.
18. Lazzeri A, Zebarjad SM, Pracella M et al. Filler toughening of plastics. Part 1 - The effect of surface interactions on physico-mechanical properties and rheological behavior of ultrafine $CaCO_3$/HDPE nanocomposites. Polymer (Guildf) 2005;46:827–844. https://doi.org/10.1016/j.polymer.2004.11.111.
19. BSI Group. BS 4611:1989 - Methods of test for polyolefin tape yarns. 1989.
20. American Society for Testing and Materials. D-1238 Standard Test Method for Melt Flow Rates of Thermoplastics by Extrusion Plastometer. ASTM 2013.
21. Rao IJ, Rajagopal KR. Study of strain-induced crystallization of polymers. Int J Solids Struct 2001;38:1149–1167. https://doi.org/10.1016/S0020-7683(00)00079-2.
22. Tadmor Z, Gogos C (2006) Principles of Polymer Processing, 2 nd. Wiley, New York, USA
23. Eirasa D, Pessan LA. Mechanical properties of polypropylene/calcium carbonate nanocomposites. Mater Res 2009;12:517 – 522. https://doi.org/10.1590/s1516-14392009000400023.
24. Zuiderduin WCJ, Westzaan C, Huétink J, Gaymans RJ. Toughening of polypropylene with calcium carbonate particles. Polymer (Guildf) 2002;44:261–275. https://doi.org/10.1016/S0032-3861(02)00769-3.
25. Thio YS, Argon AS, Cohen RE, Weinberg M.Toughening of isotactic polypropylene with $CaCO_3$ particles. Polymer (Guildf) 2002;43:3661–3674. https://doi.org/10.1016/S0032-3861(02)00193-3.
26. Guillet A.Treatment of fillers with organofunctional silanes, technology and applications. Macromol Symp 2003;194:63–74. https://doi.org/10.1002/masy.200390106.
27. Gilbert-Tremblay H, Mighri F, Rodrigue D. Morphology development of polypropylene cellular films for piezoelectric applications. J Cell Plast 2012;48:341–354. https://doi.org/10.1177/0021955X12443687.
28. Kloziński A, Jakubowska P. The evaluation of extensional viscosity of highly filled polyolefins composites films with calcium carbonate. Polym Eng Sci 2019;59:E155–E163. https://doi.org/10.1002/pen.24894.
29. Lin Y, Chen H, Chan CM, Wu J. The toughening mechanism of polypropylene/calcium carbonate nanocomposites. Polymer (Guildf) 2010;51:3277–3284. https://doi.org/10.1016/j.polymer.2010.04.047.
30. Yang K, Yang Q, Li G et al. Mechanical properties and morphologies of polypropylene with different sizes of calcium carbonate particles. Polym Compos 2006;27:443–450. https://doi.org/10.1002/pc.20211
31. Audet E, Mighri F, Rodrigue D, Ajji A. Cellular morphology optimization of polypropylene/$CaCO_3$ composite films designed for piezoelectric applications. Cell Polym 2018;37:103–119. https://doi.org/10.1177/026248931803700301.
32. Exxon Mobil. Value-added solution for PP raffia tapes. 2016;1–2.

Chemical Evaluation and Probiotic Potential of Kefir Different Nutrient Media

Suzana Casaes de Jesus Teodoro[1*], Matheus Chaves de Jesus[1], Crissia dos Santos Rocha[1], Roseane Santos Oliveira[1], Ingrid Lessa Leal[1]
[1]SENAI CIMATEC University Center; Salvador, Bahia, Brazil

Kefir is a gelatinous mass composed of bacteria and yeast. This study aims to develop beverages obtained from kefir grains' fermentation in different nutrient media. Thus, kefir fermentation was performed in an aqueous solution of sucrose, whole milk, whole grape juice, and water-soluble coconut extract. The fermentation process was analyzed from grain growth, beverage yield, lactic acid determination, pH, total soluble solids, and microbiological analysis. The results showed the beverages had pH and lactic acid values following the legislation. Furthermore, it identified the probiotic potential of the coconut and milk water-soluble extract beverages.
Keywords: Probiotic Beverage. Kefir Benefits. Fermented Beverage. Gut Microbiota.

Introduction

Consumers are increasingly committed and concerned with issues associated with health and quality of life [1]. Thus, they opt daily for products that have functionality claims. In this sense, the food industry progressively invests in developing lines with these functional and nutritional characteristics to satisfy the public's preferences [2].

An excellent example of foods that present functional characteristics is probiotics. They are defined as a food supplementation composed of microorganisms that regulate the intestinal microbiota, conferring good health to the user [3]. In addition, to maintain the advantages of these supplements, it should be consumed regularly [3].

We performed this study using kefir probiotic drink, which according to Brazilian legislation, is defined by the food in lactic acid cultures, fermented by kefir grains composed of bacteria of *Lactobacillus* and diverse species of the genera *Lactococcus, Acetobacter,* and *Leuconostoc*. In addition, they can have yeasts of the type *Kluyveromyces marxianus*, which are lactose fermenting agents, and *Saccharomyces omnisporus, Saccharomyces cerevisiae, Saccharomyces exiguus*, which do not ferment lactose. We emphasize that for the beverage to be considered probiotic, the microorganisms must be abundant in the final product [4].

There is a tendency to add fruit pulp to improve the acceptance of probiotic beverages [2] because these fruit pulps add better characteristics to the product, such as flavor and color. In addition, it increases the nutritional value of these products since many fruits contain bioactive compounds in their composition, which can help prevent some diseases [5]. Thus, innovation with new substrates for fermented products has proved attractive because it adds satisfactory sensory characteristics to the product, helping consumer acceptance [6].

This probiotic drink strengthens the immune system because, according to Pereira and colleagues (2011) [7], kefir has live microorganisms that can improve the intestinal microbial balance, helping to eliminate pathogenic microorganisms and resulting in health benefits to those who consume it [7].

Based on the benefits and thinking of people who are looking for functional foods, this work was carried out to produce the fermented kefir drink in different nutrient media to do a physicochemical analysis and perform microbiological analysis of molds and yeasts, lactic acid bacteria and aerobic bacteria, to evaluate the probiotic potential of the drinks.

Received on 26 November 2022; revised 18 January 2023.
Address for correspondence: Suzana Casaes de Jesus Teodoro. Rua Primeira Travessa José Araújo, 27 - Itapuã, Salvador - BA - Brasil. Zipcode: 41620850. E-mail: suzanacasaes123@gmail.com. DOI 10.34178/jbth.v6i1.272.

J Bioeng. Tech. Health 2023;6(1):10-14

Materials and Methods

After the survey of methodologies for producing kefir, the fermentation process was established in the nutrient media: water kefir in water with sucrose, water kefir from water-soluble coconut extract, water kefir in whole grape juice, and milk kefir in milk.

In previously cleaned recipients, we prepared different culture media. We mixed water (1L) with organic brown sugar (100g) at room temperature to prepare the water with sucrose solution. In another container, 1L of grape juice was placed. For the water-soluble coconut extract, 1 coconut (229.61g), water (1L), and organic brown sugar (100g) were used, and the material was processed in a blender and filtered, and finally, pasteurized whole milk (1L).

We inoculated sucrose, grape juice, water-soluble coconut extract, and water kefir grains (200 g) for the media of the water solution. Moreover, we inserted milk kefir grains (13.192 g) for milk. The containers were closed with a thin cloth, and the fermentation process was carried out at room temperature in a place with little light for 24-48h. Then, the kefir was filtered, and the beverage was stored in the refrigerator at approximately 4°C [8-10]. Finally, the grains were stored for further use. We used the Nogueira and colleagues' method (2016) [11] to cell growth of fermented kefir grains (▲m) on different substrates. For the results, the grains were weighed before and after fermentation; after that, the numbers obtained were applied to the following equation [11]:

$$\blacktriangle m(\%)=(mkf-mk0)/mk0*100 \quad (1)$$

In equation 1, ▲m(%) is the change in mass of kefir grains, (mk0) is the weight at the beginning, and (mkf) after fermentation. The Nogueira and colleagues' method (2016) [11] determined the yield, the beverage mass was measured before and after fermentation, and the results were applied to the following equation [11]:

$$R(\%)=msf/ms0*100 \qquad (2)$$

In equation 2, R(%) corresponds to the beverage yield, ms0 corresponds to the initial mass, and msf to the final mass of the fermented kefir beverage in the substrates, respectively [11].

The titratable acidity method of Adolfo Lutz (2005) [12] was performed twice after 24 hours of the fermentation process. The results were expressed in g/100mL of lactic acid. For the pH evaluation, direct reading was done using a calibrated ph meter. In addition, the soluble solids content (°Brix) was measured by direct reading in a digital refractometer [10].

Microbiological analysis was performed on the beverages after 24h of fermentation to quantify the presence of different microorganisms.

For lactic acid bacteria analysis, samples were used at a dilution of 10^{-7} and 10^{-8}, in duplicates in 3MTH PetrifilmTM Lactic Acid Bacteria Count (LAG) Plates, following the manufacturer's guidance [13].

Mold and yeast analysis was done at 10^{-3}, 10^{-7}, and 10^{-8} dilutions in duplicates on 3MTN PetrifilmTM Rapid Yeast and Mold Count (Rym) plates, following manufacturer's guidance (3M Petrifilm, 2021). In addition, aerobic mesophilic bacteria analysis was done at 10^{-7} and 10^{-8} dilutions in duplicates on 3MTM PetrifilmTM Aerobic Count (AC) plates, following the manufacturer's guidance [13].

Results and Discussion

We analyzed the grains' growth, comparing the final and initial mass of the grains grown in each medium separately. Table 1 shows the variation in mass and the percentage of mass acquired.

After the analysis of the kefir grains' yield (Table1), we observed that the grains of water kefir fermented in water-soluble coconut extract and whole grape juice grew, on average, 12.9% more than the grains of water kefir in water with sucrose, which is its standard culture medium. The results showed that adding these 2 substrates in the kefir fermentation made the medium more nutritious, benefiting the grains. The grains of

Table 1. After fermentation in different nutrient media, the yield of kefir grains and kefir drinks.

Grain	Nutrient Media	Yield Grains (%)	Yield Drink (%)
Water kefir	Water solution with sucrose	8.7	100
Water kefir	Entire grape juice	21.3	100
Water kefir	Water-soluble coconut extract	21.9	85
Milk kefir	Milk	36.2	100

milk kefir also had a good yield. So, for producing the fermented milk kefir drink, a smaller amount of grains is necessary compared to the number of grains needed to produce the water kefir drink. In the study directed by Pereira and colleagues (2011) [7], the kefir grains obtained an average growth of 20% concerning the initial weight of the grains, similar to the present study, in which the average grains' growth was 22% [7].

The yield of the drinks was analyzed with the drinks before and after fermentation, comparing the final and initial volume of the drinks (Table 1). Table 1 shows that the yield of kefir fermented beverages in the different nutrient media was good (100%), except for the water-soluble coconut extract, which had an estimated loss of 15%. The high content of lipids in the coconut caused this loss. These lipids solidified in the water-soluble coconut extract during fermentation, so they were removed from the beverage through filtration.

The soluble solids index was checked before and after the fermentation process, in the 4 different culture media, with the help of a digital refractometer. Table 2 presents the results of the brix degree.

Table 2 presents the number of soluble solids (basically as sugar or sucrose) consumed by the grains in each culture medium. The water kefir grains that obtained the highest sugar consumption were those fermented in water-soluble coconut extract. This higher consumption of sucrose in this medium was responsible for causing a higher yield of the grains in this substrate. Tu and colleagues (2019) [14] found a significant reduction in the contents of soluble solids from 9.20 to 4.43 ºBrix in 48 hours of water kefir grains' fermentation. The results found in the literature were similar to those exposed in this work, considering that the fermentation in this study was only for 24h. Tu's study also observed that the grape juice presented a very high result of soluble solids at the beginning and end of the fermentation. This high sugar content in this substrate was not favorable for fermentation and resulted in a compromise in the grains' health, similar to the present study, in which the average growth of the grains was 22% [14].

Our results indicated the quantification of lactic acid in the samples, and the pH analysis was performed separately on each medium after fermentation (Table 3).

Table 3 presents the fermented beverages' percentages of lactic acid lower than 1%. According to the legislation, Resolution No. 46 determines that kefir should have a maximum acidity (expressed as lactic acid) of 1% [4]. Thus, the fermented beverages

Table 2. Quantity of soluble solids per degree Brix.

Grain	Nutrient Media	Total Soluble Solids Before Fermentation (°Brix)	Total Soluble Solids After Fermentation (°Brix)
Water kefir	Water solution with sucrose	9.8	7.5
Water kefir	Entire grape juice	22.2	19.5
Water kefir	Water-soluble coconut extract	8.7	5.7
Milk kefir	Milk	8.0	7.6

prepared in this study showed percentages of lactic acid within the limit established by legislation. A study conducted by Alves (2020) [10] regarding the production of lactic acid found a variation of acidity from 0.68 to 1.01 g/100mL in 24 hours of kefir grains' fermentation [4].

The pH values found in the study of physicochemical characterization of fermented products by kefir grains are usually in the range between 4.2 and 4.5. In the present study, we noted more excellent proximity of the pH level found in the products based on milk, water and sucrose, and water-soluble coconut extract, which showed more intense changes in the fermentative process. On the other hand, the product developed from whole grape juice showed a pH level farther from the range found in previous studies, and the average found in the analyses (mean pH = 4.00, with a value of 3.41) may indicate one of the reasons for the low effectiveness of microorganisms in the medium.

The microbiological analysis indicated the microorganisms' colony-forming units desired to evaluate each beverage's probiotic potential. Table 4 shows the values found for each order.

Following the amount of UFC presented for each drink (Table 4), the milk kefir and water kefir drinks in water-soluble coconut extract are probiotics because they meet the minimum viable amount of lactic acid bacteria in probiotic foods, which should be between the range of 10^8 to 10^9 UFC in the daily recommendation of the product ready for consumption [4]. On the other hand, the water kefir drinks in sugar water and grape juice did not show probiotic potential. This result in the grape drink may have been caused by the high amount of soluble solids, which made the culture medium unviable for these microorganisms.

The quantity of colony-forming units of molds and yeasts (Table 4), we observe that all drinks presented between 10^3 and 10^4 UFC. In kefir production, yeasts play an important role in the fermentative process because in addition to providing essential nutrients for growth, such as amino acids and vitamins, changing the pH, and helping to expel ethanol and produce CO_2, produces metabolites, which contribute to improving the flavor of kefir [15]. Nevertheless, to fulfill their role and enrich the fermented beverage, yeasts must be

Table 3. Determination of lactic acid by titratable acidity.

Grain	Nutrient Media	Lactic Acid After Fermentation (g% LA)	pH at Post-Fermentation
Water kefir	Water solution with sucrose	0.16	4.00
Water kefir	Entire grape juice	0.70	3.41
Water kefir	Water-soluble coconut extract	0.41	3.91
Milk kefir	Milk	0.67'	4.71

Table 4. Microbiological analysis of fermented beverages.

Grain	Nutrient Media	Lactic Acid Bacterias (UFC/mL)	Aerobic Mesophiles	Molds	Yeasts
Water kefir	Water solution with sucrose	1.80×10^7	2.00×10^7	6.50×10^3	8.00×10^3
Water kefir	Entire grape juice	1.00 x 10 est.	1.00 x 10 est.	1.00×10^3	2.50×10^3
Water kefir	Water-soluble coconut extract	2.22×10^{10}	1.63×10^{10}	8.60×10^4	4.95×10^4
Milk kefir	Milk	7.74×10^9	1.04×10^{10}	3.30×10^4	9.50×10^4

in controlled quantity. According to the Technical Regulation of Identity and Quality of Fermented Milks, the mold and yeast count should equal or less than 10^4 UFC/mL [4]. Generally, the samples had mold and yeast counts equal to or below the minimum established by the Technical Regulation of Identity and Quality of Fermented Milks.

In the microbiological result of mesophilic aerobic count (Table 4) we note the high value of the same in milk kefir and coconut water-soluble extract kefir. According to Franco (2007) [16], mesophilic bacteria, when present in high counts (more significant than 10^6 UFC/mL), can cause the deterioration of the product and decrease the shelf life of foods [16]. The results obtained in this research exceeded this value, except for the fermented water kefir drink in water with sucrose, which found 2.00 x 10^7 UFC. There was no sign of fermentation and bacterial growth in the whole grape juice due to the high amount of soluble solids.

Conclusion

Observing the behavior of kefir in the different media, we note that all beverages presented pH and lactic acid values within the norms released by the legislation, being suitable for consumption before this requirement. The probiotic potential of the beverage and the yield of grains were favorable in water kefir fermented in water-soluble coconut extract and milk kefir. The beverages had a good yield, except for the water-soluble coconut extract, which lost approximately 15% of the beverage due to the high lipid content present. The grape juice did not obtain satisfactory results, as it was not a suitable medium for kefir fermentation due to its high soluble solids content.

For future research, the behavior and probiotic potential of kefir in coconut milk will be evaluated using milk kefir and diluted grape juice, thus reducing the number of soluble solids fermented with water kefir.

References

1. Silva EO.Kefir: Propriedades Funcionais e Gastronômicas. 1.ed. Cruz das Almas - Bahia: UFRB, 2015. p. 7-123.
2. Borgovoni TF.Biocompostos das polpas de maracujá e de buriti: caracterização e aplicação em leite. São José do Rio Preto: Universidade Estadual Paulista “Júlio de Mesquita Filho”. 2018. 90p. (Dissertação, Mestrado em Ciências de Alimentos).
3. Fooks LJ et al. Probiotics as modulators of the gut flora. Br J Nutr 2002:88:S39-S49.
4. Brasil. Ministério da Agricultura, Pecuária e Abastecimento (MAPA). Instrução Normativa nº 46, de 23 de outubro de 2007. Adota o Regulamento Técnico de Identidade e Qualidade de Leites Fermentados, anexo à presente Instrução Normativa. Diário Oficial da República Federativa do Brasil, Brasília, 24 out 2007.
5. Chen C et al. Probiotics and prebiotics: role in clinical disease states. Adv Pediatr 2005; 52:77-113.
6. Paiva YF et al. Iogurte adicionado de polpa de abacaxi, base mel: elaboração, perfil microbiológico e físico-químico. Revista Verde de Agroecologia e Desenvolvimento Sustentável 2015;10(5):22-26.
7. Pereira GM et al. Caracterização físico-química e sensorial de kefir tradicional e derivados. Arquivo Brasileiro de Medicina Veterinária e Zootecnia 2011;63(2):473-480.
8. Santos FL. Produção artesanal de kefir. Ferlando Lima Santos, 2004.
9. Almeida FA et al. Análise sensorial e microbiológica de kefir artesanal produzido a partir de leite de cabra e de leite de vaca. Rev Inst Latic “Cândido Tostes” 2011;378(66):51-56.
10. Alves V. Desenvolvimento de bebida fermentada com kefir de água em extrato vegetal hidrossolúvel de coco (*Cocos nucifera l.*) com adição de inulina. 2020.
11. Nogueira LK,et al. Milk and açaí berry pulp improve sensorial acceptability of kefir fermented milk beverage, ActaAmazônica 2016;46(4):417-424.
12. Instituto Adolfo Lutz. Métodos Físico-Químicos para Análise de Aimentos.Instituto Adolfo Lutz. 4ª Edição. 2005.
13. Segurança Alimentar. 3M Petrifilm, 2021. Disponível em: <https://www.3m.com/3M/en_US/food-safety-us/support/package-inserts/>.Acesso em: 20, Abril de 2022.
14. Tu C, Azi F, Huang J, Xu X, Xing G, Dong M. Quality and metagenomic evaluation of a novel functional beverage produced from soy whey using water kefir grains. LWT Food Science and Technology 2019;113:108-258.
15. Ghedini TG. Qualidade microbiológica do kefir. Brazilian Journal of Development. Universidade de França. 2020.
16. Franco BDGM, Landgraf M. Microbiologia dos Alimentos. São Paulo: Atheneu, 2007.

The Increase of Wearables in Health: A Market Study

Maely Guilherme Botelho Coelho Filho[1*], Thiago Cardoso Maia[1], Carlos Augusto Bispo Dias[2], João Carlos Fregonazzi Tavares[2], Rayane Cremasco Martins[2], Thamiles Rodrigues de Melo[1], Valéria Loureiro da Silva[1], Valter Estevão Beal[1]

[1]SENAI CIMATEC University Center; Salvador, Bahia; [2]Academic Association Of Technology and Innovation in Health; Vitória, Espírito Santo, Brazil

This study aims to identify and characterize the most relevant medical devices to collaborate with in developing new technological resources for the healthcare market. A market study was carried out using the devices on the ANVISA platform. The chosen ones were divided into 5 scores, with 5 being the closest to the objective of the study, in order to compare their functionalities and connectivity. The number of features reveals that group 5 has had an average of 8.75 features per device, confirming the group with the most significant impact. However, further studies must list and analyze other health devices to categorize them, contributing to the production and advancement of this sector.
Keywords: Devices. Wearables. Sensory.

Introduction

Market Definitions and Context

Nowadays, there is a significant increase about health and well-being in all age groups. The National Health Survey (PNS), produced by IBGE, points out that in 2019 the average number of Brazilians who practiced the recommended level of physical activity during leisure time was 30.1%, while in 2013, this average was 22.7%, indicating a percentage increase in these indicators [1]. Regulated diet, physical exercise, and sleep quality are increasingly frequent guidelines. Concurrently, there is a growth of technologies that contributes to new emerging habits, such as Wearable Devices (Wearables) with health-related functions. Cooperation between technology and health has had existed for centuries, making it essential for their mutual evolution. Technological resources are essential in health support as they apply knowledge and skills to solve the population's health problems and improve the quality of life by creating devices, medicines, vaccines, and organizational and support systems [2].

Wearables allow continuous monitoring of the individual non-invasive and real-time by biochemical markers in body fluids, such as sweat, saliva, tears, and interstitial fluids [3]. Due to this, they help transform healthy activities into daily habits, allowing the individual to understand their evolution, set and achieve personal goals and prevent health complications, all with greater comfort and convenience, directly from their wearable. Another area with great potential for use is among senior citizens, especially considering Brazil's exponential increase in population aging. This population can benefit from continuous and remote monitoring of wearables, given the increasingly independent habits of the style of life among individuals in this age group [4].

Study Purpose

Due to the growth in demand for these products, the increase in investments in this technology area is also evident, resulting in the evolution and need for global adaptation to this new reality. In the second quarter of 2021 alone, this market saw a 32.3% increase in global shipments, with volumes reaching 114,2 million in this period [5]. Multinational technology companies such as Apple,

Received on 28 November 2022; revised 10 February 2023.
Address for correspondence: Maely Guilherme Botelho Coelho Filho. Rua Pedro Fonseca, 165, Monte Belo, Vitoria, Espírito Santo,Brazil. Zipcode: 29053280. E-mail: maely.filho@medsenior.com.br.DOI 10.34178/jbth.v6i1.273.

J Bioeng. Tech. Health 2023;6(1):15-20

Samsung, Amazon, Google, and Microsoft have entered significant investments in the health market, expanding access to such devices and favoring a new stage in health care with interconnected systems and information [6].

The present work aims to identify and characterize the most relevant medical devices (software, hardware, or both) for use in a hospital, home, or outpatient environment, including their current and non-current resources available in the ANVISA database (National Health Surveillance Agency), in order to collaborate with the development of new technological resources for the health market, meeting the premises set forth by the regulations of this regulatory agency and by the demand and relevance in the current market.

Materials and Methods

A cross-sectional observational analytical study was carried out to establish the medical devices available in Brazil with applications in wearables for use in hospital, outpatient, and preventive medicine settings.

The search for devices was conducted on the ANVISA platform from June to October 2021, limited to devices registered in the health sector. As a result, 94,146 devices were found of the most varied types. Of these, after the inclusion and exclusion criteria were established, 393 remained.

The inclusion criteria were:

1. Medical devices;
2. Software (whether or not linked to hardware);
3. Registered on the ANVISA platform, whether in force in their registration or not.

The exclusion criteria were:

1. Hardware-only devices (without proprietary software);
2. Imaging devices (PACS - Picture Archiving and Communication System).

Thirty-two devices were selected according to the relevance criteria. We did the screenings in 4 stages:

1. Screening by inclusion and exclusion criteria in the database;
2. Evaluation of the provisions by 3 independent reviewers, with disagreements resolved by consensus after discussion;
3. Classification of devices' relevances was performed with a score of 1 to 5, with 5 being the closest to the study's objective, by 3 independent reviewers, with the final relevance score calculated from the simple average of the scores. Each reviewer received all information about the device, its features, and its applications.
4. Compilation of each device's available functions and connectivity features into a table to compare them (Table 1).

Results and Discussion

Based on the review of the selected devices, the great potential and technology embedded in these devices presented in the ANVISA's table are evident. There are, therefore, trends, as among the most frequent features, there are primarily vital cardiac signs, with Heart Rate (HR) present in 12 devices of the total analyzed, followed by Blood Pressure (BP) in 11 devices and Electrocardiogram (ECG) in 8 devices. The fourth most frequent functionality is Oxygen Saturation ($SatO_2$), present in 7 devices, followed by two functions tied for fifth place: Glycemia and Irregular Heart Rhythm Detection (ICR) in 6 devices. Appearing on 5 devices each, Fall Prevention and Body Temperature appear, followed by CPAP/Apnea, the functionality available on 3 devices.

Regarding the total amount of functionalities (33 described in the table attached to the article), we noted that 16 are present among the four devices in the group rated 5, an average of 8.75 functionalities per device; therefore, the group with more significant impact. Likewise, the 4 devices in the 4th-grade group include 9 of the 33 features described, with an average of 4.25 features per device. On the other hand, in the grade 3 group, 9 of the 33 features described for having 7 selected devices had

Table 1. Criteria used in each relevant track.

Score	Classification Criteria
1	Challenges to convert to wearable: No long-term monitoring; In-hospital only; Difficult to connect to other devices; Monitor any vital signs.
2	Possible conversion to wearable; In-hospital only; No connection to other devices; Analysis is not real-time; Possible integration with Health Service.
3	Possible conversion to wearable: In and Out of Hospital; Connection to other devices/data storage; Non-portable; Real-time monitoring.
4	It has hardware: In and Out of the Hospital; Connection to other devices/data storage; Portable; Real-time monitoring
5	Wearable: In and Out of Hospital; Real-time monitoring; Connectivity to other devices/data storage.

Figure 1. More frequent features for the number of devices.

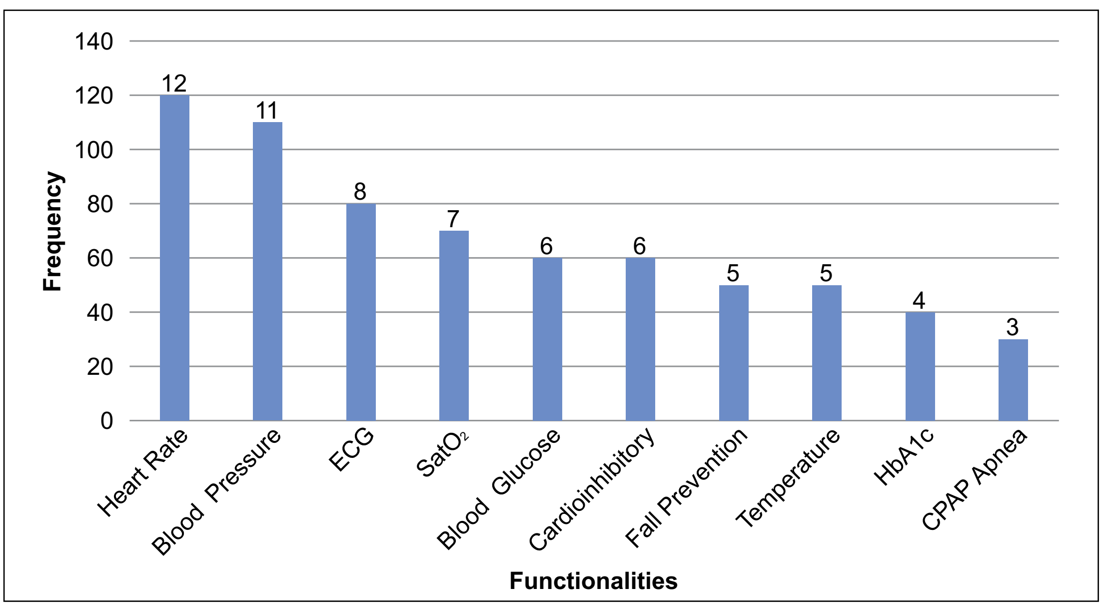

an average of 1.42 features per device. The grade 2 group, composed of 10 devices, included 13 of the 33 features, with an average of features per device 3.2. Also, the grade 1 group, with 7 devices, presented 11 of the 33 functions analyzed, reaching an average of 2.57 functionalities per device.

On the other hand, one can also point out the presence of particular features which appeared in only one device, such as Suggested Iron Dosage, Stroke Risk, Eye Pressure, Noise Monitoring, Neural Network Mapping, Fecal Calprotectin, and the Infusion Pump.

Bearing in mind the infinity of variables in the selected devices, both in terms of their functionalities, connectivity options, and the design of the products (size, shape, weight, and materials used), it became clear the need to classify these of relevance, to facilitate a macro analysis of similar devices. Because of this, we developed the relevance criteria in 5 grades in search of a product that, in our conception, would be the closest to ideal.

It would be a portable device (preferably wearable), which can monitor vital signs in real-

Figure 2. The total number of features presented in each score.

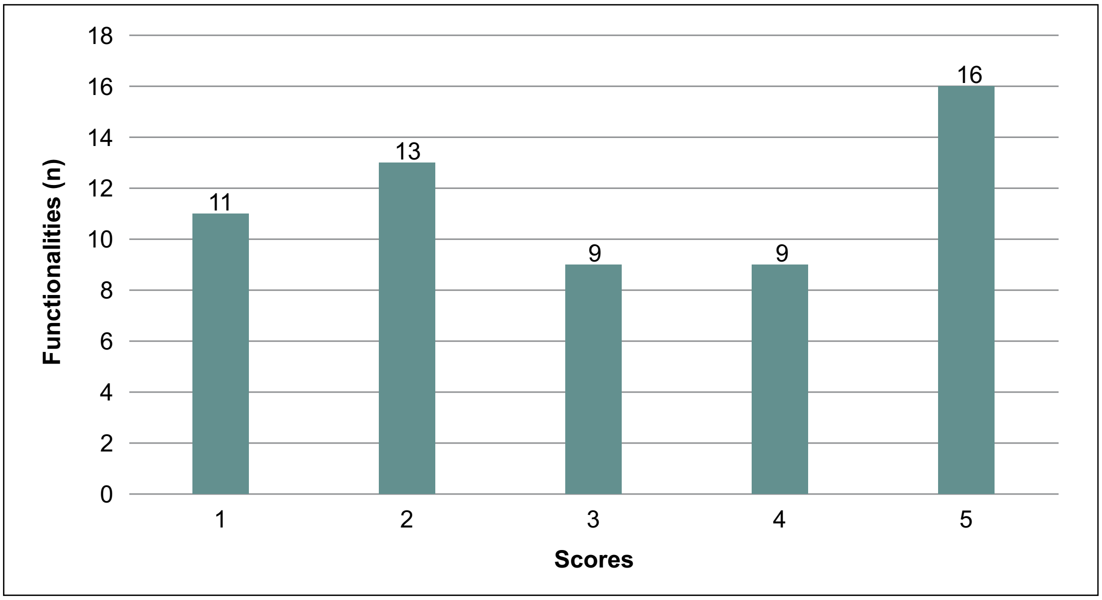

time, allows connectivity with other devices (and thus information traffic), and has data storage capacity so that the parameters records are not lost and can be used for in-depth analysis by algorithms and professionals, in addition to maintaining patient history. In addition, use resistant materials while having a competitive market price and being accessible to different social classes. It is also interesting that it can be used in different environments, both hospital and home, and its features adapt to the needs of each user.

Based on the average functionality data per device, it is evident that despite being portable (since one of the criteria for inclusion in the group is to be wearable), the devices in the grade 5 group have more technology embedded in each of their devices, while being small, light and versatile, making them the devices that most resemble the one proposed by the project. Based on this, the devices included in this classification category are the closest to ideal. They are wearable, capable of home and hospital use, have real-time monitoring, storage, and connectivity with applications and other devices, and are already available and validated by Organ's competent bodies in the Brazilian market.

Of the four devices selected, the devices in the grade 5 group, Galaxy Watch and Apple Watch fit as watch-shaped wearable devices, which have features such as heart rate monitoring, pulse oximetry, irregular rhythm notification, sleep monitoring, and detection of drop, among other functions (Table 2). On the other hand, the Libre Link device, through daily measurements, estimates the user's glycated hemoglobin using a minimally invasive sensor, which, when passing the reader that comes with the kit or the user's smartphone, allows the reading of glucose, its trend (increasing, decreasing or stable), the development of graphs and the estimated calculation of glycated hemoglobin, through the daily values - factors that made it be selected for group 5. Finally, the Wipple device has a portfolio of medical devices connected devices that can be used by synchronizing them with the Wippe Track application, thus taking advantage of features such as monitoring physical activity (calories spent, kilometers traveled, number of steps) through a wearable watch type, digital scale, Portable ECG and digital blood pressure monitor, which detects HR, BP, and RCI.

When it comes to device connectivity, the Apple Watch and Galaxy Watch are once again on

Table 2. Features available on score 5 devices.

	Devices Score 5			
Functionalities	**Apple Watch**	**Galaxy Watch**	**LibreLink**	**Wippe**
Altimeter	x	x		
Digital scale	x			x
Compass	x	x		
Cellular connection	x	x	x	x
Falls Detection/Prevention	x	x		
ECG	x	x		x
Heart rate	x	x		x
Glicemy			x	
Noise monitoring	x			
Sleep monitoring	x	x		
PA monitoring	x	x		
Water resistance	x	x		
Dust resistance	x	x	x	
Irregular heart rate	x	x		
$SatO_2$	x	x		x
SOS Emergency	x	x		

par, offering the user a range of options, including LTE, Bluetooth 5.0 (which has the advantage of spending less battery), Wi-Fi, NFC (Near Field Communication, short-range wireless network), A-GPS (Assisted Global Positioning System - which uses the cellular network to improve GPS performance) and/or GLONASS (Global Navigation Satellite System in Russian) and UMTS (3rd generation operators, popularly known as 3G) (Table 3).On the other hand, the Libre has only the NFC sensor, which transmits glucose data to the reader of Abbott's authorship or a smartphone with this technology (iOS or Android devices), making the device even more practical. Wippe, in turn, has only Bluetooth 5.0 available to connect its four devices to the user's smartphone.

With the progress of this study, the number of functionalities in the most different devices already available in the national market for different applications becomes evident. In this sense, we notice a great potential in Wearables to contribute to medical care in the world, automating processes, preventing comorbidities and accidents, and collecting data beyond the hospital environment, which with the use of these devices, can be much faster and more accurate, avoiding thus the loss of data from medical records and fraud. Furthermore, it allows us to verify that we already have the technology, the regulation by competent institutions, and the economic market that demands this type of device in our national territory.

Conclusion

Briefly, a current study of health devices present in Brazil, according to the ANVISA platform, was addressed in this work, analyzing their functionalities, connectivity, and importance in the current scenario. The relevance of this theme was noted because of the increase in the world

Table 3. Connectivity options available on score 5 devices.

	Devices Score 5			
Connectivity	**Apple Watch**	**Galaxy Watch**	**LibreLink**	**Wippe**
LTE	x	x		
Bluetooth 5.0	x	x		x
Wi-Fi	x	x		
NFC	x	x	x	
A-GPS / GLONASS / Beidou 7	x	x		
UMTS	x	x		

market for these devices, their production, and their relevance in the daily life of the population. It is concluded that the most used/relevant features were heart rate, blood pressure, and ECG, indicating concern with cardiovascular diseases that are the leading cause of death in the world [7].

The initially proposed objective of identifying and characterizing the most relevant medical devices (software, hardware, or both) was achieved, as detailed in the attached table. Finally, it is suggested to deepen market studies that list and analyze the other health devices in the world market to categorize them, contributing to the production and advancement of this sector and stimulating, in fact, their application to the final customer.

References

1. Brasil. Ministério da Saúde. Pesquisa Nacional de Saúde - Percepção do Estado de Saúde, Estilos de Vida, Doenças Crônicas e Saúde Bucal. Brasília, 2019. Available at: <https://biblioteca.ibge.gov.br/visualizacao/livros/liv101764.pdf>. Accessed on: Jan 10, 2021.
2. Health Technology Assessment. World Health Organization - Regional Office for Europe. Available at: <https://www.euro.who.int/en/health-topics/Healthsystems/health-technologies-and-medicines/policy-areas/health-technologyassessment>. Accessed on: Jan 10, 2022.
3. Kim J et al. Wearable biosensors for healthcare monitoring. Nature Biotechnology 2019;37(4):389-406.
4. Ajami S, Teimouri F. Features and application of wearable biosensors in medical care. Journal of Research in Medical Sciences 2015;20(12):1208-1215.
5. Chou J et al. Wearable Devices Market Share. IDC, Massachusetts, Dec 2021. Available at: <https://www.idc.com/promo/wearablevendor>. Accessed on: Jan 10, 2022.
6. Brasil. Agência Nacional de Vigilância Sanitária. Manual de Tecnovigilância. Brasília, 2021. Accessed on: <https://www.gov.br/anvisa/ptbr/centraisdeconteudo/publicacoes/fiscalizacao-emonitoramento/tecnovigilancia/manual-tecnovigilancia-2021v4.pdf/@@download/file/MANUAL%20TECNOVIGILANCIA%202021%20v4.pdf>. Accessed on: Jan 10, 2022.
7. Doenças Cardiovasculares. Organização Pan-Americana de Saúde (OPAS). Accessed on: <https://www.paho.org/pt/topicos/doencas-cardiovasculares>. Accessed on: Jan 10, 2022.

Study of the Technical-Economic Feasibility of a Pyrolysis/Gasification Plant for the Generation of Liquid Gas Fuels from Plastic Waste

Hugo Gomes D'Amato Villardi[1*], Fabiano Ferreira de Medeiros[1], Fernando Luiz Pellegrini Pessoa[1,2], Jailson Bittencourt de Andrade[1,2], Alex Álisson Bandeira Santos[1,2]

[1]SENAI CIMATEC Uiversity Center, [2]Postgraduate Program in Computer Modeling and Industrial Technology, SENAI CIMATEC University Center; Salvador,Bahia, Brazil

Pyrolysis can offer a practical environmental solution for recycling plastic waste, converting it into liquid and gaseous fuels of high commercial value. This article proposed the simulation in Aspen Plus® of a pyrolysis/gasification plant, having plastic residues and residual soybean oils as raw material. The products generated in the gasifier are bio-oil and synthesis gas, which can be converted into ethylene and gasoline in reactors. To calculate the plant's cost of capital, the Lang Method was used. The economic indicators NPV, IRR, PI, and Payback determined the project's viability. The works show that the current scenario studied has economic viability, but better results can be achieved with increasing project maturity.

Keywords: Plastic Waste. Pyrolysis. Gasification. Simulation. Economic Evaluation.

Introduction

The dependence on energy in its many forms by society is high. Worldwide, energy demand is expected to increase by a third between 2015 - 2040, mainly in countries outside the Organization for Economic Co-Operation and Development [1]. Moreover, the rise in the standard of domestic consumption, industrial growth, and the increase in urbanization have brought the increase in fuel consumption and in pollution caused by solid waste, with plastics being one of the leading waste discarded.

Plastic is an organic synthetic polymer produced based on petroleum, which serves as a raw material for the manufacture of the most varied objects and with high durability. In 2020, around 367 million tons of plastics were produced worldwide [2]. However, this amount produced ends up generating an environmental liability. According to Plastic Europe (2017), around eight million tons of plastic waste are released annually into the oceans.

Received on 15 December 2022; revised 23 February 2023.
Address for correspondence: Hugo Gomes D'Amato Villardi. i. Av. Orlando Gomes, 1845, Salvador, Bahia, Brazil. Zipcode: 41650-010. E-mail: hugo.amato@fbter.org.br.DOI 10.34178/jbth.v6i1.274.

J Bioeng. Tech. Health 2023;6(1):21-27

In Brazil, mechanical recycling is the most widespread for using plastic materials. However, in recent years, thermochemical conversion technologies have gained significant attention.

Pyrolysis offers a practical solution for recycling plastic waste, converting it into liquid fuel oil as the main product with high marketing value. Furthermore, the process generates by-products, such as reduced gases, due to the absence of O_2 in the process [3], in addition to carbon black as a solid material. Therefore, this technology adds environmental and economic benefits at the same time.

Pyrolysis

Pyrolysis is a thermochemical process in which organic chains undergo breakage in their original molecular structure, through a complex set of chemical reactions, due to the action of rapid heating in the absence of oxygen, reducing long-chain organic molecules into shorter molecules. The raw materials for pyrolysis is from many heterogeneous origin.

The pyrolysis of plastic material occurs in four stages: initiation, transfer, decomposition, and termination, resulting in the production of vapors and coal [4]. These pyrolysis vapors include condensable and non-condensable gases. The liquefaction of the condensable vapors forms the pyrolysis wax/oil, a complex combination of the thermal cracking products of each type of plastic. Interactions occur between the primary thermal cracking products to increase this complexity, producing secondary products [5]. Solid waste (coal) and non-condensable gases are also produced, but they are usually by-products of the pyrolysis process [6].

Three types of pyrolysis are classified by process duration and operating conditions: slow, fast, and flash (Table 1). In slow pyrolysis, which lasts longer, the reaction time is stipulated according to the raw material, which can vary from 10 min to 10 h. The low heating rates and temperatures are generally 5 to 10 K/min and 500 to 900 K, respectively [7]. Under these conditions, the percentage of carbonaceous solids is maximized; however, the yield and composition of the product are determined by the reaction parameters and the raw material. In fast pyrolysis, heating rates, and temperatures are higher, whereas gaseous products and oils tend to maximize.

This work investigates the technical-economic feasibility of obtaining combustible gases and liquids by developing and simulating a gasification/pyrolysis plant in Aspen Plus®, using plastic waste and residual soybean oil as raw material. We have been guided by economic indicators - Net Present Value (NPV), Internal Rate of Return (IRR), Profitability Index (PI) - to make the project viable.

Materials and Methods

Process Simulation of a Gasification/Pyrolysis Plant

We used a method adapted from the literature [8-10] for a simulated double-fluidized bed gasifier in Aspen Plus® v8.8 operating at 850 ºC and 1 atm. The raw materials for feeding the gasifier were plastic and residual soybean oil, both at a flow rate of 100 kg/h. The synthesis of two products, ethylene, and gasoline, is proposed from the gas produced (syngas). The criteria adopted for the gasification reactions was minimizing the Gibbs free energy coupled with the equilibrium constraint method.

For the synthesis of the final products, equilibrium reactors were used. The premises considered in this work were:

1. Steady state and isothermal operation;
2. Pressure and temperature are uniform in each reactor;
3. Load and heat losses are neglected;
4. Drying and pyrolysis stage are instantaneous;
5. Ash is inert;
6. All carbon in the biomass is gasified or converted to ash;
7. Purification steps represented by numerical separators.

The thermodynamic package selected was the Peng-Robinson cubic equation of the state with the Boston-Mathias alpha function, which models the gas phase at medium and high pressures with good accuracy. The enthalpy model used was HCOALGEN with standard code options. Each number refers to a calculation method for obtaining the heat of combustion, standard heat of formation, heat capacity, and base enthalpy of coal. For density, the model was DCOALIGT.

Figure 1 presents the process simulation's scheme. The SF stream is the heated raw material that feeds the gasifier after passing through the exchanger (TC). The EQ stream that leaves the gasifier goes to the TC as a hot stream, and the other

Table 1. Typical technological parameters of different types of pyrolysis [7].

Pyrolysis	Process Time	Temperature (K)	Heat Rate (K/min)
Slow	10 min - 10 h	500 - 900	5 - 10
Fast	10 - 20 min	700 - 900	50 - 100
Flash	< 10 min	1000 – 1300	> 100

Figure 1. Flowchart of ethylene and fuel gas production from plastics and vegetable oils.

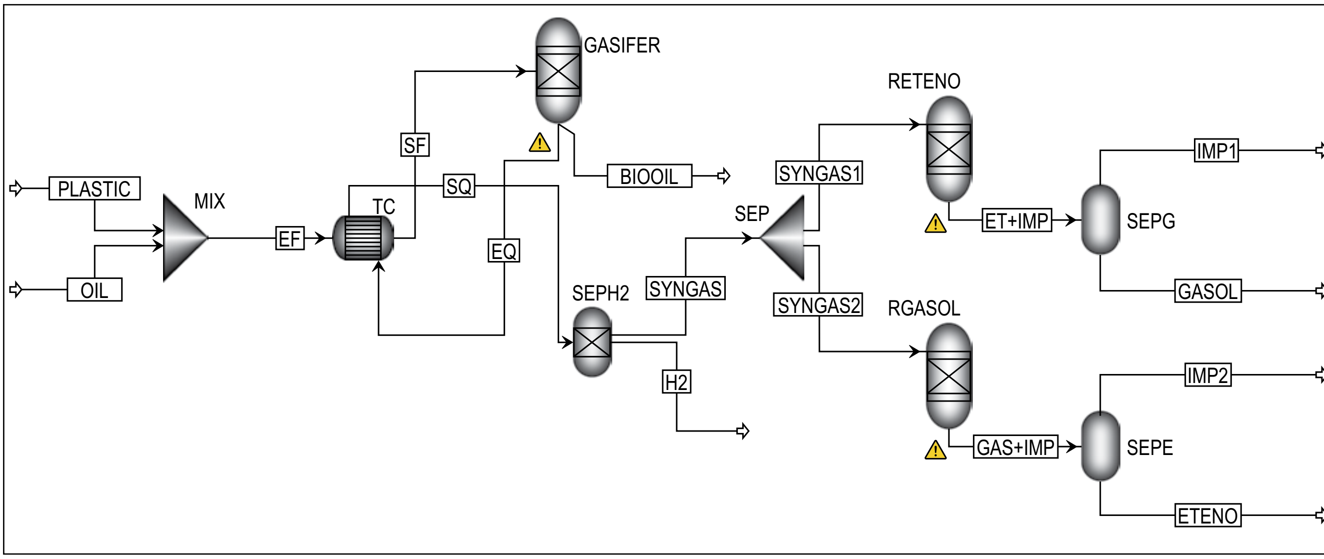

stream is the Bio-oil produced (Green Diesel - GD). The CT (SQ) output current goes to a separator (SEPH2), separating the syngas from the H_2. The SYNGAS current is divided into SYNGAS1 and SYNGAS2, where the separation percentage is defined. The currents SYNGAS1 and SYNGAS2 are sent to two different equilibrium reactors: one operating at 300 ºC and 10 bar and the other at 320 ºC and 40 bar, reaction conditions based on the literature [11]. The separator vessels (SEPG) and (SEPE) remove impurities from the final products in the streams (IMP1) and (IMP2), respectively, characterized by H_2, CO, O_2, and CO_2.

Economic Evaluation of the Gasification/Pyrolysis Plant

The Lang Method [12] was used to estimate the capital cost of the pyrolysis unit. This methodology has a degree of uncertainty of around 35 % but allows for comparing different procedural alternatives. The total investment capital (Total Capital Investment, TCI) is obtained by Equation 1:

$$C_{TCI} = 1.05\, f_L \sum i \left(\frac{PCI_i}{PCI_{b,i}}\right) C_i \qquad (1)$$

in which: CTCI is the total investment cost, including working capital; fL is the Lang Factor, which for a plant that processes solids and fluids is equal to 5.9; Ci is the cost of each of the sized equipment; PCIi and PCIb, i are the Plant Cost Index in the current year and the base year, respectively. The value of the Plant Cost Index for the year on which the correlations were based was 394. For the year 2021, this value is 680.5.

Using the data obtained in the simulation, the design was based on the equations proposed in the literature [12]. The flow rates (m^3/h), operating pressure (psig), and temperature (ºF) obtained from the ASPEN simulation data were used as input data. The quotient between inlet flow, residence time, and catalyst composition determined the reactor volume.

A scenario of 50 % hydrogen recovery and syngas separation to 25 % gasoline and 75 % ethylene was considered. The equipment was then dimensioned, and the costs were estimated for that scenario. Finally, production costs were calculated following the literature method [13], considering that the plant operates 24 hours a day and 334 days a year, totaling 8016 hours.

The base prices considered for the raw material, the products, and utilities, in addition to the catalysts, along with their composition and density, were taken from the COMEX STAT (portal for accessing Brazilian foreign trade statistics), obtained by the ratio between the f.o.b import value, in US dollars, and the net import kilogram value for 2022.

The price of electricity and water were obtained from the tariffs published by ANEEL - National Agency of Electric Energy - for the industrial sector in August 2020 and by ANA - National Agency of Water and Basic Sanitation for the same sector and period, the conversion currency was carried out using the August 2020 quotation according to the Central Bank of Brazil.

The economic indicators evaluated to propose the feasibility of the project were the Net Present Value (NPV), the Internal Rate of Return (IRR), the Profitability Index (PI), and Payback.

Results and Discussion

The operational cost (Operational Expenditure - OPEX) corresponds to the cost associated with the daily operation of the pyrolysis plant. Its calculation is a function of direct production costs, fixed production costs, and general expenses. Among the factors that affect the operational cost are:

1. Direct costs comprising raw materials, inputs, utilities, labor, preventive and corrective maintenance, and operational supplies, along with others;
2. Fixed costs comprising depreciation, taxes, plant overheads, and
3. Overheads comprising the cost of administration, distribution and sales and research and development [13].

Table 2 presents the estimates of the operational costs of the pyrolysis plant obtained through the models presented in this work. The total operating cost of the pyrolysis plant was close to US$ 640,000.00 per year.

The cost of capital (Capital Expenditure – CAPEX) includes investment costs in the pyrolysis plant to become operational. In addition, it includes the direct costs of acquiring equipment, indirect costs, contingency costs, and costs with auxiliary facilities [13]. Table 3 shows the estimates of the investment costs in the equipment of the pyrolysis plant, together with the indirect and auxiliary costs, added to the working capital necessary to keep the plant in operation. The total investment cost of the pyrolysis plant was in the order of US$ 3,145,000.00.

Table 4 shows the plant's revenue projection data, considering the formation of 4 main products based on the recovery scenario described in the methodology. Hydrogen generated the highest revenue return among products due to its higher selling price per kg (2.0 US$/kg).

A cash flow was prepared considering the estimated values of OPEX, starting operations in year 1, CAPEX, considering investment in year zero, and the projected revenue in year 1 of the project. To calculate the discounted cash flow (DCF), the net present value (NPV) formula was used, considering a minimum attractiveness rate (MAR) of 9.0 % per year and an average inflation rate (IR) of 6.0 % in the same period.

Figure 2 shows the discounted cash flow accumulated for 20 years of operation of the pyrolysis plant, considering the current economic scenario of the project and 2 additional scenarios: a pessimist with a 20 % lower revenue and an optimistic one with a revenue of 20 % higher. The results showed that the current scenario's calculated net present value (NPV) was positive, reporting a return of US$ 869,464.55. The internal rate of return (IRR) reported a return of 6 %, which is below the MAR (9.0 %). The profitability index (PI) reported a value of 1.28, which means that for every US$ 1.00 invested in the plant, US$ 1.28 is returned in present values. The payback, the time required to recover the initial investment, was 14.6 years. The economic indicators evaluated showed that the proposed implementation of a gasification plant could be economically viable under the conditions presented, except for the low value of the IRR. In a scenario where revenue is 20% lower, we found that the project is not viable within 20 years. However, in a scenario where revenue is 20% higher, the payback reduces considerably for 7.9 years, with an IRR of 13% (above MAR) and a positive NPV of US$ 3,605,316.42. Plant revenue and business

Table 2. Annual operating result of the economic evaluation of the pyrolysis plant.

Plant Operating Costs	
Direct Costs	
Raw material (CRM)	US$ 1,154.00
Plastic + Oil	US$ 1,154.00
Labor (CL)	US$ 35,456.11
Technical supervision (CTS)	US$ 5,318.42
Utilities (CUTIL)	US$ 119,701.04
Steam	US$ 0.00
Cooling water	US$ 63,854.40
Electricity	US$ 9,590.40
Catalysts	US$ 45,944.41
Adsorbents	US$ 311.83
Effluent disposal (CED)	US$ 0.00
Maintenance and repairs (CMR)	US$ 150,868.55
Operating supplies (COS)	US$ 22,630.28
Laboratory charges (CLAB)	US$ 5,318.42
Patents and royalties (CPR)	US$ 19,187.88
Indirect Costs	
Packaging and storage (CPS)	US$ 114,985.85
Local taxes (CLT)	US$ 27,717.14
Interest (CI)	US$ 12,572.38
Depreciation (non-accounting)	US$ 251,447.59
General Expenses	
Administrative costs (CADM)	US$ 28,746.46
Distribution and sale of products (CDSP)	US$ 63,959.59
Research and development (CR&D)	US$ 31,979.80
TOTAL OPERATING COST (OPEX)	**US$ 639,595.91/year**

profitability can be increased with greater project maturity.

Conclusion

This work proposed a study of using plastic and oily residues for synthesizing hydrogen, gasoline, and ethylene. The results of the simulation and economic evaluation point to a promising scenario. The total project investment was US$ 3,143,094.85 with an operating cost of US$ 639,595.91/year, and the plant generated 25 % of the products in hydrogen and 75 % of Syngas for the production of gasoline and ethylene. The economic indicators reported the feasibility of the project under the conditions presented. However, the payback time for the current scenario studied was 14.6 years, a reasonably long period with the IRR remaining below the MAR. In the optimistic scenario, the time to recover the initial investment was 7.9 years, with a positive NPV and an IRR of 13 % above the MAR.

Table 3. Capital investment results for the pyrolysis plant.

Pyrolysis Plant Investiment	
Equipment cost (Separators, gasoline, and ethylene reactors, gasifiers, and heat exchangers)	US$ 997,807.89
Indirect and ancillary costs	US$ 1,516,667.99
Working capital	US$ 628,618.97
TOTAL CAPITAL COST (CAPEX)	**US$ 3,143,094.85**

Table 4. Results of the annual revenue projection for the pyrolysis plant.

Plant Revenue Projection	
Hydrogen (H_2)	US$ 577,186.91
Bio-oil (Green Diesel)	US$ 96,192.00
Ethene	US$ 139,601.45
Gasoline	US$ 92,106.00
TOTAL REVENUE PROJECTION	**US$ 905,086.36**

Figure 2. Cumulative cash flow scenarios for a change in revenue at a MAR of 9.0 % and an IR of 6.0 % on the economic viability of the pyrolysis plant projec.

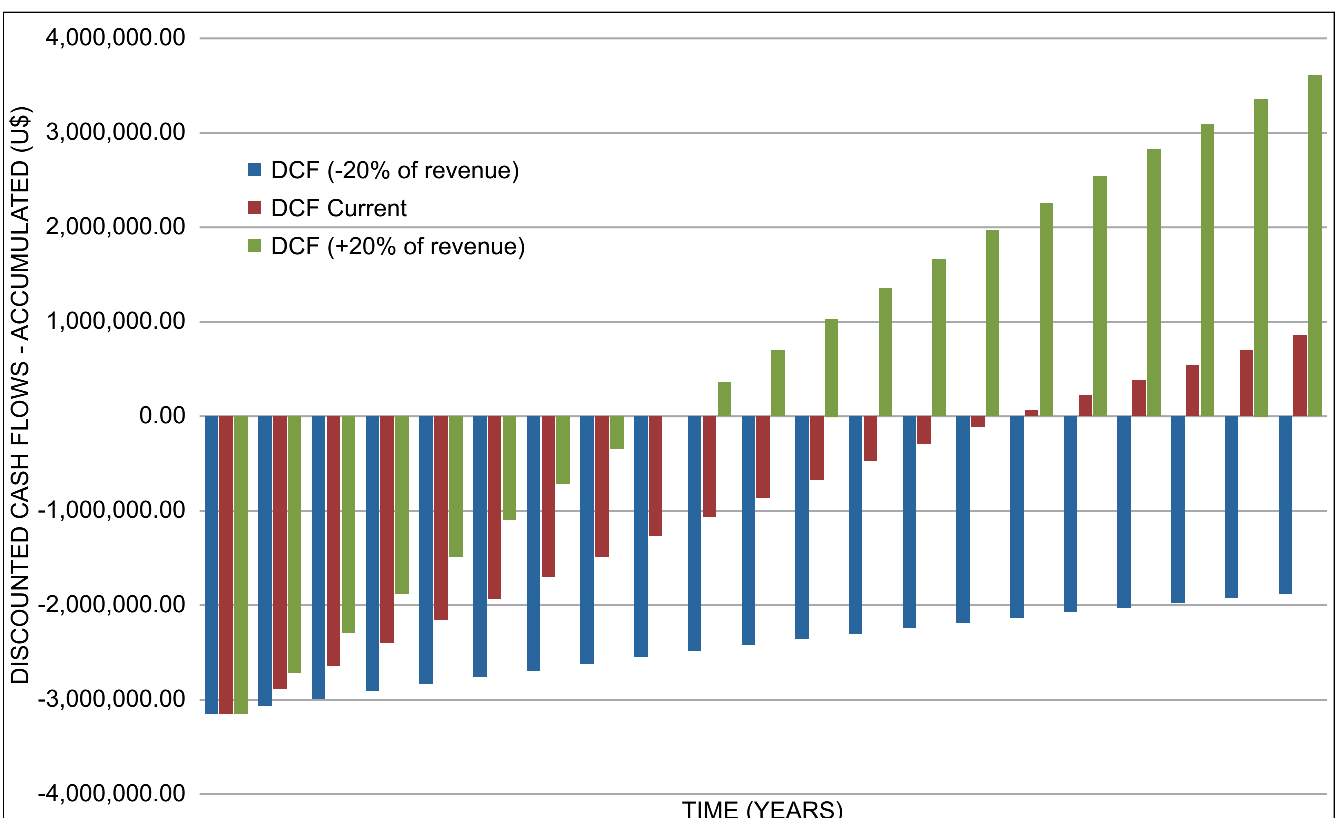

Acknowledgments

The authors thank Senai Cimatec for the opportunity to disseminate knowledge.

References

1. Energy Agency. International. World Energy Outlook 2016. Paris - France: [s. n.], 2016. Available at: www.iea.org/books.
2. Statista, Production of Plastics Worldwide from 1950 to 2018. 2020. Available at: www.statista.com/statistics/282732/global-production-of-plastics-since-1950/.
3. Fivga A, Dimitriou L. Pyrolysis of plastic waste for production of heavy fuel substitute: A techno-economic assessment. Energy 2018;149:865–874.
4. Faravelli T et al. Thermal degradation of polystyrene. Journal of Analytical and Applied Pyrolysis 2001;60(1):103–121.
5. Pinto F et al. Pyrolysis of plastic wastes. 1. Effect of plastic waste composition on product yield. Journal of Analytical and Applied Pyrolysis, v.51 (1–2), 39–55, 1999.
6. Young GC. Municipal solid waste to energy conversion processes. Economic, Technical, and Renewable Comparisons. New Jersey: John Wiley & Sons, Inc., Publication, 2010.
7. Pawelczyk E, Wysocka I, Gebicki J. Pyrolysis combined with the dry reforming of waste plastics as a potential method for resource recovery - A review of process Parameters and Catalysts. Catalysts 2022;12:362.
8. Doherty W, Reynolds A, Kennedy D. Aspen Plus simulation of biomass gasification in a steam blown dual fluidised bed. In: Materials and Process for Energy. Dublin: [s.n.]. 2013:212–220.
9. Puig-Gamero M et al. Three integrated process simulation using Aspen Plus®: Pine gasification, syngas cleaning and methanol synthesis. Energy Conversion and Management 2018;177:416–427.
10. Sikarwar VS, Zhao M. Biomass Gasification. Encyclopedia of Sustainable Technologies 2017;3:205-216.
11. Wang C et at. Investigation on hydrogen-rich syngas production from catalytic co-pyrolysis of polyvinyl chloride (PVC) and waste paper blends. Energy 2021;232:121005.
12. Seider WD, Seader JD, Lewin DR. Product and process design principles: Synthesis, analysis and evaluation. 2ª ed. New York: John Wiley & Sons, 2003, 786p.
13. Turton R, Bailie RC, Whiting WB, Joseph A, Shaeiwitz JA, Bhattacharyya D. Analysis, synthesis, and design of chemical processes. Prentice Hall - Pearson Education, Inc, 4° Ed., 2012.

Social Technology for Local Recycling of Plastic: An Example of Circular Economy

Adriano Puglia Lima[1,2*], Rosana Lopes Lima Fialho[1,2], Paulo Alberto Paes Gomes[1,3]
[1]Federal University of Bahia; [2]Industrial Engineering, Polytechnic School; [3]Institute of Humanities Arts and Sciences, Federal University of Bahia; Salvador, Bahia, Brazil

The pollution caused by an improper disposal of plastic is a problem that the current recycling model, based on large industrial plants, still needs to solve. An alternative is the so-called Local Recycling, in which people without specialized training transform discarded plastic into valuable objects in the disposal environment. This work presents a technology for recycling, with a robust social bias, which transforms plastic waste into solid bars and plates, later used in the production of furniture and other valuables. This technology is being applied in the field at the modular recycling unit in Pedra Furada – SE, where young people without technical training produce objects of high commercial value.
Keywords: Circular Economy. Equipments. Local Recycling. Social Technology. Plastic.

Introduction

Pollution due to improper disposal of plastic threatens the planet's biodiversity. Plastic waste, when found in soils, rivers, and oceans, can cause degradation or destruction of natural habitats, impact the health of fauna and flora, alter air quality, and harm biodiversity in water and land systems [1]. Despite this, the production and consumption of plastic have been increasing systematically. Global production jumped from 2 Mt in 1950 to 380 Mt in 2015 [2] and continues to grow: the amount of plastic circulating is estimated to reach 417 Mt per year by 2030 [2].

One mechanism to mitigate the problem of plastic pollution is recycling [3], whether mechanical, chemical, or energy [3-5]. Mechanical recycling is the most common form of recycling as it is cheaper than the other two. Through it, it is possible to move from an economically linear to a circular consumption model. Typically, thermoplastic polymers such as Polypropylene (PP), Polyethylene (PE), Poly(ethylene terephthalate) (PET), and Polyvinylchloride (PVC) can be mechanically recycled [6,7].

Received on 9 December 2022; revised 15 February 2023.
Address for correspondence: Adriano Puglia Lima. Rua Xisto Bahia n 33 - Zipcode: 40221080 - Bairro: Engenho Velho da. E-mail: adriplebe@hotmail.com. DOI 10.34178/jbth.v6i1.275.

J Bioeng. Tech. Health 2023;6(1):28-33

Although mechanical recycling allows the plastic produced to remain in the economy for longer [7-9], the current recycling industry cannot prevent the problem of plastic pollution from spreading [10]. Today, the global average of recycling is less than 20%. The 4 countries that produce the most plastic waste in the world are the United States, China, India, and Brazil, with recycling rates of 34.60%, 21.92%, 5.73%, and 1.28%, respectively [10].

An alternative to the current model, based on large industrial plants, is the so-called Local Recycling. In it, discarded plastic is transformed into valuable objects in the disposal environment by ordinary people without technical training [11].

Implementing Local Recycling of plastic depends on the availability of technological solutions that can effectively be appropriated by ordinary people and applied on a large scale.

This work aims to present technology for local plastic recycling with a strong social bias. Equipment has been developed that transforms plastic waste into solid bars and plates. Equipment can be specified for recycling different types of thermoplastics. The current set was designed for recycling polypropylene as a first case study. These types of equipment are low-cost and can be operated by people without specialized training. Subsequently, plastic bars and plates are used in the production of furniture and other utilitarian and decorative objects.

The parts produced have applications such as furniture, and recycled materials are being thermally and mechanically characterized to compare their properties with materials commonly used to manufacture similar objects, such as wood and steel.

This technology is being applied in the field at the modular recycling unit in Pedra Furada – SE, where young people without technical training are producing objects of high commercial value. It is believed that this technology can not only contribute to the reduction of pollution caused by the accumulation of plastic, but it can also be a tool for reducing social inequalities linked to traditional recycling.

Materiald and Methods

Figure 1 presents the method used.

Project Requirements

The first step to define the project requirements was to hold meetings with representatives of non-governmental organizations (NGOs), associations, and cooperatives, aimed to establish the necessary prerequisites.

The criteria defined were:

1. Production of parts that could compose the objects instead of producing them in a single step, giving flexibility and versatility for production.
2. Easy-to-learn technology and low execution time. The equipment must be simple enough to dispense with any operating manual.
3. Easy maintenance of the equipment to avoid specialized personnel (repairments would have to be done locally).
4. The equipment must be of low cost so that the technology is scalable.
5. The equipment must be robust, as it would usually be placed in environments with dust and other harmful elements.

Selection and Preparation of Raw Material (Plastic Material)

The plastic material (polypropylene) was selected in an Association of Collectors and crushed in a commercial shredder, generating millimeter-sized residues.

Equipment Design and Operation

Two groups of equipment were developed for the production of bars and plates.

Design of Equipment for the Production of Bars

The equipment design was done in 3D modeling software (SolidWorks).

The bar equipment group is designed to produce bars of the approximately 1-meter length and different profiles. The equipment consists of: a stainless-steel heating chamber, surrounded by electrical resistance, a thermal shielding device (shield), and a pressure device (Figure 2a), which, when manually activated, compresses the molten plastic in the heating chamber, conforming it to the shape of the profile.

Design of Equipment for Plate Production

The group of equipment that produces the small and medium-sized circular and rectangular plates has a heating chamber formed by 2 commercial aluminum molds with Teflon coating and an

Figure 1. The flowchart used in the study.

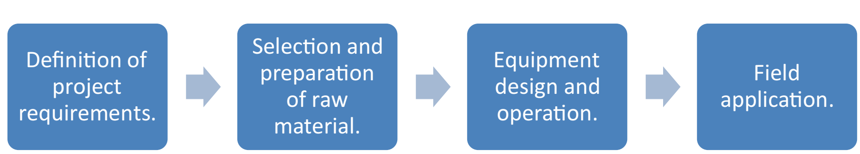

Figure 2. Three families of equipment for the local recycling of plastic. a) Equipment for the production of Bars. b) Equipment for the production of small plates. c) Equipment for the production of large plates.

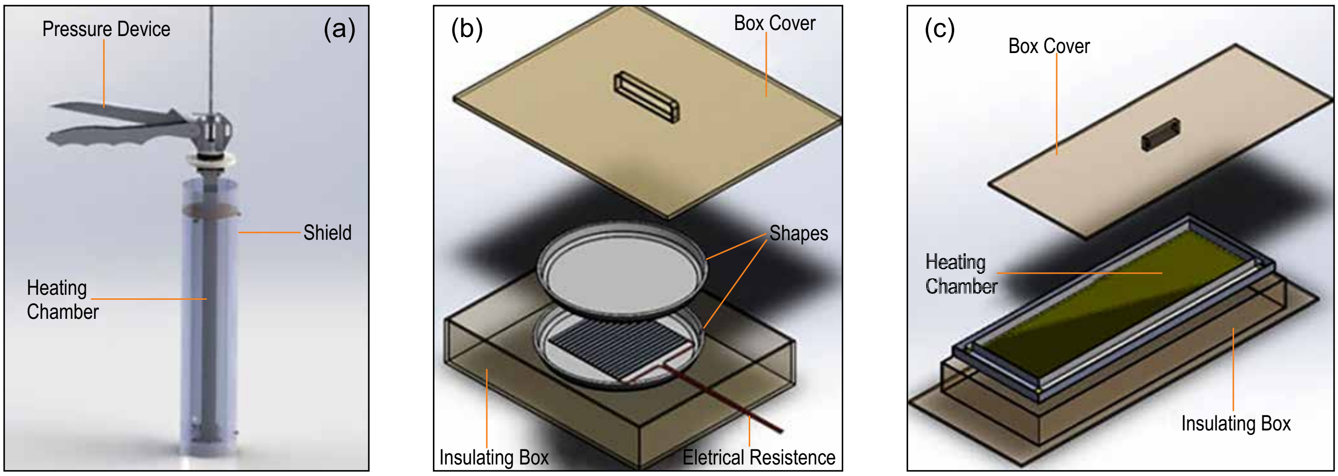

electrical heating resistance placed between them (Figure 2b). For large equipment, there is a tempered glass plate as a non-adherent surface in its heating chamber and an electrical resistance supported by a stainless-steel profile (Figure 2c). In all equipment of the two groups, there is a plywood box with an internal aluminum coating for thermal insulation. The resistance for all equipment was designed based on the thermal energy required for the fusion of the chosen plastic (PP).

Definition of Equipment Operating Parameters

By monitoring the melting temperature of the plastic material (PP) by two thermocouples coupled at the ends of the equipment, the time required for heating was defined. The manual pressure device used in bar equipment was defined by economic and ergonomic criteria and used to facilitate compressing the molten material. The compression time depends on the operator's strength of each piece of equipment.

The crushed plastic residue must be inserted on the surface of the heating chamber, varying the amount according to the desired plate thickness or profile type. The heating time and temperature were defined according to the properties of the chosen plastic material. In this case, polypropylene. Tests were performed to determine the best operating time and adjusted.

Field Application

The technology developed can be transferred to society by creating Modular Recycling Units (MRU). A complete MRU is a physical space composed of a place for storing and sorting plastic, an environment for washing and crushing plastic, a space for operating equipment and storing plates and bars, a place for producing furniture and value, and a space for administrative and commercial activities. MRUs can be created in partnership with associations and cooperatives of recycled material collectors, NGOs, municipalities, or even commercial companies.

In modular recycling units, people without technical training can be trained to operate the equipment and produce solid plastic bars and plates. Once this technology is mastered, these people will be trained to manufacture furniture and other valuables for future commercialization.

Results and Discusion

Equipment prototypes from different families were produced and tested in a laboratory environment. Modifications and improvements were carried out in dozens of development cycles using Computer Modeling and Digital Fabrication Techniques (3D Printing and Laser Cutting). In the end, equipment was produced that satisfied all project requirements. Nine pieces of equipment were produced to produce bars and plates of different shapes and sizes (Table 1).

For them to have a low manufacturing cost, materials, components, and devices available on the market in a standardized way were used for other purposes. Its estimated production cost ranges from US$140 to US$400 for plate production equipment and US$400 to US$500 for bar production equipment. The equipment has no monitoring and temperature control device, LCD panels, or adjustment buttons. They are as simple to operate as the most straightforward home appliances. Because they have few components, preventive maintenance can be carried out quickly in the working environment and with fewer tools.

Hundreds of polypropylene parts were produced in this equipment, with different shapes, dimensions, and colors (Figure 3). The pieces resemble wooden pieces, generally found in commerce, used to manufacture furniture and other objects.

Once the equipment was produced and tested, the field application stage began by implementing the first Modular Recycling Unit (MRU). This MRU is located in Pedra Furada, municipality of Santa Luzia do Itanhy, in Sergipe, Brazil. It was created with the support of the Institute for Research in Technology and Innovation (IPTI), a Social Organization that for 18 years has been developing Social Technologies to fight misery and poverty. Next, the nine pieces of equipment developed were installed at the MRU, which allows the recycling of one ton of plastic per month.

Ten young people from the village were trained to operate the equipment in this MRU. At the end of the 12-hour training, everyone could operate all the equipment, already producing usable parts (bars and plates). Two of the young women were hired by IPTI and were trained to manufacture high-added-value objects after producing dozens of bars and plates (Figure 4). As a result, their furniture begins to be commercialized, showing that the enterprise can reach its economic viability, generating decent work and income.

Table 1. Features and specifications of the equipment.

Equipment	Equipment Specifications				Produced Pieces Characteristics	
Bar Production	**Power (W)**	**Operating Time (minutes)**	**Energy (KWh)**	**Plastic Mass (g)**	**Cross Section (mm)**	**Length (m)**
Q4040	470	45	0,47	1500	40 x 40	~ 1
Q5050	620	90	0,93	2500	50 x 50	~ 1
C50	500	60	0,5	2000	50 (diameter)	~ 1
R7030	610	60	0,61	1600	70 x 30	~ 1
Plate Production	**Power (W)**	**Operating Time (minutes)**	**Energy (KWh**	**Plastic Mass (g)**	**Dimensions (mm)**	**Thickness (mm)**
D300	280	120	0.57	750	300 (diameter)	8 to 20
D350	360	120	0.72	1250	350 (diameter)	8 to 20
D500	640	120	1,28	2500	500 (diameter)	500 (diameter)
R400	420	105	0.74	1250	400 x 300	8 to 20
R1000	1500	120	3	2500	1000 x 300	8 to 30

Figure 3. Bars and plates are produced from shredded polypropylene.

Source: Authors.

Figure 4. Valued objects produced in TW.

Source: Authors.

Conclusion

This work presented a simple and effective technology for the local recycling of plastic, with a strong social bias. The equipment developed allows the production of massive plastic plates and bars from crushed polypropylene. Hundreds of pieces were produced in different formats, colors, and sizes. This equipment satisfied all previously established design requirements. Once the development phase was completed, the equipment was taken to the village of Pedra Furada, in Sergipe, where the first Modular Recycling Unit was installed, a space in which discarded plastic is transformed into objects of commercial value.

This small Modular Recycling Unit can recycle one ton of plastic per month. Young people without any technical training from the village of Pedra

Furada were trained in equipment operation and the production of furniture, utilitarian objects, and decoration. Pieces produced by these young people are starting to be commercialized, showing market potential for this type of product. It is believed that, by scaling this technology, it will be possible to contribute to reducing the impacts caused by inappropriate plastic disposal and, more importantly, to generate decent work and income for people without technical training, who are generally on the fringes of the job market.

References

1. Wit W et al. Solucionar a poluição plástica: transparência e responsabilização. Gland: WWF, 2019.
2. Geyer R, Jambeck JR, Law KL. Production, use, and fate of all plastics ever made. Science advances 2017;3(7):e1700782.
3. Schyns ZOG, Shaver MP. Mechanical recycling of packaging plastics: A review. Macromolecular Rapid Communications 2021;42(3):2000415.
4. Bucknall DG Plastics as a materials system in a circular economy. Philosophical Transactions of the Royal Society A, v. 378, n. 2176, p. 20190268, 2020.
5. Ignatyev IA, Thielemans W, Vander Beke B. Recycling of polymers: a review. ChemSusChem 2014;7(6):1579-1593.
6. Rudolph N, Kiesel R, Aumnate C. Understanding plastics recycling: Economic, ecological, and technical aspects of plastic waste handling. Carl Hanser Verlag GmbH Co KG, 2020.
7. Hahladakis JN, Iacovidou E, Gerassimidou S. Plastic waste in a circular economy. In: Plastic waste and recycling. Academic Press 2020:481-512.
8. Zhao X et al. Plastic waste upcycling toward a circular economy. Chemical Engineering Journal 2022;428:131928.
9. Letcher TM. (Ed.). Plastic waste and recycling: environmental impact, societal issues, prevention, and solutions. Academic Press, 2020.
10. Kaza S et al. What a waste 2.0: A global snapshot of solid waste management to 2050. World Bank Publications, 2018.
11. Joshi C, Seay J, Banadda N. A perspective on a locally managed decentralized circular economy for waste plastic in developing countries. Environmental Progress & Sustainable Energy 2019;38(1):3-11.

Mechanical Properties of PBAT/STARCH Films Submitted to Accelerated Weathering

Fernando de Alencar Silva Martinez[1*], Ana Paula Bispo Gonçalves[1], Michele Damiana Mota Martins[1], Paulo Romano Cruz Correia[1], Luciano Pisanu[1]
[1]SENAI CIMATEC University Center

In this study, extruded plastic films of PBAT mixed with starch in proportions of 0, 30, and 40% were submitted to the accelerated weathering procedure at 0, 360, and 720 hours under UV radiation. Mechanical properties such as tensile strength, elongation at break, and Young's modulus of PBAT films under tension were evaluated before and after the accelerated weathering. The results pointed to a significant increase in the deformation values of the films with the highest starch concentration and an increase in stiffness after the degradation process.
Keywords: Accelerated Weathering. PBAT. Starch. Ultraviolet Radiation.

Introduction

Considering the problems caused by the accumulation of waste, mainly of polymeric materials, materials with favorable decomposition properties are a promising alternative for reducing the negative impacts on the environment [1]. Notably, food packagings, such as plastic bags and films, are a significant fraction of the waste discarded in the environment [2]. PBAT, poly (butylene adipate co-terephthalate), is one of the materials used in plastic bags and films and can also be blended with thermoplastic starch. TPS is a thermoplastic starch obtained from renewable sources that can be used as a filler, along with additives, such as glycerol and citric acid, to reduce the cost of PBAT films and improve their biodegradability [3-5]. Some recent studies on PBAT have been showing promising results when it comes to mechanical and biodegradable properties. However, there are still very few analyses involving accelerated weathering by UV radiation, including blends of PBAT and starch.

The study and analysis of the behavior of these materials after their disposal in the open environment, under the action of the sun and rain, requires a long time to show the effects of degradation. Chambers with unique lamps that constantly emit UVA and UVB radiation can be used to accelerate this degradation process and simulate a scenario in which the material was exposed for an enormous amount of time. This process is known as accelerated weathering [6,7]. The study aims to analyze the mechanical properties of PBAT films (such as tensile strength, elongation at break, and Young's modulus), the effect of blending different proportions of starch with it and comprehending its behavior before and after the accelerated weathering procedure.

Materials and Methods

Materials

PBAT was supplied by BASF (ECOFLEX® F Blend C1200), and Podium Alimentos supplied the cassava starch. The glycerol used was from the Neon brand, and the citric acid was from the Synth brand.

Preparation of Films

The samples were obtained using a flat-die twin-screw extruder, Brand AX-Plásticos, Model DR1640. First, the formulations were extruded to form pellets, then extruded to generate the films. All PBAT pellets and the flat film formulations were processed at 88 RPM with temperature profile 80/9

Received on 26 November 2022; revised 18 February 2023.
Address for correspondence: Fernando de Alencar Silva Martinez. Avenida Orlando Gomes, 1845, Piatã. Zipcode: 57930-000. Salvador, Bahia, Brazil. E-mail: f.alencar.martinez@hotmail.com. DOI 10.34178/jbth.v6i1.276.

J Bioeng. Tech. Health 2023;6(1):34-37

0/110/120/130/130/130/120125°C. F1 (30% starch) had 8,55% glycerol and 0,45% citric acid, and F2 (40% starch) had 11.40% glycerol and 0.60% citric acid (Table 1).

Table 1. Formulations prepared for analysis.

Formulations	Composition
F0	PBAT
F1	70% PBAT + 30% STARCH
F2	60% PBAT + 40% STARCH

Accelerated Weathering

The accelerated weathering of the samples was carried out in a UV chamber for accelerated weathering tests, Model BASS UVV/2009, following the ASTM D 1435 standard for times of 360 and 720h (Table 2). In this process, the samples were only exposed to UV radiation, not containing moisture variation through the water spray. The process was defined after checking similar procedures [6-8].

Table 2. Accelerated weathering exposure time.

Reference	Exposure Time (h)
T0	0
T1	360
T2	720

TensileTest

The tensile test was performed on the samples with the Universal testing machine EMIC DL2000, according to the adapted ASTM D882 standard. (Test speed 25 mm/min, the distance between grips 100 mm, and sample width 25 mm. The software for data processing was TESC 2000. In the tensile test, eight specimens were tested, and five were selected for analysis of the results. The samples were removed longitudinally from the previously extruded film.

Results and Discussion

After performing the mechanical tests of the PBAT and PBAT/starch blends films, we compared the behavior of the formulations over the exposure time (Figure 1).

Figure 1A presents that F1 showed a drop in the tensile strength value with the addition of starch. According to Pellicano and colleagues [9], the addition of starch promotes the formation of a less resistant compound. Furthermore, according to the authors, the incorporation of starch reduces the mechanical properties caused by the matrix/filler interface with low compatibility and the non-occurrence of the wetting mechanism. In addition, starch acts as a stress concentrator, causing fissures and reducing tensile strength [5,9,10]. However, the 60/40 PBAT formulation showed higher tensile strength when compared to 70/30, where there may have been a better interaction between the carbonyl group of the matrix and the starch favored by the higher amount of glycerol added, about 25% more than the F1[10]. This behavior was also constant with the accelerated weathering time. After the degradation process, PBAT 60/40 samples did not lose their tensile strength, which did not occur with F0 and F1. F2, with higher starch content, appeared to be, visually, with a higher opacity. One hypothesis that could be brought up is that the whitish surface may have acted as a physical barrier to the transposition of UV light, which helped to preserve the tensile strength of the F2 samples throughout the exposure.

Figure 1B showed that the elongation at the broken property of the samples without weathering increased. This fact may probably be linked to the presence of glycerol, which was used as a plasticizer and may have interfered with the mobility of polymeric chains, causing in some cases the elongation at the break of the films to increase significantly, as shown in the work by Shanshan Lv and colleagues [10]. It can also be observed that at the time of 360h, the deformation of F2 decreased concerning time 0. It may have occurred because possibly the incidence of UV radiation

Figure 1. A.Tensile strength, B. Elongation at Break, C. Young's Modulus of PBAT formulations and their blends over exposure time.

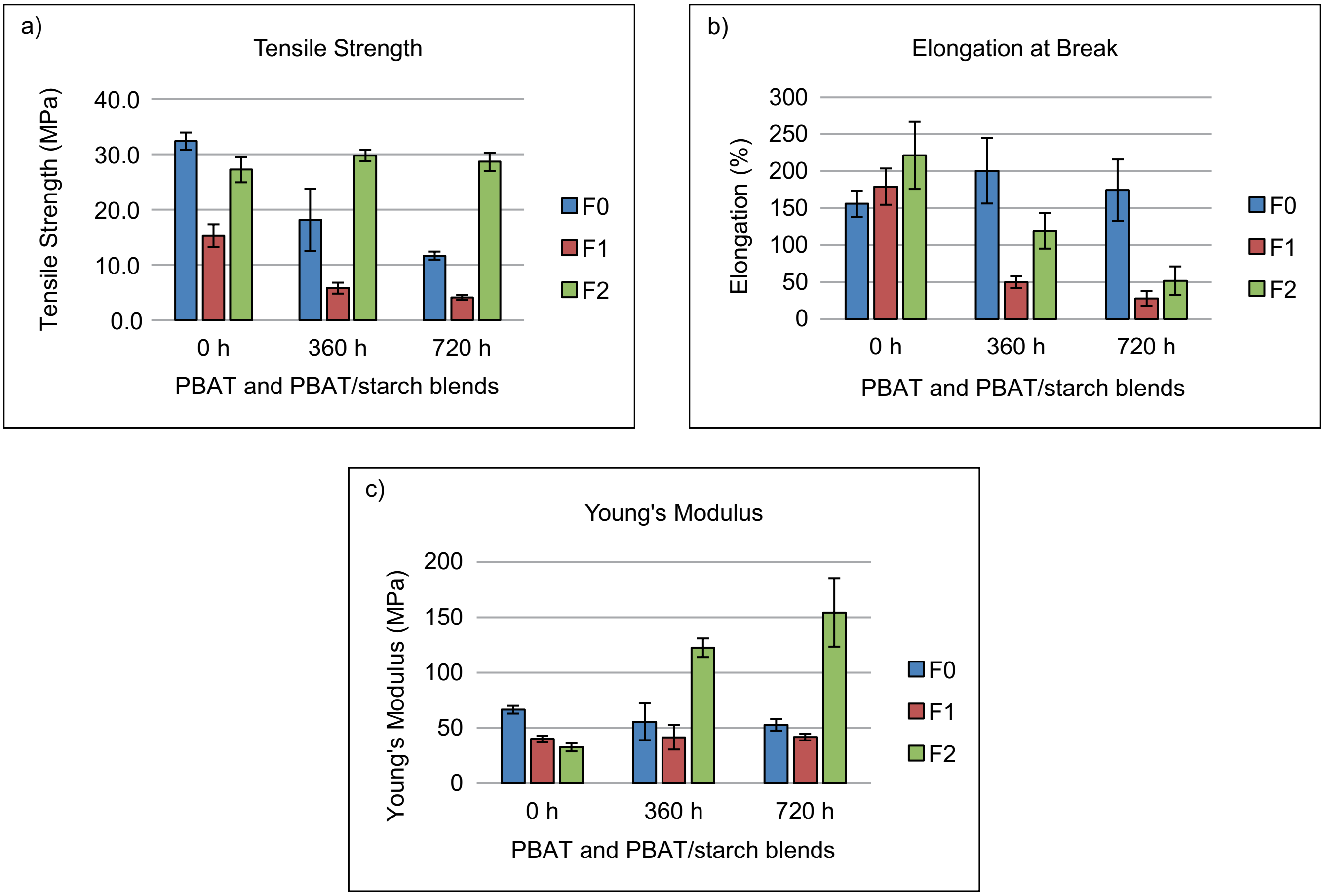

caused the glycerol to migrate to a more external region, weakening the plasticizing effect that it had previously caused, leading the PBAT films with starch to a decrease in ductility and consequently an increase in stiffness as verified in Young's modulus (Figure 1C). This behavior was also addressed in the literature by Shanshan Lv and colleagues [10]. In 720h of accelerated weathering, it is verified that the fragile behavior intensifies. The exposure may also have caused the formation of micro-fissures and reduced deformation.

In the unaged state, it is possible to observe that the material becomes more ductile with the addition of starch, in which Young's modulus decreases and the elongation at break increases. However, in the literature, it is possible to find many studies that point out that adding starch increases the stiffness of the blend since the starch has rigid characteristics, thus increasing Young's modulus of the studied samples [3,4,9,10].

Conclusion

From the results obtained, the presence of starch tends to decrease the tensile strength compared to pure PBAT. However, it is also possible to observe that the concentration with the highest presence of starch helped the films maintain their tensile strength during accelerated weathering. It was also evaluated that glycerol in the samples with starch may have increased deformation, acting as a plasticizer. However, after exposure to UV radiation, the elongation behavior at rupture was significantly altered, with the sample with higher starch content having a fragile behavior and not deforming as before due to the possible migration of glycerol to outer layers in the films.

References

1. Müller J, González-Martínez C, Chiralt A. Combination of poly(lactic) acid and starch for biodegradable food packaging. Materials. [S.l.]: MDPI AG., August 2017.
2. Djukic-Vukovic A et al. Towards sustainability of lactic acid and poly-lactic acid polymers production. Renewable and Sustainable Energy Reviews 2019;108:238–252.
3. Nayak SK. Biodegradable PBAT/Starch nanocomposites. Polymer - Plastics Technology and Engineering 2010;49(14):1406–1418.
4. González Seligra P et al. Influence of incorporation of starch nanoparticles in PBAT/TPS composite films. Polymer International 2016;65(8):938–945.
5. Ferreira FV et al. An overview on properties and applications of poly(butylene adipate-co-terephthalate)–PBAT based composites. Polymer Engineering and Science 2019;59,(2):E7–E15.
6. González-López ME et al. Accelerated weathering of poly(lactic acid) and its biocomposites: A review. Polymer Degradation and Stability. [S.l.]: Elsevier Ltd., Set 2020.
7. Copinet A et al. Effects of ultraviolet light (315 nm), temperature and relative humidity on the degradation of polylactic acid plastic films. Chemosphere 2004;55(5):763–773.
8. Coelho FA et al. Engenharia Moderna: Soluções para Problemas da Sociedade e da Indústria. Ponta Grossa - Paraná - Brasil: Atena, 2020. Doi 10.22533/at.ed.467202809. Available at: <https://www.researchgate.net/publication/344658356_AVALIACAO_DA_BIODEGRADACAO_E_ENVELHECIMENTO_ACELERADO_POR_RADIACAO_ULTRAVIOLETA_NA_BLENDA_PBATTPS>. Accessed on Jun 22, 2022.
9. Pellicano M, Pachekoski W, Agnelli JAM. Influência da Adição de Amido de Mandioca na Biodegradação da Blenda Polimérica PHBV/Ecoflex®. Polímeros: Ciência e Tecnologia 2009;19(3):212-217.
10. Amass W et al. Starch based biodegradable PBAT nanocomposites: Effect of starch morphological thermal morphological and biodegradability behavior. Journal of Polymers and the Environment 2016;19(1):736–745.
11. Shanshan LV et al. Effect of glycerol introduced into PLA based composites on the UV weathering behavior. Construction and Building Materials 2017;144:525–531.

Life Cycle Assessment of Linear Alkylbenzene Sulfonate Production: An Adaptation to the Brazilian Context

Óliver Silva Costa Barreto[1*], Jony Cley Rodrigues da Silva Cruz[2], Diego Lima Medeiros[3], Edna dos Santos Almeida[1]
[1]PPG-GETEC, SENAI CIMATEC, Salvador; [2]State University of Feira de Santana (UEFS), Feira de Santana; [3]Federal University of Bahia (UFBA), Salvador; Bahia, Brazil

Surfactants represent a class of compounds used in large-scale household sanitizers, the Linear Alkylbenzene Sulfonate being the most used. However, there is concern about these compounds' environmental aspects and impacts. This work aims to analyze the life cycle inventory of the production of Linear Alkylbenzene Sulfonate from cradle to gate for the Brazilian context aiming to propose improvements regarding cumulative energy demand and global warming potential. The total energy demand of the base case scenario was 59 MJ-Eq and a carbon footprint of 1.71 kg $CO_{2\text{-eq}}$. A scenario considering the switch in heat and electricity supply to renewable sources was proposed, and a global reduction of Global Warming Potential in 100 years of 15.73% was realized, reducing the carbon footprint of the heat supply chain by 73.07% and the electricity supply chain by 98.90%.
Keywords: Linear Alkylbenzene Sulfonate (LAS). Surfactants. OpenLCA. Life Cycle Assessment (LCA). Material Flow Analysis (MFA).

Introduction

Surfactants, or surfactant agents, are chemical compounds widely employed in a solid and liquid state for washing clothes and dishes, mainly for domestic uses but also in several industrial sectors [1]. These compounds represent a class of chemical substances with an affinity for polar or apolar substances. This characteristic is known as amphiphilic and amphipathic, which comes from its molecular structure. Therefore, part of a single surfactant molecule can interact with water, and the other part has a greater tendency to interact with oily substances, for example [2]. This property is responsible for its use in the production of detergents and hygiene products around the world. However, most commercially available compounds are produced from petroleum derivatives [3].

Linear Alkylbenzene Sulfonate, known as LAS (Figure 1), is one of the most widely used surfactants worldwide in the formulation of commercial detergents, the same in 2018 accounted for 84% of the anionic surfactant market [4,5], as it has an excellent acceptance in the market due to its high cleaning potential when compared to that of ordinary soap, the surfactant sodium lauryl ether sulfate (LESS) [6].

Even though it is widely used, this substance, like many others produced by human activities, has a production chain that implies the use of a series of processes involving extraction, manufacturing, and transportation. These processes, when operated, generate impacts on planetary systems, either by releasing carbon dioxide, consuming water, or generating chemical waste.

Figure 1. General chemical structure of Linear Alkylbenzene Sulfonate (LAS).

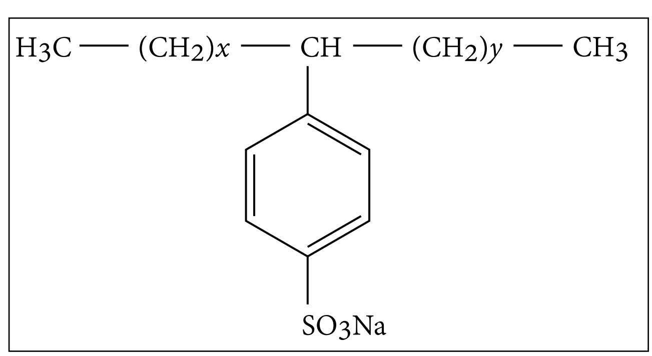

Source: Sablayrolles and colleagues (2209) [8].

Received on 22 November 2022; revised 6 February 2023.
Address for correspondence: Óliver Silva Costa Barreto. Avenida Orlando Gomes, Piatã, Salvador, Bahia, Brazil. Zipcode: 41650-010. E-mail: oliversc.barreto@gmail.com.
DOI 10.34178/jbth.v6i1.277.

J Bioeng. Tech. Health 2023;6(1):38-44

The environmental performance of a product or process throughout its life cycle can be assessed through LCA (Life Cycle Assessment), which consists of analyzing the environmental aspects of a product system in order to understand the impacts generated. The LCA study can use software to support the assessment of impacts [7]. For example, Stan allows the creation of material and energy flow diagrams. In contrast, OpenLCA allows the quantification of aspects and impacts throughout the life cycle in different energy and environmental categories.

In this context, this work aims to perform a life cycle assessment of the production of Linear Alkylbenzene Sulfonate (LAS) from cradle to gate for the Brazilian context to quantify the accumulated energy demand in order to identify opportunities for improving energy and environmental performance.

Materials and Methods

Figure 2 shows the product system considered in this study. Typical production of linear alkylbenzene sulfonate (LAS) is from the sulfonation of linear alkylbenzene (LAB) and neutralization with sodium hydroxide. LAB, in turn, is produced from the alkylation reaction of benzene with mono olefins (obtained from paraffin dehydrogenation) in the presence of the catalysts

Figure 2. Product system of linear alkylbenzene sulfonate production.

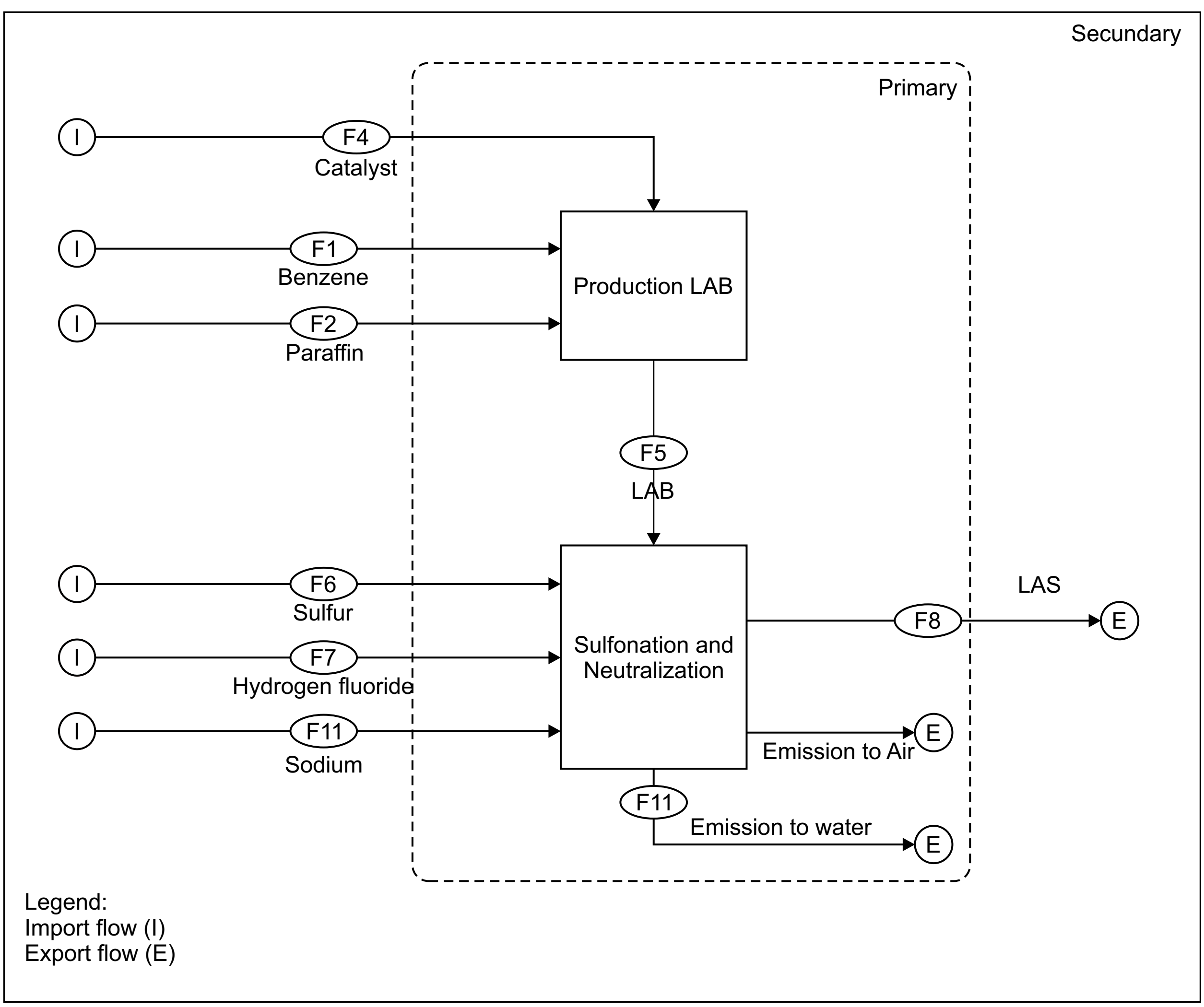

aluminum chloride (AlCl3) and hydrofluoric acid (HF) [9,10]. The use of inputs, materials, and energy and the generation of emissions were considered; however, water consumption was not included in the mass balance (Figure 1) performed in the Stan v.2.6 software.

The attributional Life Cycle Assessment (LCA) was performed based on ISO 14040 and ISO 14044 [11,12]. The function of the production system was to produce linear alkyl benzene sulfonate, and the Functional Unit (FU) reference flow used was 1.0 kg of LAS produced. The extent of the production system was from cradle to gate of the LAS plant.

The product system was modeled using OpenLCA 1.10.3 software with the Ecoinvent v3.4 database, contained in ecoinv*ent_case_studies_Ceramic_cup_vs_Paper_cup*. From the LAS production inventory (alkylbenzene sulfonate production, linear, petrochemical | alkylbenzene sulfonate, linear, petrochemical | Cutoff, U - RoW) existing in the Ecoinvent v3.4 (cutoff) inventory base.

The data from the foreground process, consisting of LAB and LAS production (Figure 2), were adapted (Figure 3), while those from the suppliers of the background processes were kept the same.

The categories evaluated in this study were Cumulative Energy Demand (CED) from the "Cumulative Energy Demand“ method, given in MJ equivalent, and Global Warming Potential (GWP) from the IPCC 2013 100a v1.03 method, which quantifies the contribution of CO_2 equivalent to global warming potential.

Figure 3 presents the input flow of the foreground inventory for the production of 1 kg of LAS obtained in OpenLCA. Adjustments were made to the heat and power supply of the foreground inventory. The electricity supply (*market group for electricity, medium voltage | electricity, medium voltage | Cutoff, U*) has been changed from RER (European data) to BR (Brazilian data), and the two heat suppliers (*market group for heat, district or industrial, natural gas | heat, district or industrial, natural gas | Cutoff*; and *market group for heat, district or industrial, other than natural gas | heat, district or industrial, other than natural gas | Cutoff, U*) have been changed from RER to GLO (global data).

Figure 4 presents the foreground inventory outputs of the LAS production corresponding to the product and emissions to air and water.

A sensitivity analysis was performed to investigate the effect of replacing the heat and electricity from non-renewable sources (fossil) with renewable sources (wood burning and low voltage photovoltaic panels) for LAS production in the evaluated category. As a result, the heat suppliers presented in Figure 3 were replaced by renewable sources (heat production, wood chips from industry, at furnace 5000kW | heat, district or industrial, other than natural gas | Cutoff, U) from the RoW region (rest of the world data) and electricity supply for also (*the market for electricity, low voltage, label-certified | electricity, low voltage, label-certified | Cutoff, S*) from the Swiss region.

Figure 3. Flow of the foreground inventory input for producing 1kg of Linear Alkylbenzene Sulfonate.

Entradas

<table>
<tr><th>Fluxo</th><th>Quantidade</th><th>Unidade</th><th>Provedor padrão</th><th>Entrada de qual...</th></tr>
<tr><td>chemical factory, organics</td><td>4.00000E-10</td><td>Item(s)</td><td>P market for chemical factory, organics | chemical factory, organics | Cutoff, U - GLO</td><td>(2; 3; 5; 2; 3)</td></tr>
<tr><td>aluminium, cast alloy</td><td>0.00320</td><td>kg</td><td>P market for aluminium, cast alloy | aluminium, cast alloy | Cutoff, U - GLO</td><td>(2; 3; 5; 2; 1)</td></tr>
<tr><td>aluminium, wrought alloy</td><td>0.00680</td><td>kg</td><td>P market for aluminium, wrought alloy | aluminium, wrought alloy | Cutoff, U - GLO</td><td>(2; 3; 5; 2; 1)</td></tr>
<tr><td>benzene</td><td>0.25100</td><td>kg</td><td>P market for benzene | benzene | Cutoff, U - GLO</td><td>(2; 3; 5; 2; 1)</td></tr>
<tr><td>electricity, medium voltage</td><td>0.03054</td><td>kWh</td><td>P market for electricity, medium voltage | electricity, medium voltage | Cutoff, U - BR</td><td>(2; 3; 5; 2; 1)</td></tr>
<tr><td>heat, district or industrial, natur...</td><td>2.87280</td><td>MJ</td><td>P market group for heat, district or industrial, natural gas | heat, district or industrial, natural gas | Cutoff, ...</td><td>(2; 3; 5; 2; 1)</td></tr>
<tr><td>heat, district or industrial, other...</td><td>1.60348</td><td>MJ</td><td>P market group for heat, district or industrial, other than natural gas | heat, district or industrial, other tha...</td><td>(2; 3; 5; 2; 1)</td></tr>
<tr><td>hydrogen fluoride</td><td>0.01000</td><td>kg</td><td>P market for hydrogen fluoride | hydrogen fluoride | Cutoff, U - GLO</td><td>(2; 3; 5; 2; 1)</td></tr>
<tr><td>paraffin</td><td>0.51600</td><td>kg</td><td>P market for paraffin | paraffin | Cutoff, U - GLO</td><td>(2; 3; 5; 2; 1)</td></tr>
<tr><td>sodium hydroxide, without wat...</td><td>0.12700</td><td>kg</td><td>P market for sodium hydroxide, without water, in 50% solution state | sodium hydroxide, without water, i...</td><td>(2; 3; 5; 2; 1)</td></tr>
<tr><td>sulfur</td><td>0.10000</td><td>kg</td><td>P market for sulfur | sulfur | Cutoff, U - GLO</td><td>(2; 3; 5; 2; 1)</td></tr>
</table>

Figure 4. Flow of the foreground inventory output of 1kg production of Linear Alkylbenzene Sulfonate .

Saídas

Fluxo	Categoria	Quantida...	Unid...	Custos / re...	Entrada de ...	Descrição
alkylbenzene sulfonate, linear...	**202:Manufacture of other chemical prod...**	**1.00000**	**kg**	**0.80500 E...**		**Linear alkylbenzene sulfonate (LAS) from b...**
Aluminium	Emission to water/surface water	1.06000E-6	kg		(2; 3; 5; 2; 1)	Literature Value. Process-related emissions ha...
Ammonium, ion	Emission to water/surface water	1.59000E-5	kg		(2; 3; 5; 2; 1)	Literature Value. Process-related emissions ha...
BOD5, Biological Oxygen Dema...	Emission to water/unspecified	1.72550E-6	kg		(4; 5; 5; 5; 5)	Calculated value. The BOD, COD, TOC and BO...
Carbon dioxide, fossil	Emission to air/high population density	0.00907	kg		(2; 3; 5; 2; 1)	Literature Value. Process-related emissions ha...
Carbon monoxide, fossil	Emission to air/high population density	4.31000E-6	kg		(2; 3; 5; 2; 1)	Literature Value. Process-related emissions ha...
Chloride	Emission to water/surface water	0.00132	kg		(2; 3; 5; 2; 1)	Literature Value. Process-related emissions ha...
Chlorine	Emission to air/high population density	7.80000E-8	kg		(2; 3; 5; 2; 1)	Literature Value. Process-related emissions ha...
Chromium, ion	Emission to water/surface water	4.28000E-6	kg		(2; 3; 5; 2; 1)	Literature Value. Process-related emissions ha...
COD, Chemical Oxygen Demand	Emission to water/unspecified	1.72550E-6	kg		(4; 5; 5; 5; 5)	Calculated value. The BOD, COD, TOC and BO...
Dissolved solids	Emission to water/surface water	0.00278	kg		(2; 3; 5; 2; 1)	Literature Value. Process-related emissions ha...
DOC, Dissolved Organic Carbon	Emission to water/unspecified	5.18273E-7	kg		(4; 5; 5; 5; 5)	Calculated value. The BOD, COD, TOC and BO...
Fluoride	Emission to water/surface water	7.58000E-6	kg		(2; 3; 5; 2; 1)	Literature Value. Process-related emissions ha...
Hydrocarbons, aliphatic, alkane...	Emission to air/high population density	0.00023	kg		(2; 3; 5; 2; 1)	Literature Value. Process-related emissions ha...
Hydrocarbons, unspecified	Emission to water/surface water	1.49000E-7	kg		(2; 3; 5; 2; 1)	Literature Value. Process-related emissions ha...
Iron, ion	Emission to water/surface water	2.40000E-6	kg		(2; 3; 5; 2; 1)	Literature Value. Process-related emissions ha...
Lead	Emission to water/surface water	1.30000E-8	kg		(2; 3; 5; 2; 1)	Literature Value. Process-related emissions ha...
Mercury	Emission to air/high population density	3.20000E-7	kg		(2; 3; 5; 2; 1)	Literature Value. Process-related emissions ha...
Mercury	Emission to water/surface water	3.00000E-8	kg		(2; 3; 5; 2; 1)	Literature Value. Process-related emissions ha...
Nickel, ion	Emission to water/surface water	2.08000E-6	kg		(2; 3; 5; 2; 1)	Literature Value. Process-related emissions ha...
Nitrogen oxides	Emission to air/high population density	0.00010	kg		(2; 3; 5; 2; 1)	Literature Value. Process-related emissions ha...
Particulates, > 10 um	Emission to air/high population density	1.64000E-5	kg		(2; 3; 5; 2; 1)	Literature Value. Process-related emissions ha...
Phenol	Emission to water/surface water	5.22000E-7	kg		(2; 3; 5; 2; 1)	Literature Value. Process-related emissions ha...
Phosphate	Emission to water/surface water	9.81000E-7	kg		(2; 3; 5; 2; 1)	Literature Value. Process-related emissions ha...
Sulfate	Emission to water/surface water	6.68000E-5	kg		(2; 3; 5; 2; 1)	Literature Value. Process-related emissions ha...
Sulfide	Emission to water/surface water	0.00011	kg		(2; 3; 5; 2; 1)	Literature Value. Process-related emissions ha...
Sulfur dioxide	Emission to air/high population density	0.00029	kg		(2; 3; 5; 2; 1)	Literature Value. Process-related emissions ha...
Suspended solids, unspecified	Emission to water/surface water	0.00024	kg		(2; 3; 5; 2; 1)	Literature Value. Process-related emissions ha...
TOC, Total Organic Carbon	Emission to water/unspecified	5.18273E-7	kg		(4; 5; 5; 5; 5)	Calculated value. The BOD, COD, TOC and BO...
Zinc, ion	Emission to water/surface water	7.70000E-7	kg		(2; 3; 5; 2; 1)	Literature Value. Process-related emissions ha...

Results and Discussion

Figure 5 presents the Material Flow Analysis for the production of LAS. Again, most of the input is derived from the petroleum products production chain, with the input with the highest mass contribution being paraffin.

Figure 6 shows the energy demand intensity of the different inputs to the product system by energy source. The total energy demand was 59 MJ-Eq, and, notably, the most significant demand is for fossil source energy, and the largest demanders of this energy are the paraffin (28.1 MJ-Eq), and benzene (18.4 MJ-Eq) supply chains, followed by the sulfur (3.0 MJ-Eq) and heat (4.0 MJ-Eq) supply chains.

Changes in the energy supply were suggested; the change of the source of heat and electricity is a feasible strategy for the production of LAS more sustainably (Figure 6) since energy is understood as a transforming resource and, therefore, the source of this energy does not affect the technology of the production process of LAS, in the figure mentioned are shown the energy sources that had higher energy consumption considering the base scenario and the proposed scenario.

We showed that the total CO_2 equivalent was 1.71 kg (Figure 7). The most significant $CO_{2\text{-eq}}$ emissions come from the petroleum chain (benzene and paraffin), which represent 0.92 kg. It can also be noted that the sum of the heat supply chains is 0.34 kg $CO_{2\text{-eq}}$. The sodium hydroxide and aluminum forging supply chains also present significant values.

In the proposed scenario (Figure 7), even with the total increase in energy demand for the system, there were reductions in GWP100a impacts in both the electricity and heat supply chains. The total contribution of the 100-year Global Warming Potential to this scenario was approximately 1.44 kg $CO_{2\text{-eq}}$, which represents a reduction of 15.73%.

Figure 5. Mass Balance of 1kg Linear Alkylbenzene Sulfonate Production with reconciled data.

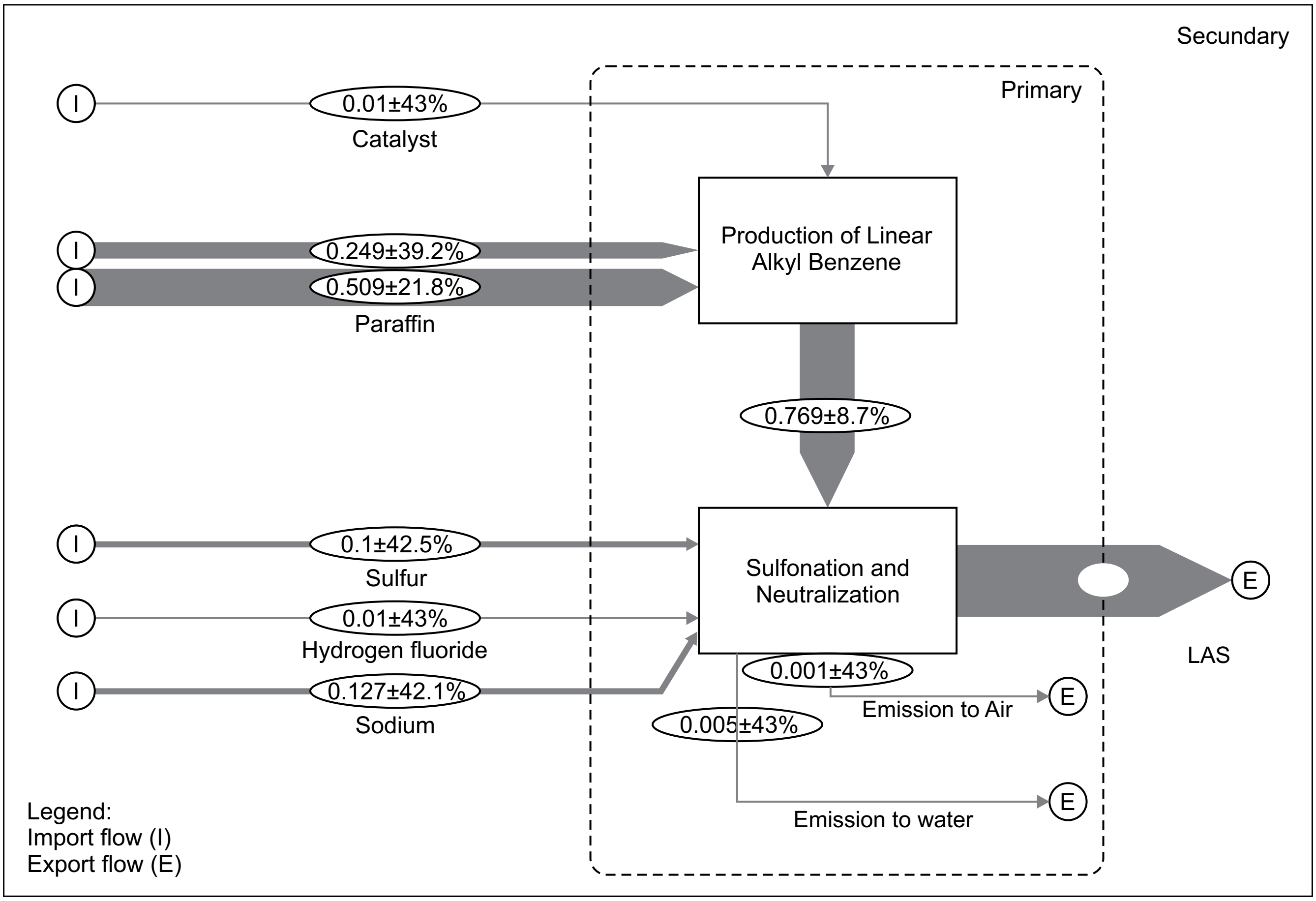

Figure 6. Cumulative Energy Demand for 1 kg of Linear Alkylbenzene production in the baseline scenario and the proposed scenario with renewable heat and electricity sources.

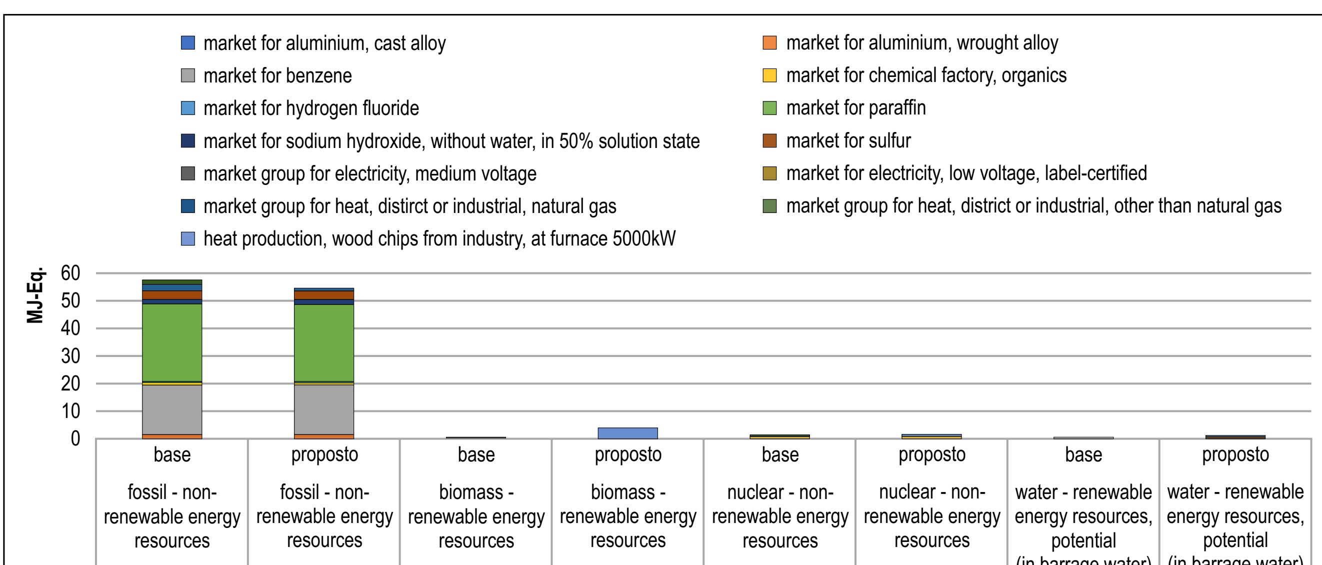

Figure 7. Impact of Global Warming Potential over a 100-year horizon for production of 1 kg of Linear Alkylbenzene with renewable heat and electricity sources.

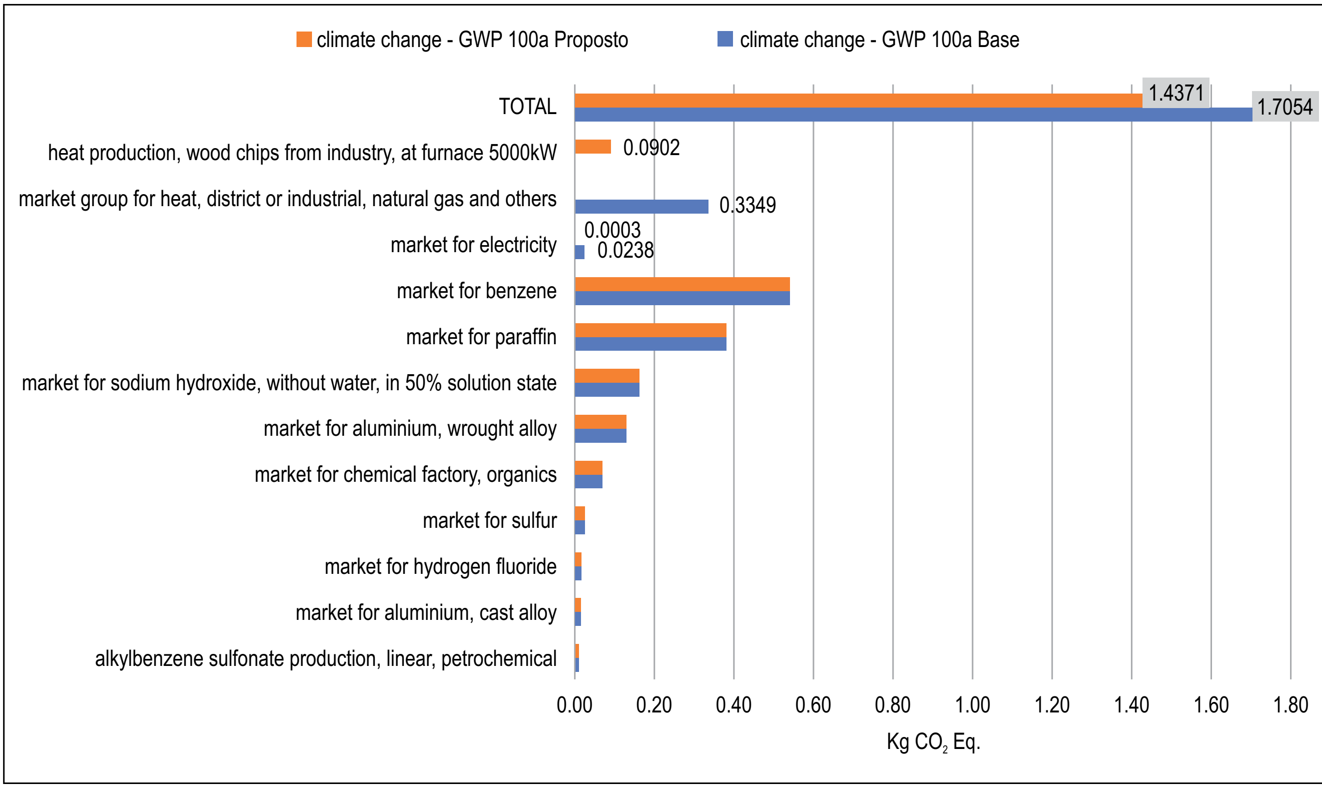

The sum of the heat sources used for the reference flow (Figure 7) is 0.09 kg $CO_{2\text{-eq}}$, reducing 0.24 kg or 73.07% from the previous scenario concerning heat supply. On the other hand, electricity supply represented a reduction of 0.02 kg or 98.90% $CO_{2\text{-eq}}$ in 100 years.

Conclusion

A life cycle assessment of the production of Linear Alkylbenzene Sulfonate from cradle to the gate was performed. It was observed that the production of paraffin and benzene inputs are the most significant contributors to the accumulated energy demand.

As a proposal for reducing the accumulated energy demand without affecting the production technology of LAS, a sensitivity analysis was considered to affect the exchange in the supply of heat and electricity, replacing them with renewable sources, the heat supply was by burning biomass in boilers and the electricity supply with the use of low voltage photovoltaic plates certified by the distribution network by overhead line cables (CH), being observed a reduction of fossil energy sources. As a proposal to reduce the environmental impacts without affecting the LAS production technology, it was considered the exchange in the supply of heat and electricity to the system, replacing them with renewable sources, The heat supply was given by burning biomass in boilers, and the electricity supply with the use of low voltage photovoltaic panels and it was possible to observe a reduction of fossil energy sources in detriment of the use of biomass for energy generation and overall reduction of Global Warming Potential (GWP) in 100 years of 15.73%, reducing the heat supply chain by 73.07% and the electricity supply chain by 98.90%.

Acknowledgments

We thank FAPESB for the grant (No. BOL0409/2021) of application No. 565/2021.

References

1. Mousavi SA, Khodadoost F. Effects of detergents on natural ecosystems and wastewater treatment processes: a review. Environmental Science Pollution Research 2019;26:26439–26448.
2. Celis MT. Emulsiones, surfactantes y polímeros: algunas implicaciones para la ciencia, la tecnología y los negócios. Revista Visión Gerencial 2020;2.
3. Suresh A, Abraham J. An Overview on the microbial degradation of Linear Alkylbenzene Sulfonate (LAS) durfactants. Phyto and Rhizo Remediation 2019:301313.
4. Villabona-Ortíz A, Tejada-Tovar C, De-La-Rosa JL.Evaluation of parameters in the removal of linear alkylbenzene sulfonate anionic surfactant using electrocoagulation. Revista Facultad de Ingeniería 2021;30(55):11570.
5. Jones-Costa M et al. Cardiac biomarkers as sensitive tools to evaluate the impact of xenobiotics on amphibians: the effects of anionic surfactant linear alkylbenzene sulfonate (LAS). Ecotoxicology and Environmental Safety 2018;151:184-190.
6. Menezes SP et al. Degradação do linear alquilbenzeno sulfonado (LAS) em reator batelada sulfetogênico e metanogênico. Uberlândia, Universidade Federal de Uberlândia: Trabalho de Conclusão de Curso do Curso de Graduação em Engenharia Ambiental, 2018.
7. Campolina JM, Sigrist CSL, Moris VAS. Uma revisão de literatura sobre softwares utilizados em estudos de Avaliação do Ciclo de Vida. Revista Eletrônica em Gestão, Educação e Tecnologia Ambiental, Santa Maria, 2015;19(2):735-750.
8. Sablayrolles C et al. Trace determination of linear alkylbenzene sulfonates: Application in artificially polluted soil—Carrots system. International Journal of Analytical Chemistry 2009.
9. Zah R et al. Life cycle assessment of energy products: environmental impact assessment of biofuels. Technical Report 2007.
10. ECOINVENT. ECOINVENT 3.4 Dataset Documentation 2021.
11. ABNT. NBR ISO 14040: Gestão ambiental – Avaliação do Ciclo de Vida – Princípios e Estrutura. Rio de Janeiro. 2009.
12. ABNT. NBR ISO 14044: Gestão ambiental – Avaliação do Ciclo de Vida – Requisitos e Orientações. 2006b.

Copernicus Program: Artificial Intelligence in Cultural Heritage

Janaina Cardoso de Mello[1*]
[1]Federal University of Sergipe; [2]Department of History, Education and Human Sciences Center, (LADOC - UFS/CNPq); Aracaju, Sergipe, Brazil

This work presents satellite remote sensing research to map data to archaeological sites at risk in regions of war conflicts, supporting the Copernicus Program and the application of Artificial Intelligence to analyze the collected information. It seeks to identify the process of using digital tools to safeguard cultural heritage in the 21st century. The qualitative, exploratory, and explanatory methodology followed the bibliographic survey, as well as the handling of the Copernicus Platform for the analysis of prototyping. The analysis of case studies of Cyprus, Pakistan, and Syria establishes a digital timeline containing the impacts of deterioration of the areas for the proposition of conservation, protection, and restoration measures.
Keywords: Remote Sensing. Satellite. Artificial Intelligence. Cultural Heritage. Safeguard.

Introduction

Created for the collection and sharing of satellite and in-situ data, the Copernicus Program has favored observing the physical conditions of planet Earth. Developed within the scope of the European Union and collaborative partnerships with some Latin American countries such as Brazil, Chile, and Colombia. An agenda of satellite missions, called Sentinel, coordinated by the European Space Agency (ESA), the European Organization for the Exploitation of Meteorological Satellites (EUMETSAT), the European Centre for Medium-Range Weather Forecasts (ECMWF), EU Agencies and Mercator Ocean, focuses on an aspect of observation of the Earth, atmosphere, oceans, and land cover. The images generate data for weather forecasts, land use and land cover, coastal areas, and oceans, monitoring the atmosphere. Environmental issues receive special attention in providing information on air quality, carbon emissions, and the state of the ozone layer [1].

Received on 20 December 2022; revised 18 February 2023.
Address for correspondence: Janaina Cardoso de Mello. Av. Gonçalo Rollemberg Leite, 2143/601, Ed. Itatiaia, Aracaju - Sergipe, SE- Brazil. Zipcode: 49045-280. E-mail: janainamello.ufs@gmail.com. DOI 10.34178/jbth.v6i1.278.

J Bioeng. Tech. Health 2023;6(1):45-51

The advances in artificial intelligence (AI) made possible the consolidation of the Copernicus Program since it integrates the definition of a system's ability to interpret external data correctly, to learn from such data, and to use those learnings to achieve specific goals and tasks through flexible adaptation [2]. Recent AI successes attributed to new ML techniques include building models in their internal representations. They are support vector machines (SVMs), random forests, probabilistic graphical models, reinforcement learning (RL), and deep learning neural networks (DL) [3].

Integrated with IT research and application in identifying, cataloging, and preserving cultural heritage, AI data from the Copernicus program seeks to detect archaeological objects with images obtained by satellites equipped with AI – capable of recognizing even very subtle variations in vegetation. Due to the intensity of the flow and a large amount of information and images, AI can help reduce manual work and optimize the delivery of more accurate analysis. The initiative came from the Italian Institute of Technology (IIT) in partnership with the European Space Agency (ESA) in the creation of the Cultural Landscapes Scanner (CLS) project, allowing for a broader reading of the soil and more accurate results with the help of Artificial Intelligence. The project was led by Arianna Traviglia, coordinator of the Cultural Heritage Technology Center (CCHT) of the IIT in Venice, whose research area is dedicated to technological mediation in the studies and management of cultural heritage [4].

As a general objective, it seeks to analyze the cultural heritage protection processes provided using digital technologies with satellite images. The specifics objectives of the study are:

1. To Publicize the application of digital technology resources in mapping, data collection, analysis, and protection of cultural heritage;
2. To present the potential of using the Copernicus Platform and the derived projects for applying AI in the analysis of data and images of archaeological sites;
3. To demonstrate how land surface data collected by satellite can help preserve archaeological heritage from the effects of climate degradation.

The hypothesis of the study comprises:

1. In emerging economy countries, there is still a significant lack of knowledge about the application of digital technologies in safeguarding cultural heritage;
2. There is no significant difference between prospective teachers in their awareness of healthy dietary habits concerning the following background variables;
3. Greater dissemination of the Copernicus Platform can build digital skills for future generations of archaeologists from different geographies aimed at preserving sites, avoiding the high cost of invasive prospecting;
4. Monitoring environmental impacts such as global warming provide more data requiring human and digital cognition in decision-making.

Significance of the Study

Studies of cultural heritage in the 21st century have demanded the use of digital technologies capable of aggregating information to analog procedures previously used, discovering new perspectives previously thought of, with high potential for information analysis, storage, and sharing with researchers from different geographies. Essential knowledge of ancestral civilizations comes from forgotten topographies, hidden by dense vegetation or submerged in fresh or saltwater flows (rivers, lakes, and seas) formed from melting or changing paths. These spaces, seen with the naked eye by researchers, do not show the social uses of the past, the buried artifacts, and the composition of the cultural landscape itself. The digital elevation model (DEM) is most frequently generated from airborne sensors, drones, terrestrial laser scanners, and satellite remote sensing (with an overview of the semantic categorization of potentials and practicality of such platforms for elevation data acquisition) [5]. With unprecedented data acquired continuously, the Copernicus satellite constellations provide essential information for analyzing and monitoring the Earth's surface and atmosphere [6].

The use of Copernicus data combined with AI in guaranteeing the analysis of a more significant amount of data in less time demonstrates the possibility of making the management of archaeological and cultural heritage in several countries more efficient. Studies that favor disseminating AI and remote sensing via satellite in the treatment of cultural heritage are essential to reinforce the continuity of funding and international cooperation, inspiring new research and researchers, especially in developing countries.

Review of Related Studies

Studies reveal that the use of Machine Learning (ML) techniques within Cultural Heritage (CH) is still limited [7]. As state-of-the-art techniques become popular in other fields such as CH, it is intuitive that more classical classification and regression techniques, such as Linear and Logistic regression, have a distinct and valuable application within CH. While these can be applied in conservation efforts, such as historical building integrity prediction, for example, the application of

Support Vector Machines (SVM) refined the hyper-parameter estimation to support multiple instances of learning for recognizing iconographic elements in artworks. With increasing efforts to digitize CH assets, the progression to Deep Learning models is natural, where modern data-trained models are fine-tuned to CH data.

Borie and colleagues [8] show that remote sensing archaeology in recent years has emphasized using high-precision and high-accuracy tools to achieve the detailed documentation of archaeological elements. The researchers claim that satellite remote sensing has also benefited from increased spatial and spectral resolution of the sensors, enabling the discovery and documentation of new archaeological features and sites worldwide. Thus, they studied a vast area of the Atacama Desert in Northern Chile, covering 22,500 km^2.

That airborne and spaceborne remote sensing in archaeology generates at least two critical issues for discussion: technology and visualization [9]. Technology opens new cognitive perspectives for archaeology and keeps researchers increasingly fascinated by its capabilities. Acquired data, primarily via remote sensing methods, can be studied after processing and visualizing. The research raises several issues related to the new cognitive situation of archaeologists facing the development of new technologies within remote sensing methods. These issues are discussed from ontological, epistemological, and discursive perspectives, supporting an exploration of the role of technology and visualization. Analyzing the most significant volumes of data efficiently by human operators is exceptionally challenging [10].

The English Heritage National Mapping Program (primarily aerial image interpretation) achieves a coverage rate of approximately 1 km^2 per person per day; this project has been running for over 20 years employing on average 15-20 staff, and has covered an area of 52,000 km^2 by 2012, in contrast, the Baden-Württemberg study, whilst still a primarily manual approach, took advantage of automated processing where possible, allowing an estimated coverage rate of over 35,000 km^2 by a single operator in six years. Exist an indication of the speed advantages of integrating automated processes into an analysis workflow.

With current advances in computing power, the potential to pre-process entire national datasets in weeks rather than decades is now a distinct possibility. This approach would be precious for countries that do not have many existing historical site records; a rapid Artificial Intelligence (AI) scan would provide a primary database that could be developed further as more resources become available. Due to the few time and cost overheads required for automated processing, there can be complementarity between achieving the quantity of the automated results *versus* the quality of traditionally generated databases, which can proceed to be created as usual in tandem with the automated processing. Even if imprecise, these machine learning tools could identify the more significant trends in the data, allowing human resources to be prioritized to the areas with many potential sites for detailed precision mapping. Especially when sites are under threat from development, rapid identification and mapping will give cultural heritage managers more time to act.The studies about the Copernicus platform observed that the dataflow concepts provide mechanisms to handle diverse challenges. The Copernicus architecture integrated two components aimed specifically at sampling problems: A peer-to-peer network and a workflow execution engine [11]. The software network layer handles the infrastructure and communication within the system, even as the underlying physical network change. With heterogeneous computing resources, it is portable and written in Python 2.7, available on virtually all *nix systems. Furthermore, it was designed to handle different types of network setups by using its peer-to-peer features. The network comprises three components communicating securely using Transport Layer Security (TLS).

Materials and Methods

The research on the digital technological procedures used in the satellite mapping of archaeological sites configured as cultural heritage adopted qualitative, exploratory, and explanatory procedures, based on the collection of data in books, articles, websites, and the use of the Copernicus platform.

The digital tools used in this research covered the manipulation of the Copernicus Platform, with the projection of sectorial information and the experimental treatment of the cartography inserted in the case studies.

The monitored topography includes satellite and AI digital technology projects applied to archeology in the following geographies: Cyprus, Pakistan, and Syria.

Results and Discussion

In 2015, the island of Cyprus was hit by a magnitude 5.6 earthquake. Researchers used Sentinel-1 SAR images to map two UNESCO World Heritage sites: Nea Paphos and the Tombs of the Kings (Figure 1) [12].

D-InSAR investigation was the first step to map the displacement pattern over large areas, such as the Paphos district, with cultural heritage sites, providing fast and reliable information to local stakeholders and policymakers about the hazard. Vulnerability maps were developed based on this evaluation and considering the structural stability of standing and/or buried monuments. For authors, D-InSAR processing can be part of a continuously updated risk management plan of cultural heritage sites and landscapes aligned with state-of-the-art geoinformation technologies such as those provided under the Copernicus umbrella [12].

Other researchers used data from Copernicus Sentinel-1 and Sentinel-2 to analyze the Cholistan

Figure 1. Final displacement map at (a) Nea Paphos; (b) Tombs of the Kings; and (c) the historic center of Paphos [12].

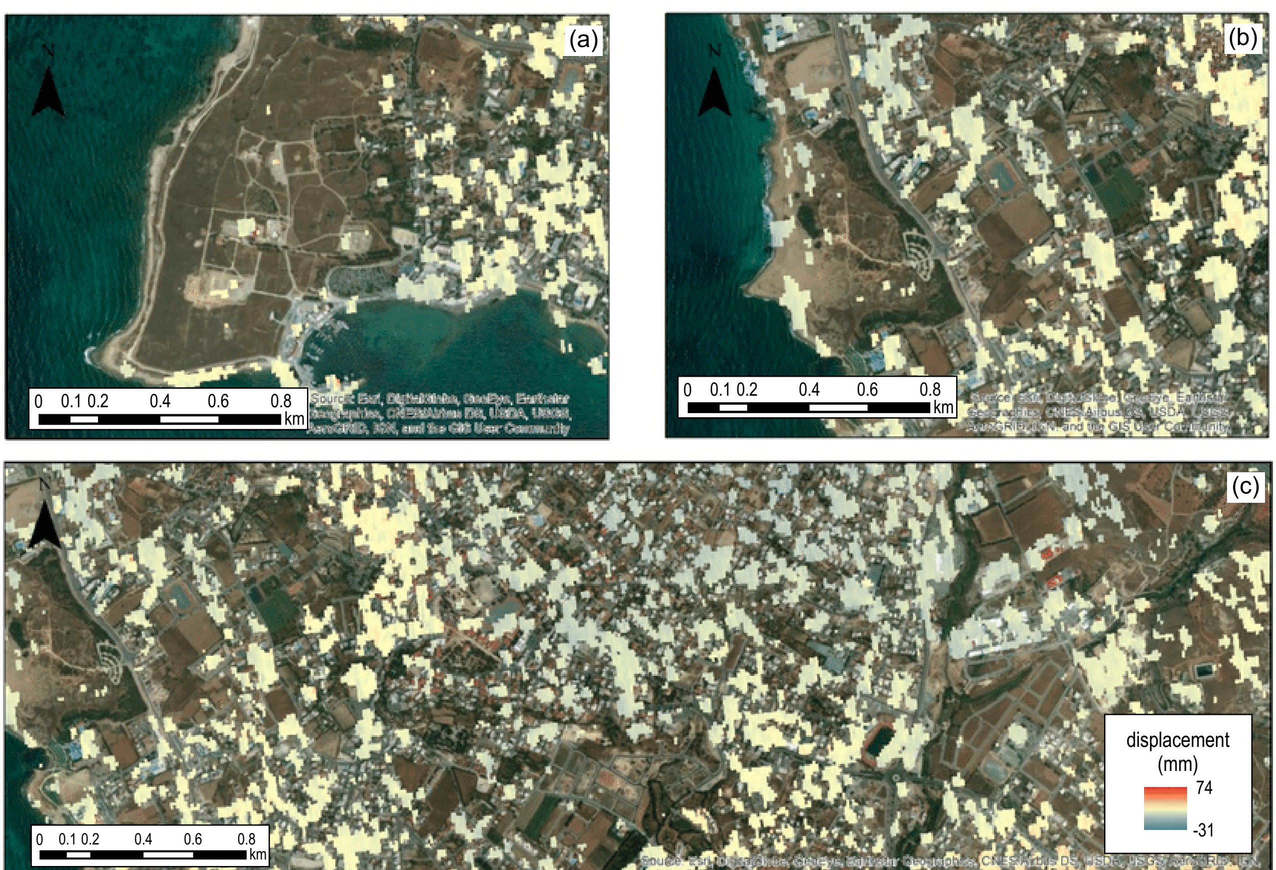

Desert area in Pakistan, historically linked to the Bronze-Age Indus Civilization, to detect archaeological mounds from this era [13]. A combination of multitemporal, multi-polarisation, and multiangle SAR bands, like multitemporal optical bands, were analyzed. The research showed more mounds over a larger area than previously recorded. Also detected were small to large mounds that suggest a continuous shift of settlements likely due to changes in the climate and hydrological network throughout history (Figure 2).

As attested in a deep study, the dataset provides a collection of Sentinel 1 and Sentinel 2 spectral signatures for mound-like archaeological features in drylands. The resulting mound locations can now be addressed regarding RF probability values [13].

The Copernicus platform services have also been used to identify areas of military conflict, terrorism, and depredation of cultural heritage, such as the geographies of Iraq and Syria.

Thus, Copernicus Optical and SAR imagery has also been used by researchers to establish a systematic monitoring tool for looting observation and prevention by detecting so-called looting pits, which typically appear as dark/black holes and can be recognized thanks to their sharp color contrast with the surrounding sand/grass surface. Similarly, another group of researchers from the European Union Satellite Centre, which implements Copernicus SEA, used satellite imagery to evaluate the extent and severity of damage on the important ancient sites of Nineveh and Nebi Yunus in Iraq, as well as looting and smuggling activities in Iraq in the context of ISIL's domination over the area. The results showed that looting activities existed even before the armed conflict. However, during ISIL's presence looting and smuggling were replaced by military and fundamentalist activities [14].

In Figure 3, the first image shows the UNESCO World Heritage Ancient City Limits of Aleppo in a 30 m resolution Global Digital Elevation Model ASTER (GDEM), indicating the Citadel's elliptical track. ASTER GDEM is a product of METI and NASA. The second photo contains the view of the walls of the Citadel from August 1, 2005 (Source: Wikimedia Commons). Finally, the third image is a view of the Citadel of Aleppo (Syria) from Sentinel-2 images acquired at very high resolution

Figure 2. Distribution of newly detected mounds about regional land cover [13].

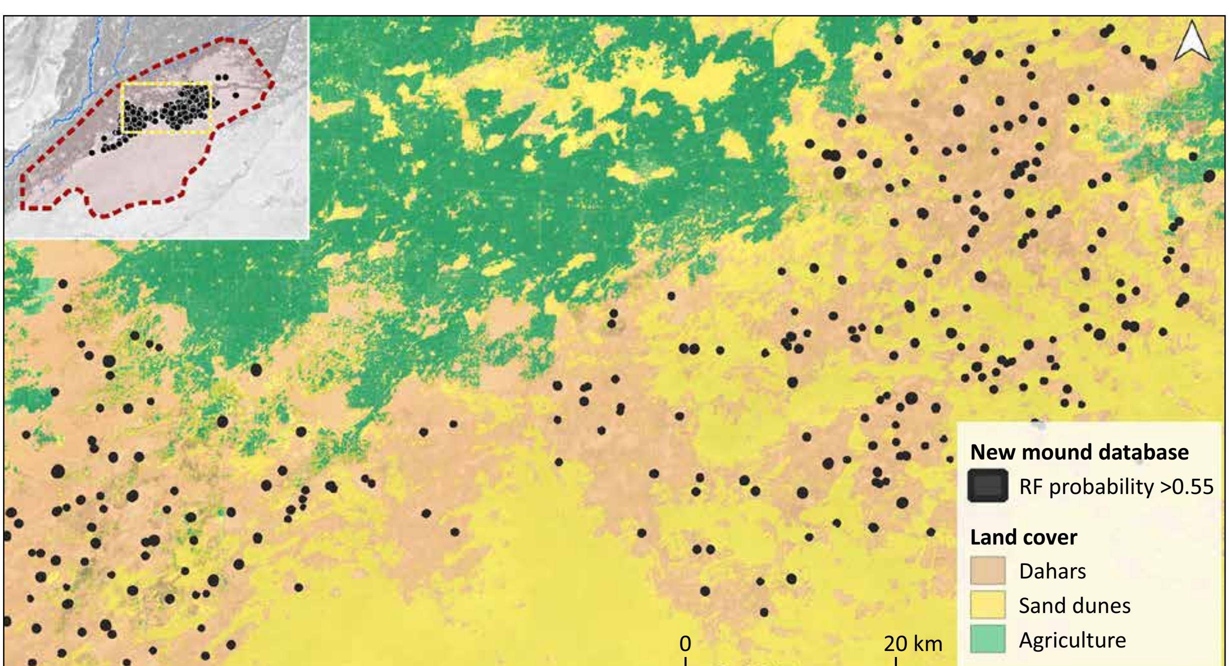

Figure 3. UNESCO World Heritage Ancient City Limits of Aleppo in three moments [15].

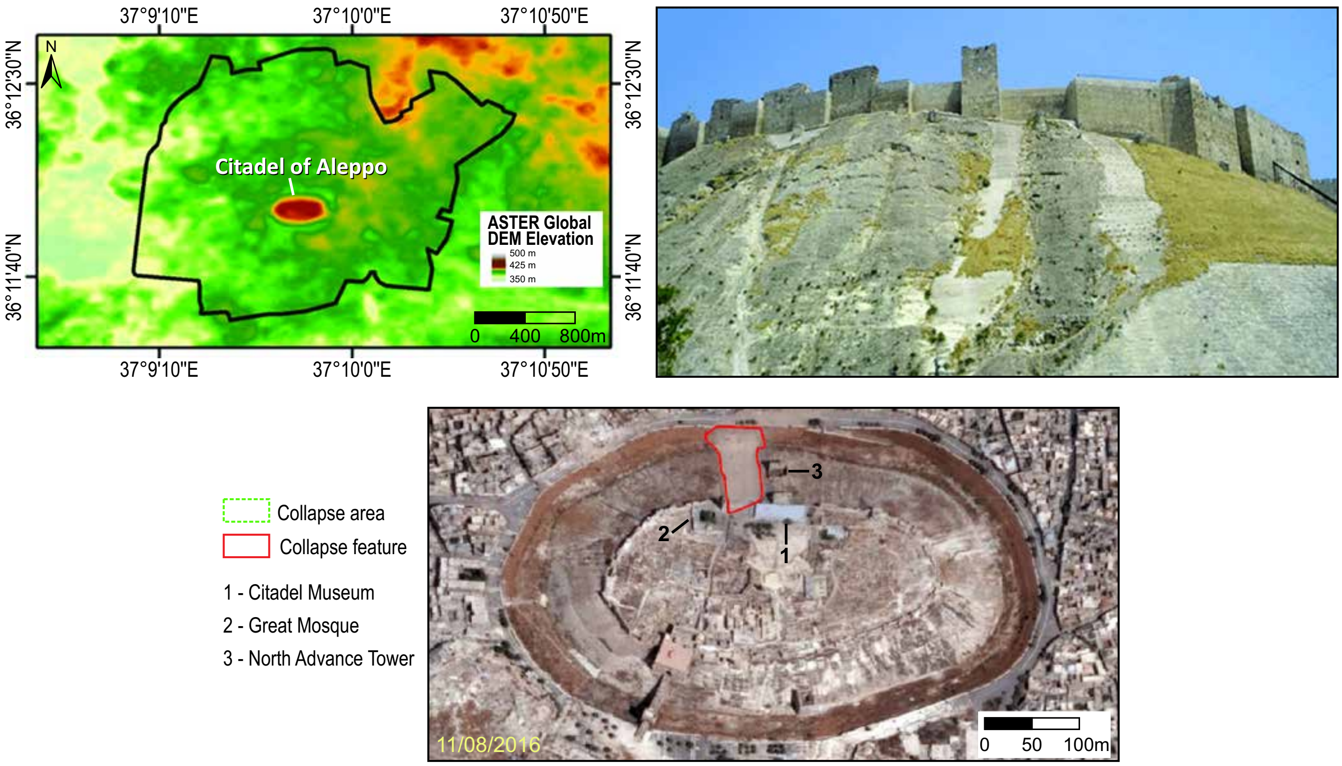

(VHR) Google Earth image taken on August 11, 2016. Labels and polygons indicate the area of the wall collapse that took place on August 11, 2016 (Sources: European Space Agency - ESA; Google Earth Image © 2018 DigitalGlobe) [15].

Conclusion

The study of digital satellite mapping tools with data capture of changes in topography allows applying Artificial Intelligence to quantify the information, favoring qualitative analyzes capable of defining parameters to safeguard cultural heritage in high-risk regions.

Acknowledgments

Acknowledgments to the National Council for Scientific and Technological Development (CNPq, Brazil).

References

1. RNP. Copernicus: tecnologia aliada à Observação da Terra. Available at: <https://www.rnp.br/noticias/copernicus-tecnologia-aliada-observacao-da-terra>. 2020. Accessed on May 5, 2021.
2. Haenlein M, Kaplan A. A brief history of artificial intelligence: On the past, present, and future of artificial intelligence. California Management Review, 2019.
3. Gunning D et. al. XAI-Explainable artificial intelligence. Science Robotics 2019;4(37), eaay7120.
4. Torres W. Inteligência Artificial será usada para descobrir sítios arqueológicos ocultos. Yahoo! Available at: <https://esportes.yahoo.com/noticias/intelig%C3%AAncia-artificial-ser%C3%A1-usada-para-132000792.html>. Accessed on Jun 18, 2022.
5. Tapete D et al. Regional-scale systematic mapping of archaeological mounds and detection of looting using cosmo-skymed high-resolution dem and satellite imagery. Remote Sensing 2021;13(16):1-29.
6. Guzzonato E et al. RUS Copernicus: An expert service for new sentinel data users. IOP Conference Series: Earth and Environmental Science 2020;509:1-3.

7. Fiorucci M et. al. Machine learning for cultural heritage: A survey pattern recognition letters 2020;133:102-108.
8. Borie C et al. Beyond Site Detection: The Role of Satellite Remote Sensing in Analysing Archaeological Problems. A Case Study in Lithic Resource Procurement in the Atacama Desert, Northern Chile. Remote Sensing, 2019;11(869):5-31.
9. Raczkowski W. Power and/or penury of visualizations: Some thoughts on remote sensing data and products in archaeology. Remote Sensing 2020;12(2996):33-55.
10. Gallwey J et al. Bringing lunar LiDAR back down to earth: Mapping our industrial heritage through deep transfer learning. Remote Sensing 2019;11(1994):57-78.
11. Pouya I et. al. Copernicus, a hybrid dataflow, and peer-to-peer scientific computing platform for efficient large-scale ensemble sampling. Future Generation Computer Systems 2017;71:18-31.
12. Tzouvaras M et al. The use of Sentinel-1 Synthetic Aperture Radar (SAR) images and open-source software for cultural heritage: An example from Paphos area in Cyprus for mapping landscape changes after a 5.6 magnitude earthquake. Remote Sensing 2019;11 (15):1-13.
13. Orengo HA et. al. Automated detection of archaeological mounds using machine-learning classification of multisensor and multitemporal satellite data. PNAS 2020;117(31):18240-18250.
14. Copernicus Observer. How does Copernicus help discover, monitor, and protect archaeological and cultural sites? Available at: <https://www.copernicus.eu/pt-pt/node/10702>. Accessed on Dec 19, 2021.
15. Tapete D., Cigna F. Appraisal of opportunities and perspectives for the systematic condition assessment of heritage sites with Copernicus Sentinel-2 high-resolution multispectral imagery. Remote Sensing 2018;10(4); 1-22.

Path Planning Comparison Strategies for Mobile Robot Navigation

Anderson F. de S. Lima[1*], Marcella G.S. dos Santos[1], João V.S. Mendes[1], Matheus A. da Silva[1], Marco A. dos Reis[2]
[1]Robotics and Autonomous Systems Competence Center, SENAI CIMATEC University Center; [2]Computational Modeling and Industrial Technology Program, SENAI CIMATEC University Center;Salvador, Bahia, Brazil

Autonomous navigation is an essential application because it allows the robot to perform activities without human interference. It enables the execution of tasks that pose a risk or difficulty to the human being. This material aims to present the research to evaluate the performance of different navigation algorithms. The results obtained in the first phase of the research will be highlighted, in which the A* (A Star) and Dijkstra techniques were evaluated. The robot was integrated into the Robot Operating System (ROS) framework, and the navigations were performed in a labyrinth-like environment.
Keywords: Autonomous Navigation. ROS. A*. Dijkstra.

Introduction

Mobile ground robots are increasingly common in robotics in hazardous environments. They are classified as Unmanned Ground Vehicles (UGVs), used in many areas, and may have applications in disaster rescue, nuclear inspection, planetary exploration, and military combats [1]. These robots navigate autonomously, requiring intelligence to define the most efficient routes to complete their missions. In a robotic navigation platform, there is a layer responsible for obtaining information from the environment and another layer responsible for reading and interpreting this data. Path planning algorithms are used to find a path between one point and another as efficiently as possible, such as Dijkstra and A* [2].

Robotic System

Autonomous robots are systems capable of interacting with the work environment without human action throughout their task execution. One of the most common applications in mobile robotics is autonomous navigation through unfamiliar environments, where many navigation techniques can be used to achieve an end goal.

The robotic system used in this work was the Turtlebot, a low-cost, open-source mobile robotics platform designed to be user-friendly and with the same capabilities as platforms from large robotics companies [3]. Turtlebot (Figure 1) has several devices in its structure to move, which allows the robot to recognize the environment around the asset, process this information and control its actions.

A 2D LIDAR is responsible for collecting information from the environment, using a laser beam fired by the device so that the system can identify close objects based on the reflection time [4]. A Raspberry is responsible for processing this data, which is presented as a low-cost, portable solution for integrating the sensor into the robotic system [5]. Hence, an OpenCR control board was used to control the robot actuators and distribute power to the devices [4].

Robotic systems may also be able to explore unknown spaces. For example, explorations can be dedicated to getting a robot out of a residence, a maze, getting a map of an unknown region, along with others.

Robotics Navigation

Navigation is essential for mobile autonomous systems because mobile robots need to move in environments with little or no human intervention

Received on 12 September 2022; revised 21 February 2023.
Address for correspondence: Anderson F. de S. Lima. Anderson F. de S. Lima. Rua Senador Quintino - 1984 - Brasília. Feira de Santana, Bahia, Brazil. Zipcode: 44088-720. E-mail:eng.andersonfsl@gmail.com.DOI 10.34178/jbth.v6i1.279.

J Bioeng. Tech. Health 2023;6(1):52-57

Figure 1. TurtleBot3 - Burger Version.

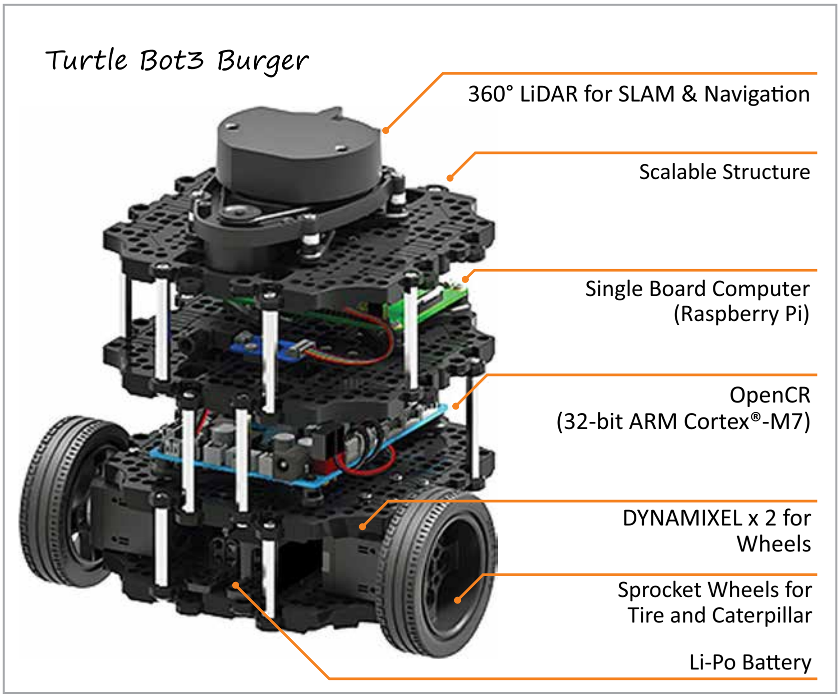

in many applications. A framework is needed that supports the navigation. ROS2 contains several packages that are used in robotic applications. Among them, NAV2 seeks to find a safe way to move a robot from point A to point B. It runs in several robot navigation applications, such as the following dynamic points. It completes dynamic path planning, calculate motor speeds, avoid obstacles, and structure recovery behaviors. The package uses behavior trees to call modular servers, so it completes an action, which can be, calculating a path, controlling effort, recovery, or any other activity related to navigation [6].

Some algorithms are used in navigation to do trajectory planning to perform the trajectory and achieve the proposed goal at a lower cost. The minimum path discovery algorithms can be classified into two forms: Uninformed search, when the algorithm does not use heuristics to find the shortest path between origin and destination, and informed search when the algorithm uses heuristics to estimate the minimum cost path [7]. Some examples of these algorithms are Dijkstra and A*, which use uninformed and informed search, respectively.

Dijkstra

Dijkstra's algorithm is a technique that is often used in differential mobile robots because it uses uniformed search capable of obtaining a trajectory between two nodes. These two nodes are points in the environment. From a specific node in space, the Dijkstra algorithm calculates from all available nodes a trajectory to the other node where the goal is. Figure 2 illustrates the possibilities of the paths to be used by the Dijkstra algorithm.

Dijkstra solves the single-origin shortest path problem on a directed or undirected graph when all edge weights are non negative. Equation 1

Figure 2. Algorithm Dijkstra.

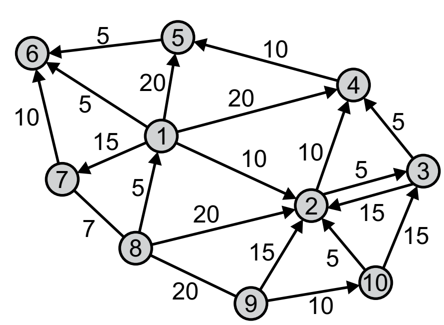

illustrates the time cost of Dijkstra's algorithm, in which V is the number of vertices, and E is the number of edges [8].

$$O\left[E + \frac{V}{Log(V)}\right] \quad (1)$$

*A**

The A* search algorithm is used in various fields of computer science and can also be applied to search problems related to mobile robotics.

The A* was created as part of a general-purpose mobile robot project called Shakey [9]. One of Shakey's most notable results was using this search algorithm. The A* algorithm uses graphs as the basis of the search system (Figure 3). The initial vertex represents the starting point of the search, and the endpoint is the final goal. The algorithm is formulated using weighted graphs to find a path to the given objective with the lowest cost (shortest distance traveled, along with others). The algorithm keeps several paths originating from the starting point and expands these paths one point at a time until its search criteria are satisfied.

The search is performed through minimal paths using heuristic functions, i.e., the selection of nodes is based on the distance from the start node plus the approximate distance to the destination. This approximation estimate can be represented by the function f(n) = g(n) + h(n) [10].

According to Rachmawati and Gustin [11], the star algorithm and the most widely known form of best-choice search solution, A star evaluates nodes in graphs by combining the cost of reaching a particular node already visited and the cost of going to the destination node.

Figure 3. Graphs of A*' algorithm.

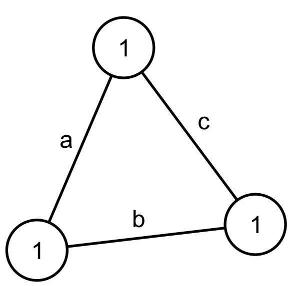

Materials and Methods

This research aims to compare the performance of trajectory planning strategies in ROS using Turtlebot3, and the scope of the paper is to present the results of the comparison made between the A* and Dijkstra techniques. Figure 4 presents the Methods used to perform the comparison between planning strategies.

In the first stage, a literature search was done to understand the concepts of the A* and Dijkstra techniques, how to use them, and thus define the system architecture. After that, the algorithms were configured on the robotic platform to be tested in a simulation environment, and the first samples of the system were collected. After collecting the samples, a normality test is done to know if the sample is

Figure 4. Methods used to compare strategies' plans.

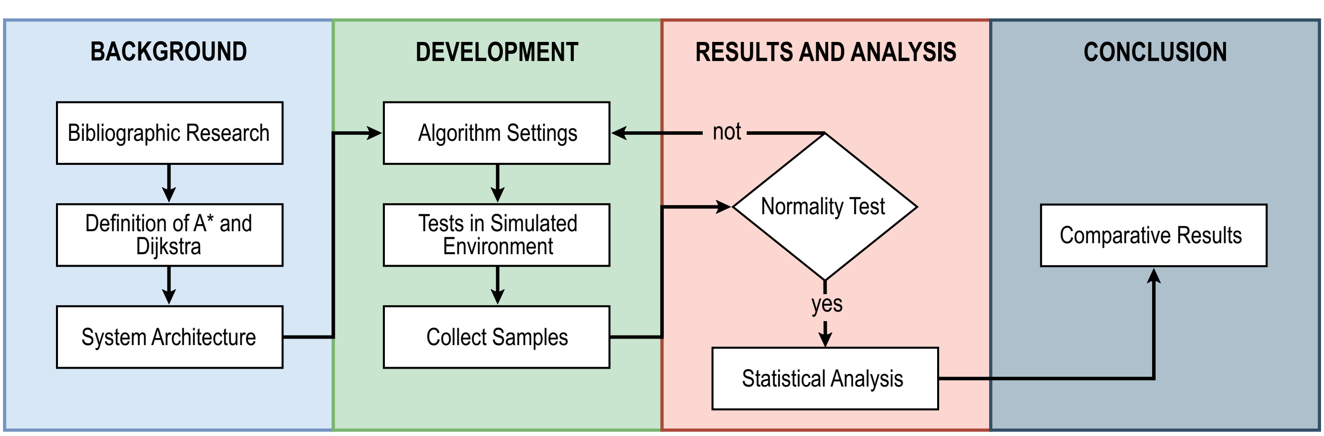

viable for analysis. If not, a new configuration is made, and the tests are done again. However, when the samples pass the test, a statistical analysis will be done to present the comparative results between the techniques.

Reults and Discussion

The Mission

We proposed a misison to Turtlebot3 to analyze the performance of the algorithms (Figure 5). The mission was to move it from an initial point to a final point in the simulated gazebo environment.

The robot uses AMCL to locate itself and plans the path using the A* and Dijkstra, enabling observing each algorithm's time spent completing the mission and comparing them. Thirty trials were run for each to perform the task to compare the algorithms' performance (Figure 6).

Observing the navigation missions, we observed the trajectory generated by each path-planning algorithm (Figure 7). Meanwhile, Figure 8 presents the time samples for each algorithm.

For the analysis, the normality of the dataset was initially verified through the Shapiro-Wilk test. The data for the Dijkstra algorithm had a p-value of 0.404. For the A star, the p-value was 0.150 for a significance level of 5% for both cases. This value confirms that the data is usually distributed. The average execution time for the mission using the Dijkstra path planner was 20.04 seconds with a standard deviation of 0.158 seconds, and the average time using the A star path planner was 20.14 seconds with a standard deviation of 0.207 seconds. Figure 9 shows the comparison between the two algorithms. For the sample values, we conclude that there was no relevant difference between the navigation time based on the mean and standard deviation.

We used the t-test to compare the average navigation population time between the algorithms. The null hypothesis was Dijkstra, and A star algorithm has an equal average navigation time. The null hypothesis for the significance level of 5% was rejected for a p-value of 0.042, concluding that the population means time for this navigation mission using the A star and Dijkstra algorithms are not equal, with little significance.

Conclusion

We performed a comparison between A* and Dijkstra to make UGVs more efficient in the trajectory planning process, using statistical comparison methods to understand the differences.

Figure 5. Gazebo simulation.

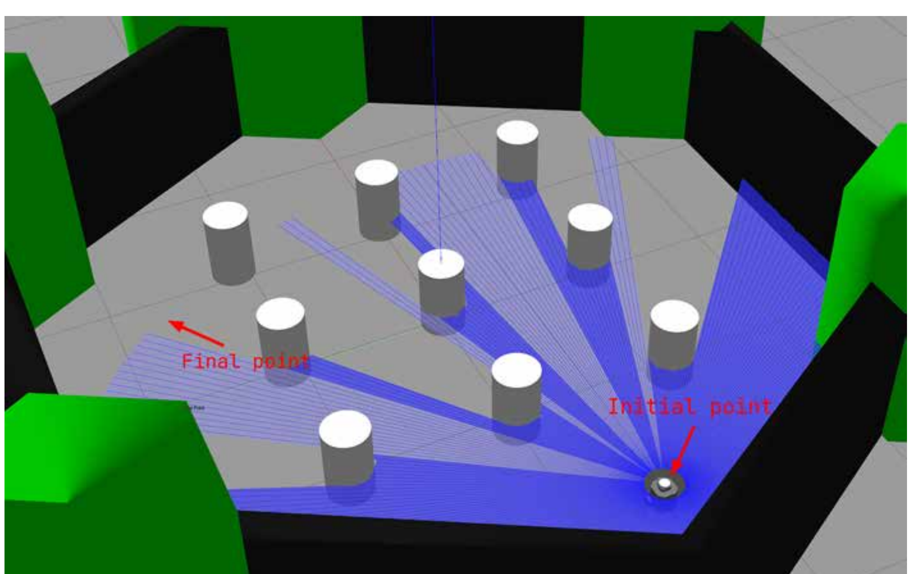

Figure 7. Path planned for each algorithm.

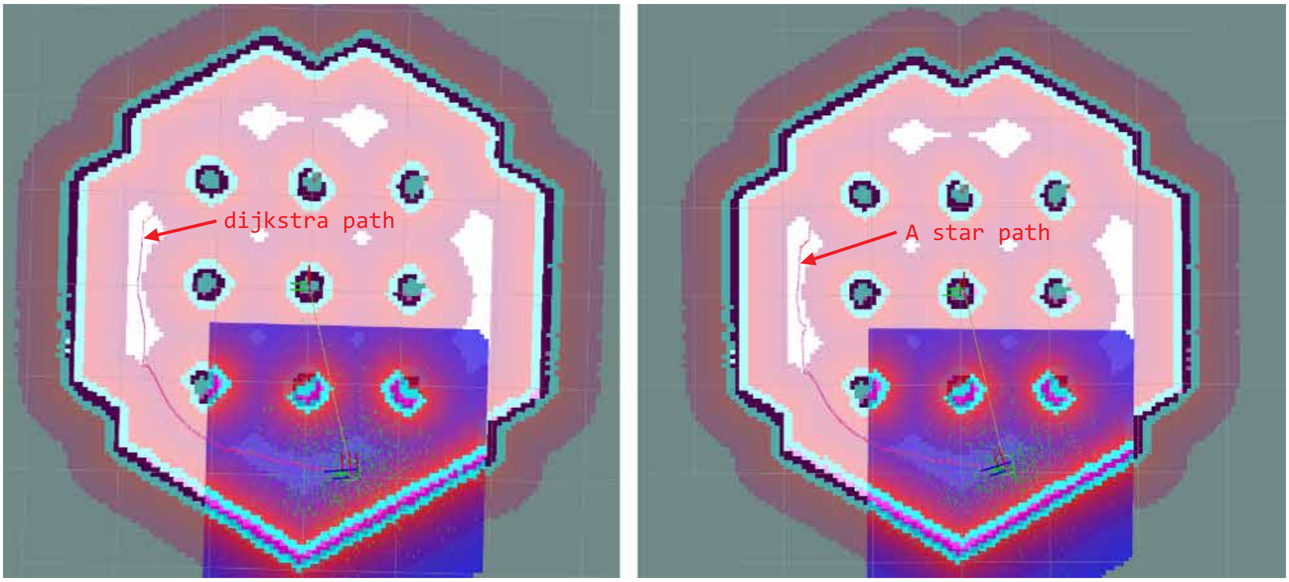

Figure 8. Time samples for each algorithm.

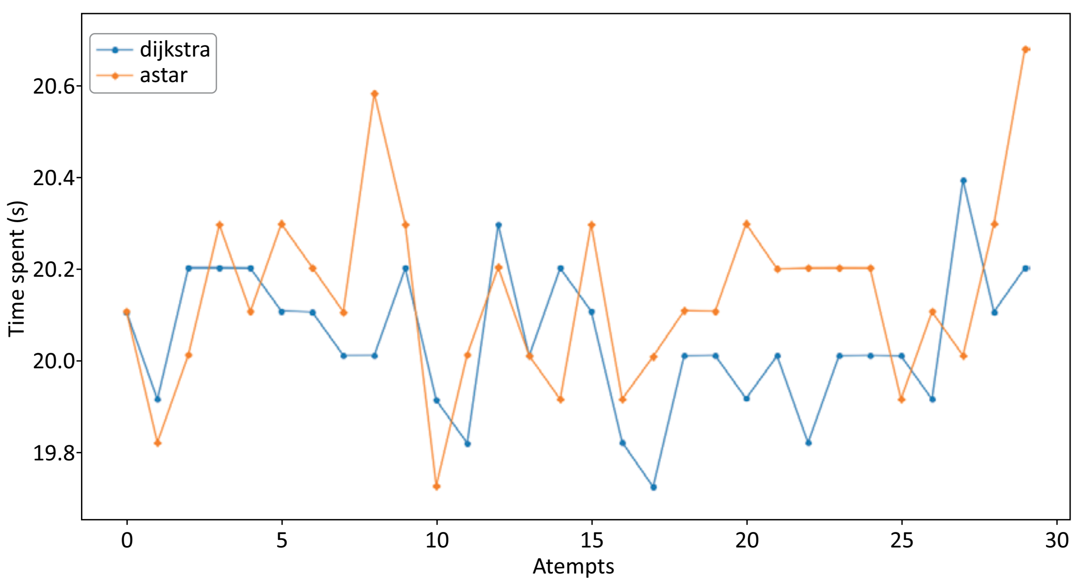

From the data obtained, we observed that the amplitude of the minimum and maximum time for the two algorithms was one second, which within the total time was too small for a definition of which method showed a better performance through graphical analysis. The t-test were used to verify the averages of time spent by each algorithm, and the value obtained to reject the hypothesis was irrelevant.

In this sense, we deduced that the Dijkstra and A* trajectory planning techniques present very close performances in a simulated environment.

At this point, we concluded that the difference between the algorithms for short trajectories becomes irrelevant even if Dijkstra is considered a greendy search algorithm leading to a longer mission time. According to Rachmawati and Gustin [11], the A* algorithm only scans toward the final

Figure 9. Algorithm time comparison.

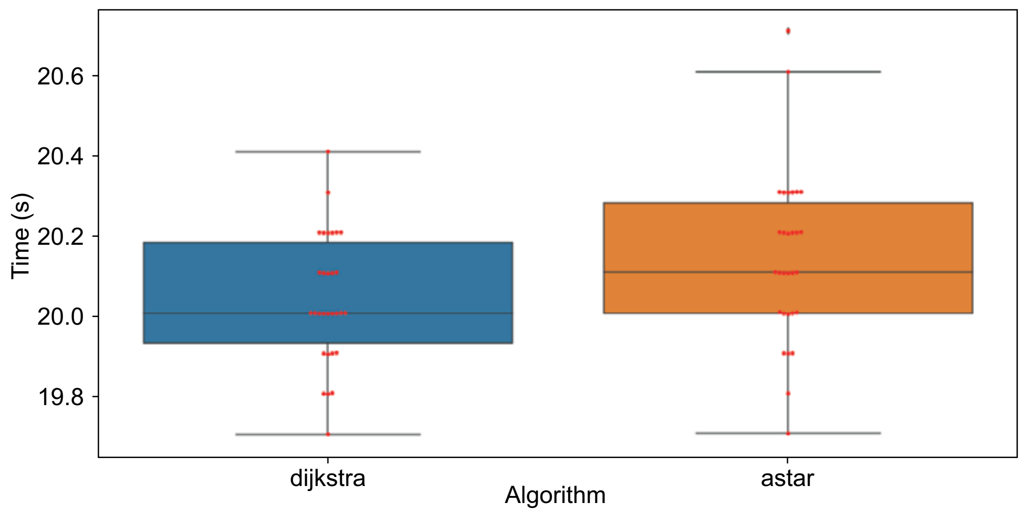

destination. In contrast, the Dijkstra algorithm does an equally expanding scan for each point ending in exploration with a larger area before finding the final objective.

For future studies on the topic, it is recommended to consider new mission possibilities, mainly regarding the increase in trajectory distance, the presence of more obstacles, and varying scenarios, enabling the analysis of each technique's performance in more contexts.

References

1. Hua C et al. A global path planning method for unmanned ground vehicles in off-road environments based on mobility prediction. Machines MDPI 2022;10(5):375.
2. Guruji AK, Agarwal H, Parsediya D. Time-efficient A* algorithm for robot path planning. Procedia Technology Elsevier 2016;23:144–149.
3. What is TurtleBot? Disponível em: <https://www.turtlebot.com/about/>.
4. Amsters R, Slaets P. Turtlebot 3 as a robotics education platform. In: Springer. International Conference on Robotics in Education (RiE). [S.l.], 2019:170–181.
5. Zhao CW, Jegatheesan J, Loon SC. Exploring iot application using raspberry pi. International Journal of Computer Networks and Applications 2015;2(1):27–34.
6. NAV2 — Documentação da Navegação 2 1.0.0. <https://navigation.ros.org/>. Accessed on June 30, 2022.
7. Inteligência Artificial - 3ª Ed. 2013. <https://www.cin.ufpe.br/~gtsa/Periodo/PDF/4P/SI.pdf>.Accessed on June 30, 2022.
8. Russel PN. Artificial intelligence: A modern approach by Stuart. Russell and Peter Norvig contributing writers, Ernest Davis et al., 2010.
9. NilssonNJ. Shakey the robot. In: [S.l.: s.n.], 1984.
10. Zhao CW, Jegatheesan J, Loon SC. Exploring iot application using raspberry pi. International Journal of Computer Networks and Applications 2015;2(1):27–34.
11. Rachmawati D, Gustin L. Analysis of Dijkstra's algorithm and A* Algorithm in shortest path problem. In: Journal of Physics: Conference Series. IOP Publishing, 2020:012061.

Chi² Test to Determine the Cut-Off Value for Anomalies Detection with Mahalanobis Distance

João Felipe de Araújo Caldas[1*], Caique Augusto Cardoso de Moraes[1], Flávio Santos Conterato[1]
[1]SENAI CIMATEC University Center; Salvador, Bahia, Brazil

This work aims to contemplate the detection of possible anomalies in a dynamic, robust, and effective way using Mahalanobis distance readily with the Chi² test. Tests were performed with p-values of a data set and the cut-off value, both generated by the Chi² test, reliably and dynamically detected possible anomalies. Therefore, this anomaly detection method is more effective for regular anomaly determination based on points farthest from the center.
Keywords: Chi². Mahalanobis. Anomalies.

Introduction

The use of distance calculation dates back to 650 BC as an attempt to define the shortest possible distance from two points. Thales of Miletus began calculating distances between different objects using two-point references [1,2], for instance, the distance between a ship and shore or height from the top of a pyramid to the example etcetera. Subsequently, Euclidean geometry contributed to calculating the Euclidean distance, and nowadays, we can see its use in the objective life of any person. However, in machine learning, the need to estimate the metric of two points comes from the demand of the data clustering process [1].

Clustering, which is a powerful data mining technique, in turn, is formed by the proximity relationship of the defined methods, being able to be distinguished between two types by the distance of the defined points, using the defined formulas and mathematics methods, or by the degree of similarity based on their characteristics [3].

There are some measures to determine the interval between points; among them are Hamming distance, the Minkowski distance, the Manhattan distance, and the most famous, the Euclidean distance [4]. Even so, the article's primary subject was the statistical measure created by the Indian scientist Prasanta Chandra Mahalanobis, called Mahalanobis distance, used in the experiment [5.

The χ^2(chi-square), or simply Chi²(chi-square) test, is described as a non-parametric test; that is, it does not depend on population parameters; in addition to being a hypothesis test, the principle basic to this test is to compare proportions, that is, possible divergences between the observed and expected frequencies for a specific event [6].

An example of Chi² application was the usability to assess the significance of each parameter considered for risk stratification and mortality prediction for definitive values about COVID-19 [7], dealing directly with data processing to improve the final results. Mahalanobis distance is an effective multivariate distance metric that measures the distance between a point (vector) and a distribution [5,6] as per Formula 1. This metric is a multivariate distance calculation metric, efficiently measuring spatial distributions between points and vector distributions at intervals, thus having prominence in anomaly detection applications, classification of untreated datasets, and in some cases in classifications of classes and most ignored use cases [5].

The formula for the Mahalanobis distance is given by [6]:

$$D^2 = (x - t)^T \cdot C^{-1} \cdot (x - m) \qquad (1)$$

In which, D² is the square of the Mahalanobis distance; x is the observation vector; m is the

Received on 12 December 2022; revised 10 February 2023.
Address for correspondence: João Felipe de Araújo Caldas. Conjunto Jardim das Limeiras, 32 - São Marcos, Salvador, Bahia, Brazil | Zipcode: 41250-440. E-mail: jfdac11@gmail.com. DOI 10.34178/jbth.v6i1.280.

J Bioeng. Tech. Health 2023;6(1):58-61

vector of mean values of the independent variables; C^{-1} is the inverse of the covariance matrix of the independent variables.

Formula 1 also has some observations; if the matrix (x - m) is diagonal, then the distance measure is analogous to the normalized Euclidean distance [5].

This article proposes to showcase the efficacy of anomaly detection in conjunction with the distance between a distribution and Mahalanobis points. Arguments supporting the use of this technique will be presented in dissonance with the current literature approach [8,9] regarding anomaly detection in a database. After experimentation and comparisons with the Chi² test, the x values farthest from a centroid-based method lacked dynamism and showed high chances of detecting false positives. Hence, the correlation between Chi² and Mahalanobis distance is displayed to evidence the accuracy of the cut-off values for anomaly detection proposed by the result of the Chi² test (or p-value) present in this paper.

Materials and Methods

The dataset used was obtained from the learning and challenge platform Kaggle [10], a well-known platform in the Data Science area; the dataset is called World Happiness Report, which contains information about world happiness. There are two main reasons for the choice of the dataset. The first is that the dataset needs to have a high degree of relationship, i.e., that presents a precise functioning with highly correlated data in contrast to neural networks and especially in Pearson functional networks [11] so that the Chi² can stand out in the results of possible anomalies to facilitate the understanding and comprehension of the content, the second reason was that after the pandemic, socioeconomic behaviors were impacted, such as happiness and quality of life [12], for these factors the database proved to be more attractive, thus hoping to return not only anomalous results but also the difference in the degree of happiness over time. The dataset has the period from 2015 to 2022; however, it was used from 2020 to 2022 to detect possible anomalies, considering that the COVID-19 virus started spreading in January 2020 and causing the pandemic in March 2020 [13] and that this pandemic impacts to society [12]. That had as motivation for the search for the possible impacts of the COVID-19 pandemic on world happiness. During the development, it was verified that the columns with higher correlation using the Pearson correlation coefficient resulted in the upper and lower whisker columns with 99% correlation between them, thus, being chosen by the high degree of correlation to the experiment. Subsequently, the clustering was performed by defining only one cluster (group), the calculation of the data centroid, the computation of the Mahalanobis distance for each point, and the Chi² test were performed with the help of the scipy library [14], and using the cdf function (cumulative distribution function).

Consequently, finding the p-value of each point was possible to establish the cut-off values for anomaly determination. Then the possible anomalies were separated. All tests and experiments were done using Python version 3.7.10 [15].

Chi² is used as a statistical hypothesis test and as a cut-off value, i.e., a value to determine whether a piece of data is anomalous or not. The statistical hypothesis test is performed because the Mahalanobis distance results in the squared distance, the ‘D²’ [16].

To find the cut-off value, one needs to know the limits of the grouping of the data and the degree of freedom (c) will be the number of variables/ columns present in the database [11]. This calculation is represented by Formula 2, which is given by the formula in which the variable O is the observed value and E is the expected value.

$$X_c^2 = \sum \frac{(O_i - E_i)^2}{E_i} \quad (2)$$

Mahalanobis distance is closely related to Chi² in the way that [6,18] proposed: the squared Mahalanobis distance of a Gaussian (normal) distribution is distributed by Chi². Therefore, the

Chi² test will result in a variable called p-values, intended to demonstrate whether the test results are quantitatively significant. The following considerations are essential to perform a Chi² test and obtain the p-values [6]:

- The degree of freedom is defined as the number of categories minus 1 [6].
- The tester chooses the alpha level (α). Usually, the alpha level is 0.05 (5%), but one can also have other levels, such as 0.01 or 0.10 [6].

The advantages of Chi² include its robustness in data distribution, easy calculation, and detailed information that can be obtained from testing. The caveat to using this methodology in studies is that they cannot meet the parameter assumptions and flexibility in handling two aspects of group data and multi-group studies [16].

Results and Discussion

After the experiments had been carried out, the result of the detection of anomalies was compared using p-values and the cut-off value of the Chi² hypothesis test. Figure 1 shows three ellipses based on the Chi² test for the database chosen. The values outside the limit of the first ellipse (blue) are considered anomalies (annotated with their respective index). In this case, the delimitation of the ellipse is the critical cut-off value found by performing the Chi² test. It is worth pointing out that the alpha level value was set to 0.01. The standard deviation of the first ellipse measures the ellipses in red and yellow. For example, the red ellipse is the standard deviation multiplied by two, and the yellow is multiplied by three.

In Figure 2, the ellipse continued to be made similarly, but the cut-off value was determined by the p-values also generated by the Chi² test. P-values that have a significance level lower than 0.01 are considered anomalies. Therefore, both methods can be used equally for the same purpose. However, to find the p-value, only one calculation is needed, while the critical cut-off values of the Chi² test are found after more calculations. Depending on the alpha value used in the Chi² test, the result of possible anomalies may be equal to the result of using p-values as a cut-off value. In the case of this database, when using the alpha value as 0.001, the result of both methods are the same. The critical value used in the first method and the p-value of the second method are two different approaches to the same result [17].

Figure 1. Chi² critical value cut-off.

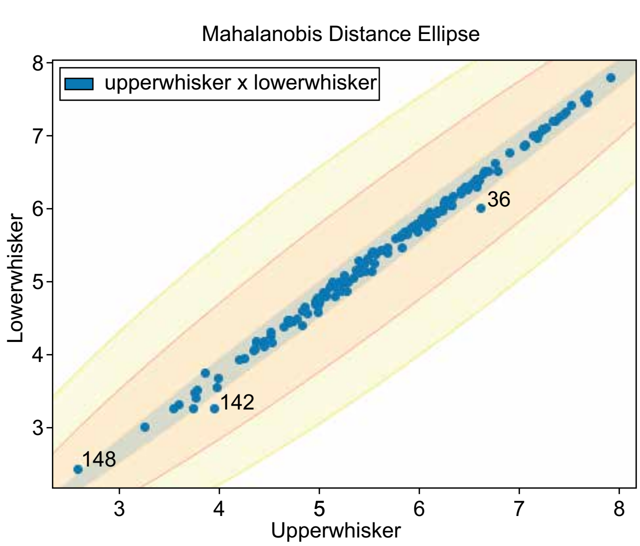

Figure 2. Chi² p-value cut-off.

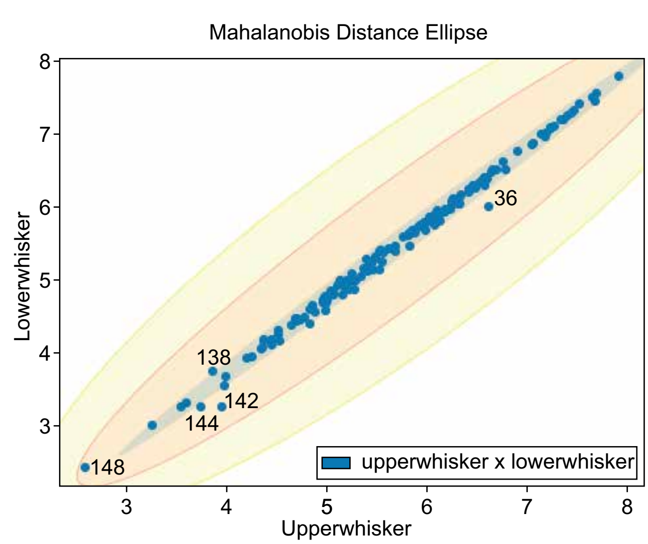

Conclusion

The anomaly detection is successfully performed, and the need to streamline it is successfully met. The values determined as possible anomalies are established according to a cut-off value calculated by hypothesis testing, unlike how it is commonly performed, measuring a certain amount of points furthest from the centroid.

The results collected in this research are of paramount importance to detecting anomalies since they demonstrate the detection of anomalies through a specific cut-off value, that is, dynamically and more reliably. Therefore, verifying and testing the effectiveness of Chi^2 with other distance metrics or with many categories is recommended for future work.

Acknowledgments

We thank Conterato Analytics and Aton Engenharia for supporting and directing the work done and for the opportunity for growth and learning.

References

1. Rezende EQF, Queiroz MLB. Geometria Euclidiana Plana e Construções Geométricas. Campinas: Editora UNICAMP, 2000.
2. Dante LR. Matemática: Contextos & Aplicações - Volume 1. São Paulo: Editora Ática, 2011.
3. Pinto R. Entendendo porque é que a distância certa faz toda a diferença. 2020. Available:https://medium.com/data-hackers/entendendo-porque-%C3%A9-que-a-dist%C3%A2ncia-certa-faz-toda-a-diferen%C3%A7a-648030c9bae2. Accessed: Jun 23, 2022.
4. Brownlee J. Distance Measures for Machine Learning. 2020.Available:https://machinelearningmastery.com/distance-measures-for-machine-learning/#:~:text=Perhaps%20four%20of%20the%20most,Manhattan%20Distance. Accessed: Jun 25, 2022.
5. Prabhakaran S.Mahalanobis Distance – Understanding the math with examples (python). 2019. Available:https://www.machinelearningplus.com/statistics/mahalanobis-distance/. Accessed: Jun 24, 2022.
6. Glen S. Chi-Square Statistic: How to Calculate It / Distribution. www.StatisticsHowTo.com. Available:https://www.statisticshowto.com/probability-and-statistics/chi-square/. Accessed: May 7, 2021.
7. Alle S et al. COVID-19 Risk stratification and mortality prediction in hospitalized Indian patients: Harnessing clinical data for public health benefits. PloS One2022;17(3):e0264785.
8. Data Tech Notes. Anomaly Detection Example with K-means in Python. May 13, 2020. Available from:https://www.datatechnotes.com/2020/05/anomaly-detection-with-kmeans-in-python.html. Accessed: Sept 10, 2022.
9. Dino L. Outlier detection using K-means clustering in python. April 19, 2022. Available from: https://towardsdev.com/outlier-detection-using-k-meansclustering-in-python-214188fc90e8. Accessed: Sept 10, 2022.
10. World Happiness Report up to 2022. Kaggle, 2022. Available:https://www.kaggle.com/datasets/mathurinache/world-happiness-report. Accessed: Jul 1, 2022.
11. Ivanov AI, Vyatchanin SE, Lozhnikov PS. Comparable estimation of network power for chi-squared Pearson functional networks and Bayes hyperbolic functional networks while processing biometric data. In: 2017 International Siberian Conference on Control and Communications (SIBCON). IEEE 2017:1-3.
12. Qiu W et al. The pandemic and its impacts. Health, Culture and Society. 2017;9:1-11.
13. Strabelli TMV, Uip DE. COVID-19 e o Coração. Arquivos Brasileiros de Cardiologia 2020;114:598-600.
14. Scipy. scipy.stats.chi2. 2022. Available:https://docs.scipy.org/doc/scipy/reference/generated/scipy.stats.chi2.html. Accessed: Jun 30, 2022.
15. Python, Python Release, 2022, Available: https://www.python.org/downloads/release/python-3710/. Accessed: 30 Jun, 2022.
16. McHugh ML. The chi-square test of independence. Biochemia medica 2013;23(2):143-149.
18. Glen S. P-value *vs*. critical value. Jul 26, 2020. Available from:https://www.datasciencecentral.com/p-value-vs-critical-value/. Accessed: Sept 9, 2022.
19. Thill M. The relationship between the Mahalanobis distance and the Chi-squared distribution. ML & Stats. 2017. Available:https://markusthill.github.io/mahalanbis-chi-squared/. Accessed: May 7, 2021.
20. Cansiz S. Multivariate outlier detection in python. towards data. Science. 2020. Available:https://towardsdatascience.com/multivariate-outlier-detection-in-python-e946cfc843b3. Accessed: May 3, 2021.

Plastic Recycling Feasibility with the Triple-Layered Business Model Canvas

Oscar Chamberlain[1,2*], Yago Araujo Vieira[3], Alessandra da Rocha Duailibe Monteiro[4]

[1]Federal University of Rio de Janeiro – UFRJ, Rio de Janeiro, Rio de Janeiro; [2]National Service of Industrial Learning - Integrated Center of Manufacture and Technology – SENAI-CIMATEC, Salvador, Bahia; [3]Federal University of Santa Catarina – UFSC, Florianópolis, Santa Catarina; [4]Fluminense Federal University – UFF, Rio de Janeiro, Rio de Janeiro; Brazil

The massive consumption of plastic material and its waste worldwide has made it necessary to find alternative solutions to reduce the size of landfill areas and recover their energy content. Pyrolysis is one of the chemical recovery technologies for plastics whose return on investment is estimated between 16% and 21%. This article aims to use the Triple Layer Business Model Canvas tool, which considers the elements of a business model visually and dynamically based on the three pillars of sustainability (economic, environmental, and social). This approach allowed for a comprehensive analysis of the sustainability-oriented business model. As a result, we concluded that pyrolysis is viable as a complementary process to other means of mechanical recycling and energy recovery.

Keywords: Pyrolysis. LCA. Sustainability.

Introduction

The growing production and demand for plastic materials, coupled with the disposable use of most polymers by the consumer sector, exacerbates the problem of plastic waste, mainly when the "environmentally adequate“ final destination is restricted to landfills. According to data from Plastics Europe, 359 million tons of plastic materials were produced worldwide in 2018, of which 39.9 % went to packaging use [1]. This fact implies that a considerable part of the plastic generated in the world is consumed and disposed of after a single use, thus becoming a threat to the integrity of ecosystems [2]. This issue raises the need to look for alternatives such as chemical recycling, in which, in addition to reducing the sizes of landfill areas, it is possible to take advantage of the energy source of these materials [3].

Pyrolysis is a chemical recycling technique involving the degradation of long-chain polymers into smaller molecules [4]. The polymeric chemical structure is modified by heat or a catalyst, generating less complex molecules. These products can be used as raw materials to manufacture new petrochemicals. Depending on the process conditions and the type of feed residues, the products obtained from pyrolysis reactions can be liquid, gaseous, or solid residues such as ash, tar, and pigment [5]. The processing of Polyethylene (PE) and Polypropylene (PP), for example, has olefins, paraffin, and waxes as main products [6]. Usually, pyrolysis processes only require a little infrastructure, making it possible to set up small and mobile units [6]. One of the most apparent advantages of pyrolysis processes is converting materials with low energy density into products with a high energy density [7]. Pyrolysis has received attention in recent years from the scientific community due to its operational and environmental advantages, considering the demand for energy and the instability of the fossil fuel market [3].

Monteiro (2018) [5] provided in his thesis a detailed study on the contribution of chemical recycling to sustainable development, presenting the Life Cycle Analysis (LCA) as a tool for the prevention and minimization of adverse environmental impacts. Joyce and Paquin (2016) [8] developed a methodological approach called Triple Layered Business Model Canvas (TLBMC) to address the elements of a business model

Received on 15 December 2022; revised 26 February 2023.
Address for correspondence: Oscar Chamberlain. Rua Estrada dos Três Rios, 1721, – BL 2 apto 403 – Ri de Janeiro- RJ, Brazil | Zipcode: 22745-004. E-mail: ochamberlainp@gmail.com. DOI 10.34178/jbth.v6i1.281.

J Bioeng. Tech. Health 2023;6(1):62-68

visually and dynamically based on the three pillars of sustainability (economic, environmental, and social). This tool enables effective decision-making that includes all aspects of sustainable development, generating value and benefits for society and the environment. In addition to these works, a literature review was carried out on the positive and negative impacts of the increasing use of pyrolysis processes worldwide. This work aimed to build a model that simulated the implementation of a pyrolysis unit in Brazil based on data found in the literature and applied it to the TLBMC model.

Materials and Methods

A literature review was carried out, which initially focused on data collection. The topics investigated dealt with installing pyrolysis plants and their economic feasibility analysis, the Life Cycle Analysis for the chemical recycling of plastic waste, and the social impact of recycling plastic materials. The bibliographic research was developed in four sub-steps, which were: the definition of the database (SCiELO, ScienceDirect, Web of Science, along with others), the definition of descriptors (use of terms such as LCA, pyrolysis, canvas, chemical recycling, along with others); definition of titles and abstracts, and finally, the analysis of the texts. In this last stage, not only a textual analysis was carried out, but also an interpretive one, leading to discussions on the author's message and a re-elaboration of this message based on personal reflection. All of this allowed for delimiting the focus of the work on applying the Triple Layer Business Model Canvas (TLBMC) to a hypothetical pyrolysis unit. Finally, the documents in question were analyzed to collect data that complemented the assembly of the business model.

Results and Discussion

Economic Layer

The business model initially proposed by Osterwalder and Pigneur (2010) provided only an economic analysis based on nine interconnected components: value purpose, customer segment, customer relationship, channels, partnerships, key activities, critical resources, costs, and benefits [9]. Figure 1 brings an infographic depicting the Canvas model setup with the display components applied to a pyrolysis unit, which are still shown individually.

Value Proposition

Pyrolysis uses Waste-derived Fuel (WDF), generally PE and PP, from packaging and other applications. This WDF can be obtained by shredding substantial amounts of waste, enabling the reuse of what is neither organic nor recyclable. Urban solid waste (household and commercial) and non-hazardous industrial waste undergo mechanical sorting and homogenization to obtain the best ratio between dry and wet materials. One such processing unit is located at ESTRE in Paulínia, São Paulo, with a daily processing capacity of 1,000 to 2,000 tons.

Customer Segments

Due to the nature of the plastic recycling operation, there are three segments of interested customers: the waste processor, the polymer producer, and the municipalities. The waste processor can add value to the WDF material through pyrolysis by marketing the product as a higher calorific fuel or a raw petrochemical material. The polymer producer may have a raw material source recognized as renewable, with associated image gains. Municipalities responsible for waste collection and treatment may have a sustainable option.

Customer Relationship

Considering the polymer producer, issuing a sustainability seal will allow the disclosure of the recycling action. The relationship between the municipalities and the waste processor will be through contracts to supply raw materials and minimum recycled quantities.

Channels

A web page will be able to collect all information on the logistics of collection and subsequent sale of

Figure 1. Infographic of the economic layer analysis of the Triple Layer Business Model Canvas of a hypothetical pyrolysis unit.

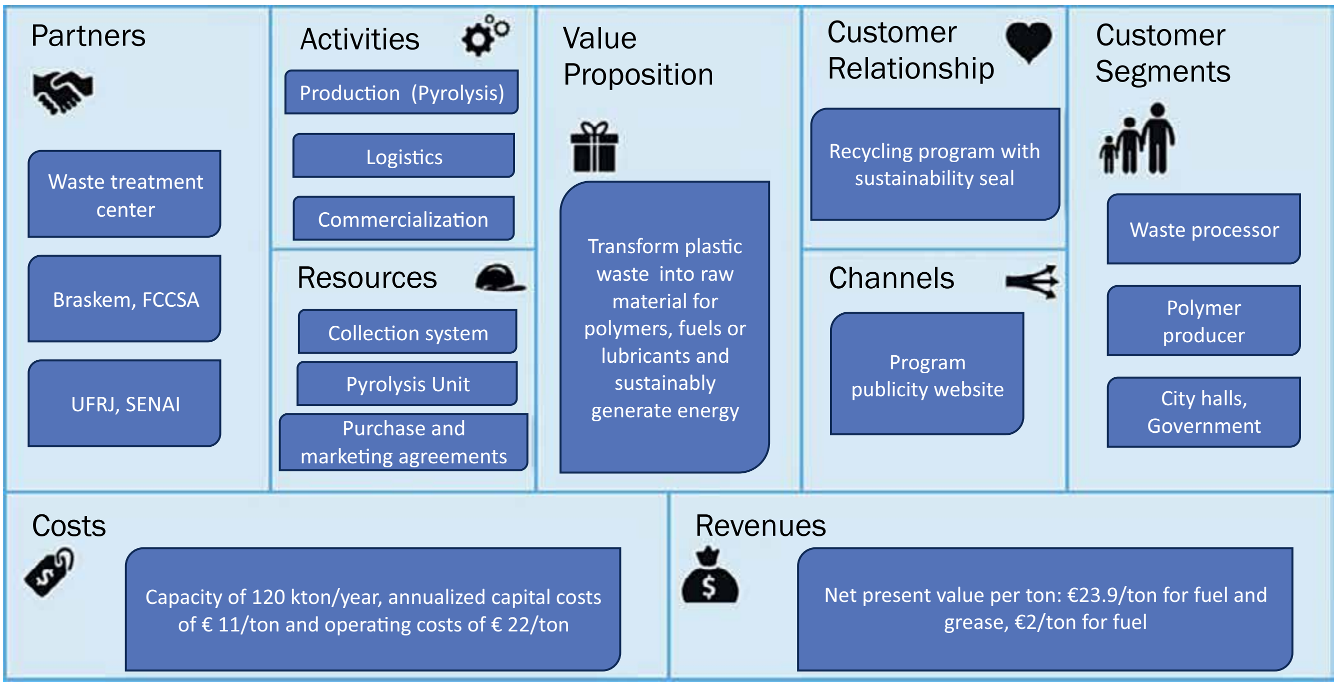

Source: Joyce and Paquin (2016) [8].

materials. The traditional channels of municipalities and the processor will be used to carry out the whole collection, processing, conversion, and sale cycle.

Partners

The critical point of partnerships depends on establishing a relationship between the city and the recycler. Other partnerships with the academy and the polymer producer or other associated industries will be of excellent value in facilitating the required investment and the disclosure of the entire process.

Activities

The process has three key steps: waste collection and segregation, the pyrolysis conversion process, and the logistics and commercialization of products.

Resources

The collection and segregation system must be available, i.e., financial investment for installing the pyrolysis unit and contracts signed between the city and the processor and between the processor and consumers of the pyrolysis products, either as fuel or as petrochemical raw material.

Costs

A plant production capacity of one ton/hour with 0.3 £/kg or R$ 2.1/kg is adopted as a cost basis.

Revenues

A rate of return between 16 and 21% and a net present value per ton between R$ 12 and R$ 15 were assumed for the expected profit based on data collected in the literature [10].

Environmental Layer

A purely economic analysis, disregarding the environmental impact data discussed worldwide, is inefficient. In this sense, a new tool requires direct integration between economic and environmental values in a holistic view that addresses corporate sustainability [8]. The environmental layer of Canvas integrates nine other components and an infographic of the environmental layer analysis

(Figure 2). The values described in this section are based on the values expressed in the work of Khoo (2019) [11]. A scenario was adopted in which 82.1% of the plastic waste received would be sent to energy recovery by incineration, 10.6 % to mechanical recycling, and 7.3 % to pyrolysis.

Functional Value

This value uses lifecycle evaluation to simulate a functional unit with a quantitative description of service performance. According to the State Inventory of Municipal Solid Waste, 39,859 tons of municipal solid waste were collected throughout São Paulo in 2018, totaling 14.54 million tons annually [12]. Unfortunately, data on the selective collection were unavailable in the literature, so estimating the amount of plastic waste that could be adequately separated from this amount was not feasible. Therefore, for this work, we assumed that 15.6 % of all residues are of plastic composition [13], reaching a functional value of 2.37 million tons of mixed plastic waste per year. Considering the above scenario, the pyrolysis unit receives 7% of this residue, i.e., 165,900 tons of plastic waste are processed yearly.

Materials

The composition of the plastic residue was estimated at 40 % polyethylene, 17 % vinyl polychloride, 12 % polypropylene, 4 % polystyrene, 4.8 % polyethylene terephthalate and 22.2 % of other mixed polymer fractions.

Production

It was estimated that 650 kg of diesel oil per ton of plastic residue production was sent to pyrolysis. Annual production of 107,835 tons of diesel oil was calculated in this sense.

Supplies and Out-Sourcing

This component considers plastic waste collection partner companies. Khoo (2019) analyzes the implementation of pyrolysis along with other alternatives, such as mechanical recycling,

Figure 2. Infographic of the environmental layer analysis of a pyrolysis unit's Triple Layer Business Model Canvas.

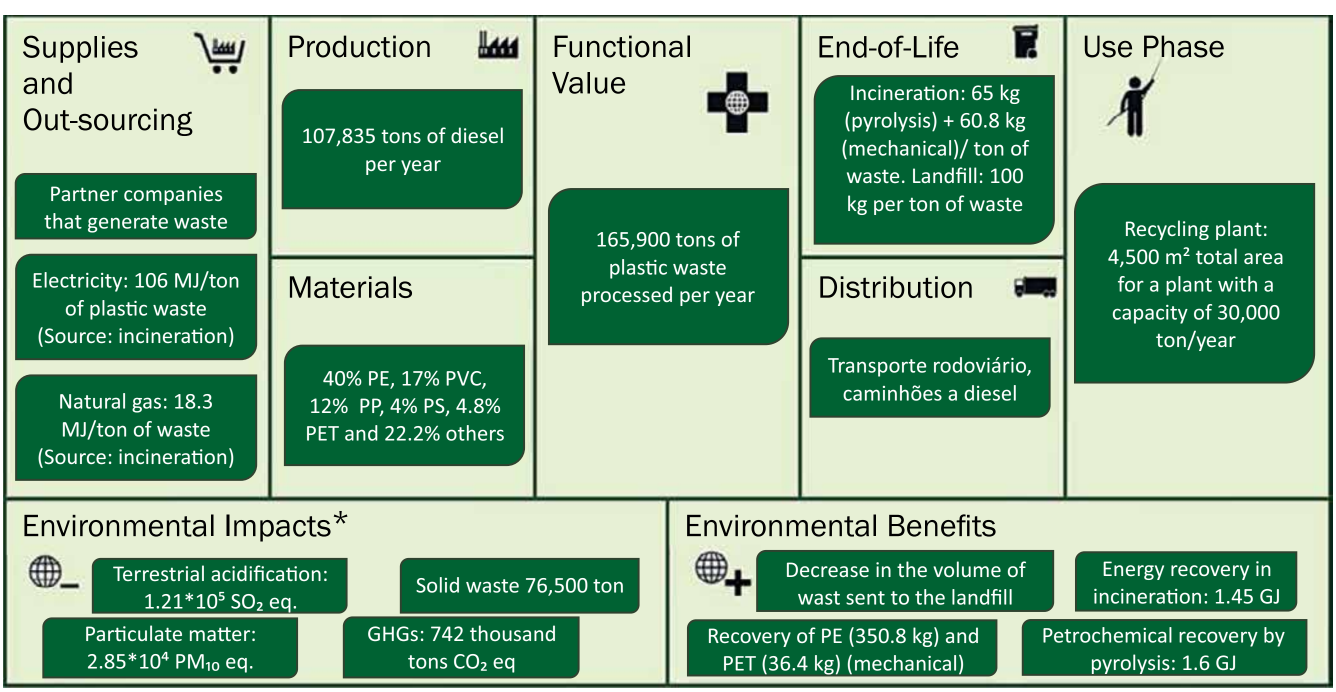

*Scenario: 87.5 thousand tons (mechanical recycling), 674.7 thousand tons (incineration), and 60 thousand tons (Pyrolysis). Source: Joyce and Paquin (2016) [8].

incineration, and gasification, determining what percentage of the waste is directed to each unit to generate higher profit and lower environmental impact [11]. In addition, the pyrolysis unit has an electrical energy demand of 124.3 mJ per ton of plastic waste processed, which the incineration unit can supply.

Distribution

Diesel trucks will be used in the logistics of the plastic waste and in the distribution of the products. Pollution generated by land transportation between units was not considered due to its minimal impact.

Use Phase

It is estimated that a pyrolysis chemical recycling plant capable of processing 30,000 tons of plastic waste per year would require a usable area of 4,500 m^2 [11]. In the Brazilian reality, to process all the plastic waste destined for the pyrolysis unit, an area 5.53 times larger would be needed.

End-of-Life

Plastic waste collected and sent for pyrolysis and mechanical recycling produces solid residue. 65 kg and 60.8 kg per ton of plastic are estimated to be processed, respectively. This waste goes to the incineration plant, generating 100 kg of solid waste per ton of processed material destined for the landfill.

Environmental Impacts

The calculations for the environmental impact require the use of software to which we did not have access, so we could not apply the State of São Paulo generation values in this component. We consider the scenario described by Khoo (2019), where 87,500 tons of waste are sent for mechanical recycling, 674,700 tons for incineration, and 60,000 tons for pyrolysis, used as sustainability indicators for the LCA. The potential for climate change was characterized by the emission of greenhouse gases (742,000 tons of $CO_{2\text{-eq}}$), terrestrial acidification (121 tons of $SO_{2\text{-eq}}$), and the formation of particulate matter (28.5 tons of PM 10-eq). In addition, 76,500 tons of waste from recycling processes were ultimately sent to landfill. It is worth noting that this value corresponds to less than 10 % of the total waste sent for recycling [11].

Environmental Benefits

A significant reduction in waste volume sent to landfills can be calculated. The estimated recovery of petrochemicals by pyrolysis is ~ 1.6 GJ, the energy recovery is ~1.45 GJ, the recovery of polyethylene is 350.8 kg, and of PET is 36.4 kg per mechanical recycling.

<u>Social Layer</u>

A sustainable business model also requires the development of a social layer that considers social value through the actions of an organization [8]. The Figure 3 presents the assembly of the Business Model Canvas from a social perspective.

Social Value

The conversion of plastic waste through pyrolysis contributes to reducing the impact of marine contamination and improves the integration of stakeholders such as the polymer producer, balanced commercial relationships with waste pickers' cooperatives, and support to municipal governments in their urban waste treatment missions.

End Users

Fuel, grease, and polymer producers can use the pyrolysis product. Working with NGOs or waste pickers' cooperatives may promote a change in how society deals with the problem.

Range

Development with NGOs at the national or international level, such as Precious Plastic (https://preciousplastic.com/), polymer-producing companies, and polymer end-using companies and their circularity actions with society, should be evaluated.

Figure 3. Infographic of the social layer analysis of a pyrolysis unit's Triple Layer Business Model Canvas.

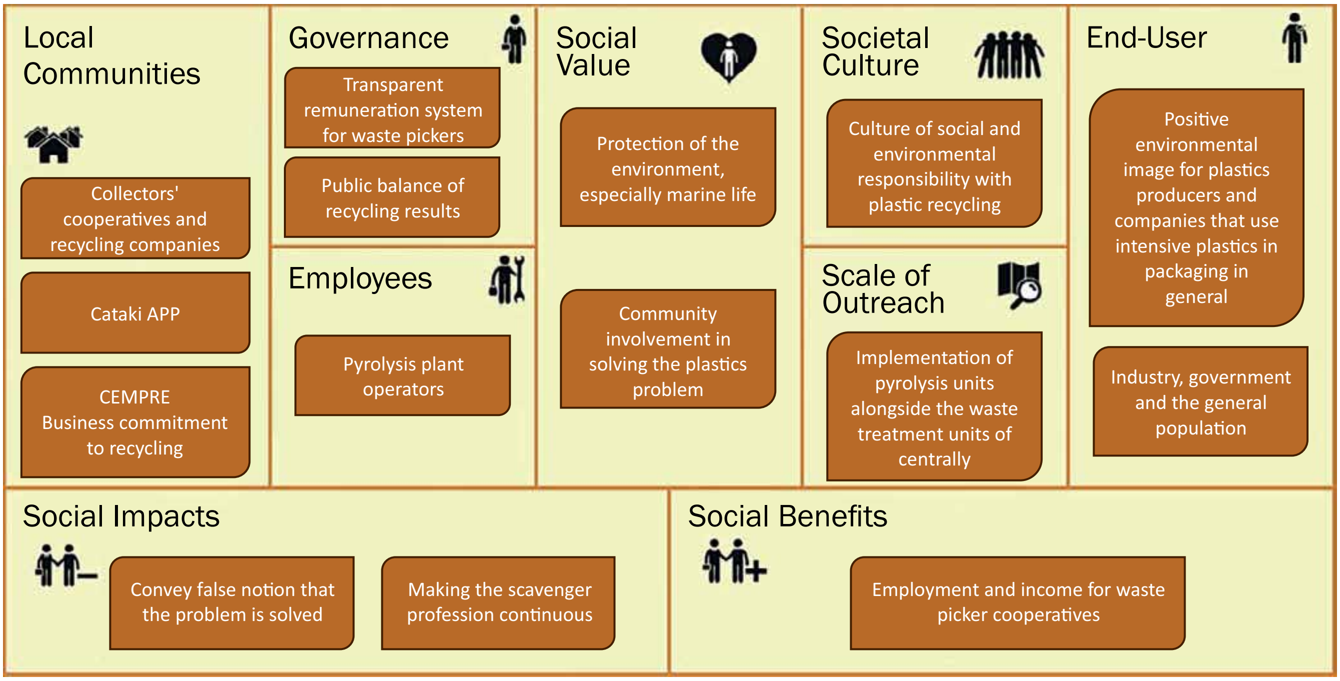

Source: Joyce and Paquin (2016) [8].

Social Culture

This component recognizes the potential impact of an organization in society. How do people behave towards plastic waste, and what actions must be developed to promote recycling? NGOs and business organizations (e.g., CEMPRE – Business Commitment for Recycling, AEPW – Alliance to End Plastic Waste) collaborate in developing a more conscious positioning of society.

Governance

This component captures the organizational structure and decision-making policies, defining which stakeholders an organization will likely identify and engage. Polymer producers and governments as stakeholders have critical decision-making responsibilities. The recycler is responsible for a transparent system that considers adequate remuneration of waste pickers and an audited public balance sheet on recycling performance.

Employees

Employees are the central part of the organization. It must be considered the number of jobs, types of functions, and essential demographics such as wage variations, gender, ethnicity, and education within the organization. The number of recycling jobs can range from 10 (sorting centers) to 300 (cooperatives/recycling associations).

Local Communities

Here, the role of waste pickers' cooperatives is fundamental because they are a relevant link in the supply of waste.

Social Impact

The social impact component addresses the social costs of an organization. It complements the financial costs of the economic layer and the biophysical impacts of the environmental layer. There are two issues: taking the false conclusion that the recycling problem is solved and perpetuating the current working conditions of waste pickers.

Social Benefits

These are the positive aspects of social value creation from the organization's actions. A clear indicator of social benefits will be the improvement of income and working conditions of waste pickers' associations.

Conclusion

This article analyzed the chemical recycling of plastic waste using the Canvas of triple layer business model application from a sustainable development perspective with economic, environmental, and social impacts. This approach allowed a comprehensive analysis of the sustainability-oriented business model. Pyrolysis is one of the plastics' recovery technologies. Although the return-on-investment rates are estimated between 16 and 21%, is not enough to justify a project because of the risks of a reliable supply of the material to be processed or the product to be commercialized, being necessary to consider also the environmental and social benefits. The collaboration of value chains is critical to achieving the full benefits of plastic regeneration. We can conclude that pyrolysis is viable only as a complementary process to other mechanical recycling and energy recovery methods. We can also identify clear social benefits for waste pickers' cooperatives in structuring a more dignified and sustainable relationship, as well as image and recycling obligations on the part of companies and waste treatment obligations on the part of municipal governments.

References

1. Europe P. EPRO. Plastics - the Facts 2019. An analysis of European latest plastics production, demand, and waste data. Plastics Europe 2019. Annual Report.
2. Kakadellis S, Harris ZM. Don't scrap the waste: The need for broader system boundaries in bioplastic food packaging lifecycle assessment – A critical review. Journal of Cleaner Production 2020;274:122831.
3. Al-Salem SM et al. A review on thermal and catalytic pyrolysis of plastic solid waste (PSW). Journal of Environ. Management 2017;197(1408):177–198.
4. Anuar SD et al. A review on pyrolysis of plastic wastes. Energy Conversion and Management 2016;115:308–326.
5. Monteiro ARD. Contribuição da reciclagem química de resíduos plásticos para o desenvolvimento sustentável. 2018. Universidade Federal do Rio de Janeiro, 2018.
6. QureshiMS et al. Pyrolysis of plastic waste: Opportunities and challenges. Journal of Analytical and Applied Pyrolysis 2020:104804.
7. Das P, Tiwari P. Valorization of packaging plastic waste by slow pyrolysis. Resources, Conservation and Recycling 2018;128:69–77.
8. Joyce A, Paquin RL. The triple layered business model canvas: A tool to design more sustainable business models. Journal of Cleaner Production 2016;135:1474–1486.
9. Osterwalder A, Pigneu Y, ClarkT, Smith A. Business model generation: A handbook for visionaries, game changers, and challengers, 2010.
10. Larrain M et al. Economic performance of pyrolysis of mixed plastic waste: Open-loop *versus* closed-loop recycling. Journal of Cleaner Production 2020;270:122442, 2020.
11. Cetesb. Inventário Estadual de Resíduos Sólidos Urbanos: 2018. Companhia Ambiental do Estado de São Paulo: 120 p.49, 2019.
12. Khoo HH. LCA of plastic waste recovery into recycled materials, energy and fuels in Singapore. Resources, Conservation and Recycling 2019;145:67–77.
13. Gutierrez RF, Gitahy L. A comercialização dos resíduos sólidos urbanos de plásticos no estado de São Paulo. Catadores Mater. Recicláveis um encontro Nac. 1ed. Rio de Janeiro: 2016:537–558.

Evaluation of the Store Potential of Green Hydrogen in Bahia, Brazil

Maíra Silva Andrade[1*], Carolina Sacramento Vieira[1], Vitório Donato[1]
[1]SENAI CIMATEC University Center;Salvador, Bahia, Brazil

The use of green hydrogen (GH_2) as an energy source is considered essential for decarbonizing the world energy matrix. It is a central element of the investment plans announced by many countries toward carbon neutrality. Brazil occupies a privileged position since the national energy matrix is composed of about 85% of renewable energy, mainly hydroelectric, in addition to the growing presence of wind, solar, and biomass energy, combined with an interconnected transmission system and the availability of potable water. However, there are still many challenges for the insertion of this renewable energy source in the Brazilian electrical matrix, including the storage of GH_2. In this context, the present article aims to evaluate the storage potential of GH_2 in the State of Bahia, analyzing the identity of 27 territories at the State.
Keywords: Green Hydrogen. GH_2 Storage. Renewable Energy.

Introduction

Green hydrogen has emerged as a basis for global energy transformation. It can contribute to reducing CO_2 emissions by about 60% until 2050, considering an increase in the world population to approximately 11 billion people [1].

The advent of an industry for hydrogen production will require the planning of new and updated logistical assets such as gas pipelines, road infrastructure, and specific technologies for storage. These actions will demand capital, a continuous and qualified workforce, resources for construction, and access to new technologies.

Brazil occupies a privileged position in the energy transition process underway in the world because of the tremendous competitive potential for producing green hydrogen due to the generation of electricity from renewable sources and the availability of potable water. However, for the insertion of this renewable energy source in the Brazilian electrical matrix, there are still many challenges to be overcome. In this context, the main objective of this article is to evaluate the storage potential of GH_2 in Bahia.

H_2 storage is a big challenge and a key element in its large-scale use. Storing hydrogen on a large scale is necessary to increase its density through high storage pressure, low temperature, or using a material that adsorbs hydrogen molecules [3-6]. The main complexity in the storage of H_2 is its low density under Normal Conditions of Temperature and Pressure (CNTP) (0.084 kg/m^3). This density, whether in the liquid or gaseous state, results in a low density of contained energy, making it necessary to store large volumes. Consequently, it is necessary to modify its density through pressure and/or temperature variations for its storage [7].

Currently, there are four possible techniques for storing hydrogen. They are i) pressurized tanks (gaseous hydrogen), ii) cryogenic tanks (liquid hydrogen), iii) carbon steel tanks (LOHC - Liquid Organic Hydrogen Carriers), and vi) carbon steel tanks (storage in the solid state-adsorption). These different H_2 storage technologies differ mainly in terms of efficiency, energy density, tightness, level of development, safety, availability, installation complexity, and process maturity [8]. Therefore, this study will classify hydrogen storage techniques into two main categories: physical and chemical storage [3].

In physical storage, hydrogen is stored in one of its physical states: gaseous or a supercritical liquid. Equipment such as pressurized, cryogenic spheres,

Received on 22 November 2022; revised 28 February 2023.
Address for correspondence: Maíra Silva Andrade. Rua Pataro Machado, 450, Cond. Solar de Vilas, apt. 208, Torre 3. Zipcode: 42702-260. Lauro de Freitas, Bahia, Brazil. E-mail: maira.andrade@fieb.org.br. DOI 10.34178/jbth.v6i1.282.

J Bioeng. Tech. Health 2023;6(1):69-75

or salt caves can be used in this case. Currently, this hydrogen storage method is the most used and mature technology. Despite the high storage pressure, the energy content per weight remains low due to the very low density of H_2. Although it is commercially available, this form of storage generates losses of around 10% [3].

The H_2 liquefaction process ensures better storage in terms of higher energy density. However, this technique requires a cryogenic system to maintain the hydrogen in the liquid state under pressures of 0.1 MPa and temperatures of -253 °C [8]. The liquefaction of hydrogen presents substantial advantages since, in this case, hydrogen's density enormously increased (by about 833 times). However, this process consumes much energy (in the H_2 liquefaction stage), and there are evaporative losses (in the storage stage). Because of this, the losses of this technique reach 40% of the energy content [8,9]. Underground storage of H_2 in salt caverns is an alternative to large-scale storage. Despite its storage potential, low operating cost, and the fact that underground salt locations are well known, only a few salt caves have been created to store hydrogen. Salt caverns in Brazil are known to exist in Bahia (Down Química) and Alagoas (Braskem).

In physicochemical storage, hydrogen can be stored through the chemical composition of pure H_2 with metal hydrides or chemical hydrides, adsorbed on carbon, stored in glass microspheres, or using Liquid Organic Hydrogen Carriers (LOHC). LOHC - Liquid Organic Hydrogen Carriers are among the most promising options for H_2 storage in large volumes. Compared to pressure storage, the advantages are reduced weight and volume and easier handling. This storage is done in two stages: initially, the H_2 is charged in the LOHC molecule (hydrogenation), and later, after transport and storage, the H_2 unloading (dehydrogenation) is carried out at the point of consumption [3]. The leading carriers used as LOHC are petroleum-based liquids, dibenzyltoluene (DBT), N-ethylcarbazole (NEC), and toluene (TOL) [10]. LOHC has excellent potential to handle hydrogen as an ordinary liquid, requiring similar environmental conditions to petroleum-based liquids (e.g., diesel, gasoline). This characteristic allows the LOHC to be stored using existing infrastructure in conventional crude oil tanks [11].

The State of Bahia has the production chain for the main LOHCs mentioned above due to the petrochemical industry and local refineries, which makes it possible to sell hydrogen and Liquid Organic Hydrogen Carriers (LOHCs). Ammonia (NH_3) is also an alternative for hydrogen storage as it allows storage in the liquid phase under mild pressure and temperature conditions with a higher volumetric density of hydrogen than liquid H_2. It also has a relatively high ignition temperature, increasing safety during storage. However, these techniques are still under development and are not considered mature.

Materials and Methods

Study Area Description

Figure 1 presents the sample space under the study, which is composed of 27 regions of Bahia. In this article, the GH_2 storage potential in Bahia was mapped to show a spatial distribution of this potential in the 27-Identities of Territory. The maps were made using the Geoprocessing software ArcGIS Pro version 2.9.2 using shapefile files from the database of the "Superintendence of Economic and Social Studies of Bahia", "Map Biomass" and the "Portal de Mapas do IBGE", (2021).

These potential territories differ because of the existing facilities and infrastructure such as Oil Refineries, Private Use Terminals (TUP), Storage and Distribution Terminals, Liquefied Petroleum Gas Bases (GLP), Processing Units Natural Gas (UPGN) and Compressor Stations. These facilities and structures have technologies for the physical storage of H_2, such as tank parks that are composed of spheres, pressurized tanks, cryogenic tanks, compression stations, decompression stations, devices for receiving, moving, and delivering gases and liquefied products, as well as, they also

Figure 1. Territories’ identitity in Bahia, Brazil.

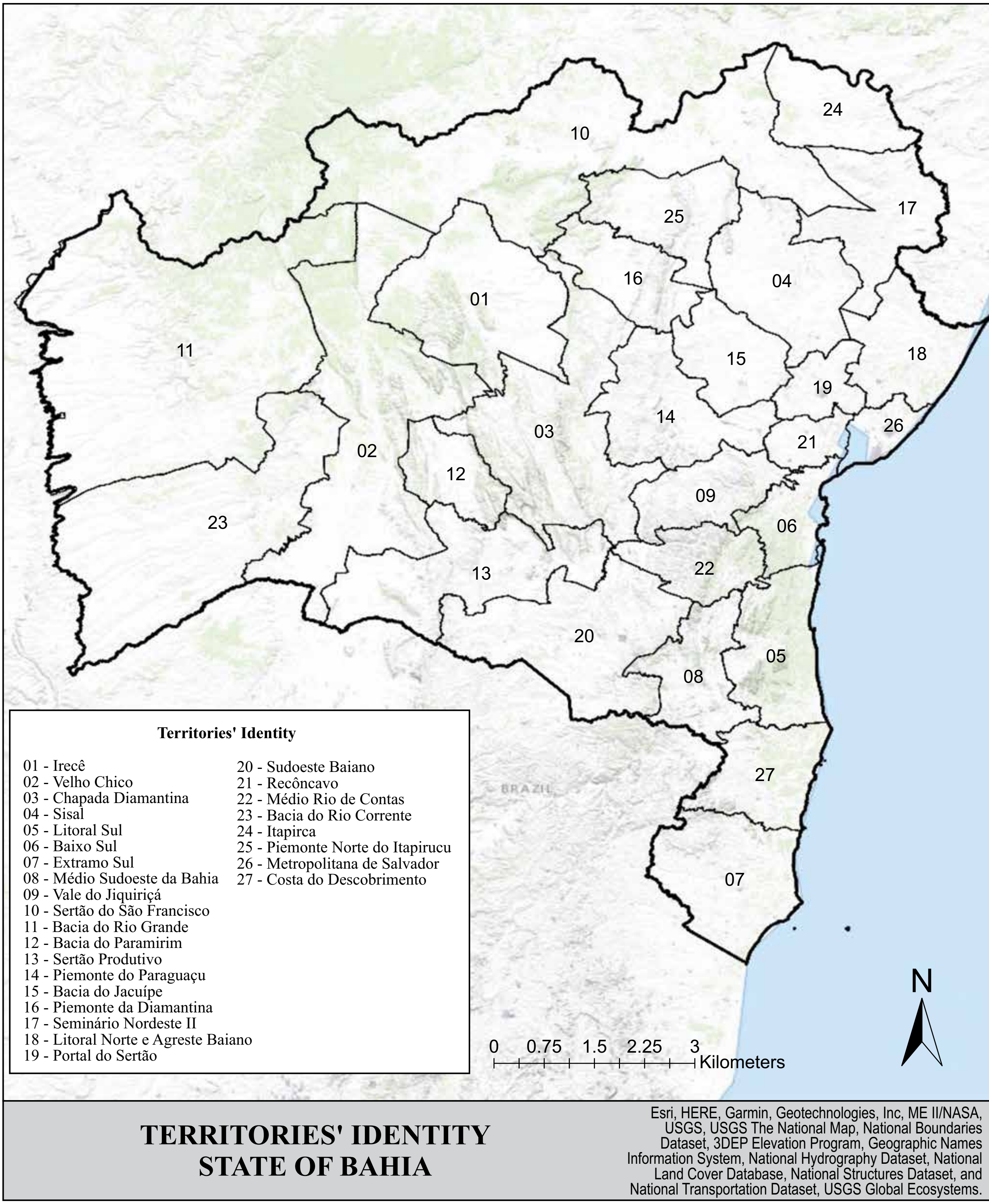

Source: Authors, 2022.

have safety and cleaning equipment, a network of internal and external pipelines.

In addition, refineries use special process conditions to keep the product below its boiling point, which is of great importance due to the difficulty of storing H_2 in the liquid state. Therefore, the storage units of this product are made up of liquefaction systems.

Results and Discussion

Figure 2 presents the updated infrastructure map with the potential for physical storage in Bahia and the existing pipeline network in the identified territories.

Bahia has six regions with infrastructure, facilities, and technologies for the storage of gases and petroleum products, and petrochemicals. The regions are Extremo Sul, Litoral Sul, Médio Rio de Contas, Litoral Norte and Agreste Baiano, Metropolitana de Salvador, and Sertão do São Francisco.

The Region Metropolitana de Salvador (RMS) has the highest concentration of facilities, infrastructure, and technologies for storing gases, petroleum products, and petrochemicals. In this region is located the Landulpho Alves Refinery (new AELEN), Petrochemical Complex, Gas Terminals, GLP Bases, and Ports specialized in gases, petroleum, and petrochemical products.

The region Litoral Sul disposes of the Oil Storage Terminal and its derivatives, the Private Use Terminal, and a GLP Base. The region Médio Rio de Contas also has an Oil Storage Terminal and

Figure 2. Physical storage potential of H_2 in Bahia.

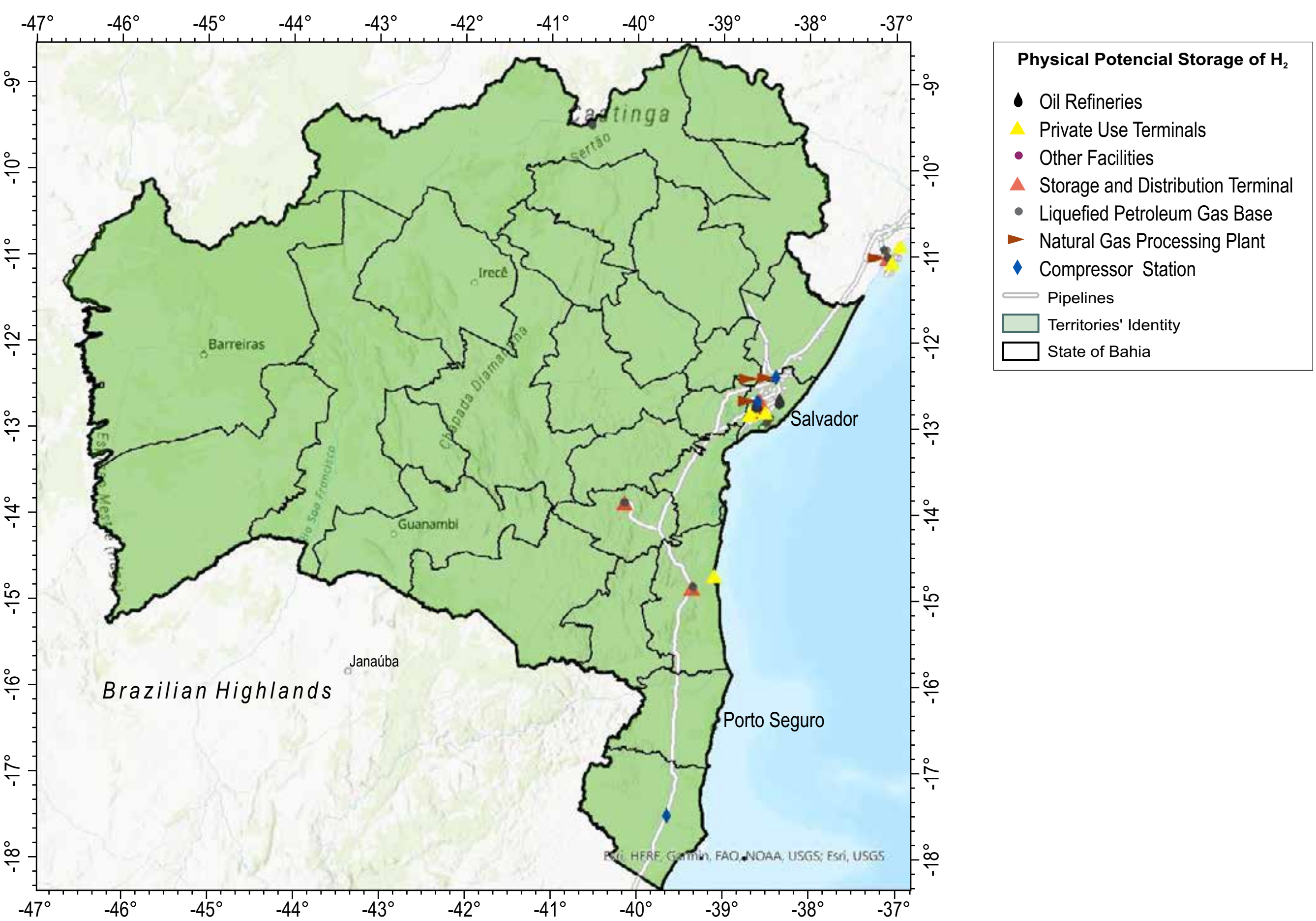

Source: Authors, 2022.

GLP Bases. Also, the Extremo Sul and Litoral Norte and Agreste Baiano Territories have Compression Stations, and the region do Sertão do São Francisco has a GLP Base. Finally, the other 20 regions do not have facilities, infrastructure, or technologies for storing gases.

Table 1 details the existing storage facilities, infrastructure, and technologies (atmospheric tanks, pressurized tanks, and spheres) with the potential for H_2 storage. The advantage of using existing facilities is to lower the infrastructure costs necessary for handling this new fuel.

Figure 3, in turn, presents the updated map of infrastructure with the potential for physicochemical storage of GH_2 in Bahia and the existing pipeline network in the territories' identity.

Figure 3 shows that only RMS has pre-existing infrastructure, facilities, and technologies for physicochemical storage, thus reducing the cost of implementation. In this territory are the

Table 1. Physical storage potential of H_2 in Bahia

Territories' Identity	Storage Technologies
N° 18 Litoral Norte	Compression System and Compressor Station (Catu)
N° 26 Região Metropolitana de Salvador	Compression System (São Francisco do Conde); **Petroleum and Derivatives Storage Terminals:** Chemical Terminal of Aratu (Candeias); VOPAK (Candeias); Transpetro (Candeias); Transpetro (Madre de Deus); **Gas Storage Terminal:** Regasification Terminal of GNL (TRBA) (Madre de Deus); Waterway Dock of Madre de Deus (Madre de Deus); Dow Aratu Ship Dock (Candeias); Cotegipe Ship Dock (Candeias); **Oil Refineries:** Landulpho Alves Refinary (RLAM), new ACELEN (Madre de Deus and São Francisco do Conde); **Other Facilities:** Braskem Basic Inputs (Camaçari); White Martins (Camaçari); Air Liquide (Camaçari); Unigel (Camaçari); Petrobrás (Candeias); UPGN: Petrobrás (São Francisco do Conde); Petrobrás (Pojuca); Petro Recôncavo (Mata de São João) Alvopetro (Mata de São João); Bases GLP: BahiaGás e NGB (Salvador); NGB, Liquigás, SuperG. and BahiaGás (São Francisco do Conde)
N° 07 Extremo Sul	Compressor Station (Alcobaça)
N° 22 Médio Rio de Contas	Petroleum and Derivatives Storage Terminal: Transpetro (Jequié); GLP Bases: Super Gás and NGB (Jequié)
N° 05 Litoral Sul	Petroleum and Derivatives Storage Terminal: Transpetro (Itabuna); GLP Bases: NGB (Itabuna)
N° 10 Sertão do S. Francisco	GLP Bases: BahiaGás e NGB (Juazeiro)

Table 2. Physical-chemical storage potential of H_2.

Territories' Identity	LOHC	Ammonia	Methanol	Natural Gas
N° 26 (RMS)	Braskem and ACELEN	Unigel	Metanor	BahiaGás

Landulpho Alves Refinery (new ACELEN), Unigel – Fafen, Metanor, Braskem, and BahiaGás. Table 2 details the existing facilities, infrastructure, and technologies with the potential for physicochemical storage of H_2.

Conclusion

This article sought to evaluate the potential for GH_2 storage in the State of Bahia. The results show that the RMS has the most significant potential for physical storage and physicochemical storage in Bahia due to the existence of infrastructure and storage technologies.

Storage is a significant challenge for the development of the H_2 economy, and the choice of the best storage technology depends on the type of application and the specific context of each situation. Several methods have proved to be technically viable for storing hydrogen, but few options have reached technical maturity and, consequently, commercial maturity for large-scale use.

Regarding the national energy transition, the gaseous storage method will be the most used at the beginning of the penetration of H_2. However, the technical difficulties of conservation and high energy demand for liquefaction mean that liquid hydrogen storage systems are not yet strong candidates for widespread use, even considering that they have an energy density twice more significant than that of H_2 compressed.

This work contributes to decision-making in analyzing the technical and economic feasibility of implementing GH_2 hubs in Bahia.

Figure 3. Physicochemical storage of H_2 in Bahia.

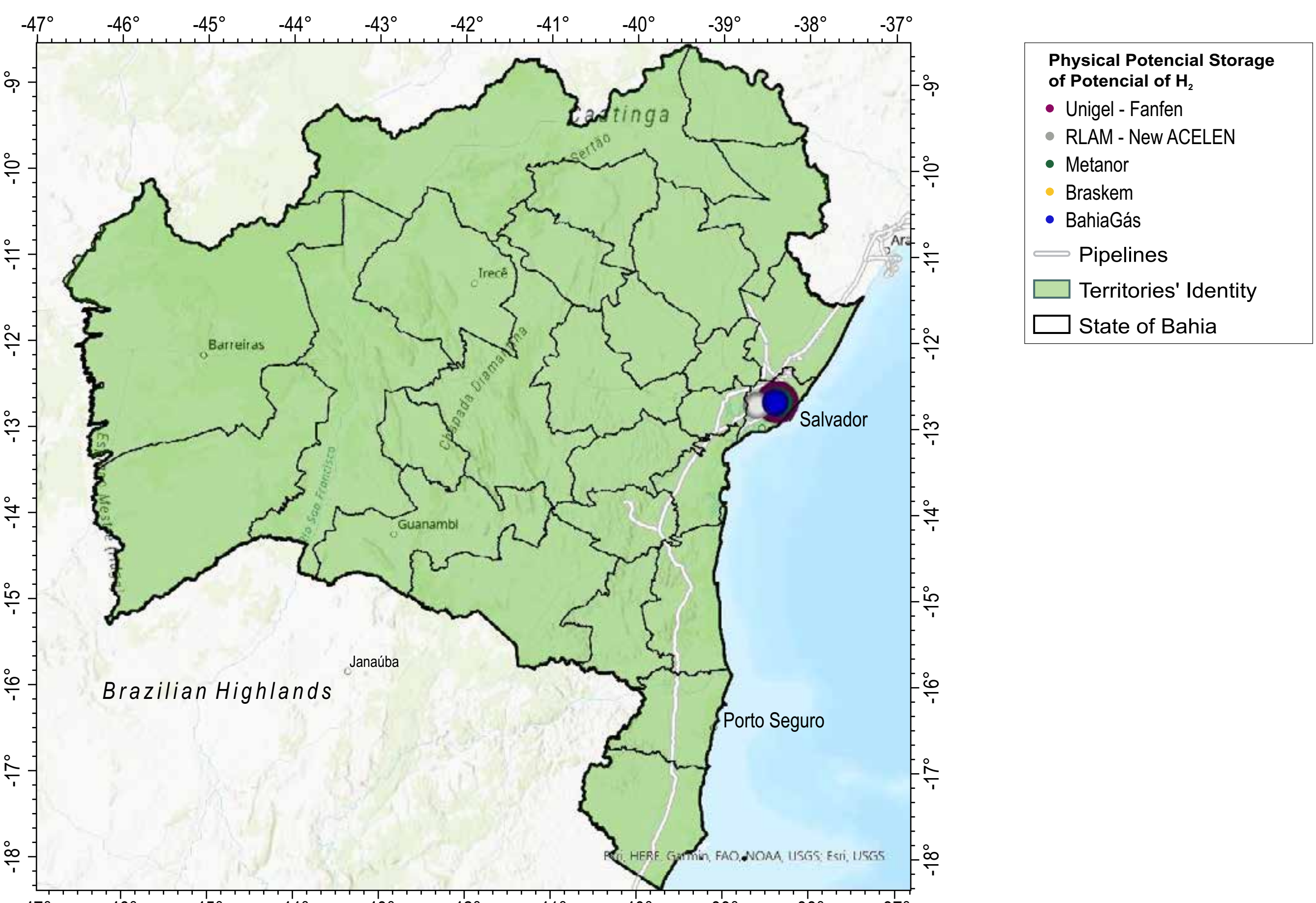

Source: Authors, 2022.

References

1. COAG Energy Council Hydrogen Working Group et al. Australia's National Hydrogen Strategy. 2019.
2. Moradi R et al. Hydrogen storage and delivery: Review of the state of the art technologies and risk and reliability analysis. International Journal of Hydrogen Energy, 12254-12269. 2019. Doi. 10.1016/j.ijhydene.2019.03.041.
3. Amaral MM. Avaliação técnica do transporte e do armazenamento de hidrogénio visando a descarbonização do sistema energético nacional. Tese de Doutorado. 2021.
4. Abe JO, Popoola API, Ajenifuja E, Popoola OM. Hydrogen energy, economy and storage: Review and recommendation. Int J Hydrogen Energy 2019;44:15072–15086.Doi:10.1016/j.ijhydene.2019.04.068.
5. Li Z et al. Development of renewable energy multi-energy complementary hydrogen energy system (A Case Study in China): A review. Energy Exploration & Exploitation 2020;38(6):2099-2127.
6. International Energy Agency. Hydrogen. 2020. Disponível em: https://www.iea.org/reports/hydrogen. Acessado em setembro de 2021.
7. Amirante R, Cassone E, Distaso E, Tamburrano P. Overview on recent developments in energy storage: Mechanical, electrochemical and hydrogen technologies. Energy Conversion and Management 2017;132:372– 387.
8. Gonzatti F et al. Fundamentos para concepção, controle e automação de uma planta armazenadora de energia utilizando hidrogênio. 2017. Tese de Doutorado. Universidade Federal de Santa Maria.
9. Abohamzeh E et al. Review of hydrogen safety during storage, transmission, and applications processes. Journal of Loss Prevention in the Process Industries 2021;72:104569.
10. Southall E, Lukashuk L. Hydrogen storage and transportation technologies to enable the hydrogen economy: Liquid organic hydrogen carriers. Johnson Matthey Technology Review 2022.
11. Niermann M et al. Liquid organic hydrogen carriers and alternatives for international transport of renewable hydrogen. Renewable and Sustainable Energy Reviews,v. 2021;135:110171.

Prospecting Adsortion Technologies for Carbon Capture

Lucas Meireles Fontes[1*], Gabriel de Veiga Cabral Malgaresi[1], Reinaldo Coelho Mirre[1]
[1]SENAI CIMATEC University Center; Salvador, Bahia, Brazil

Currently, the method of post-combustion in industries that uses the adsorption technique to capture and separate carbon dioxide from the flue gas is widely studied due to energy efficiency, ease of handling, lower cost, and environmental risk compared to other separation techniques. Regarding the adsorbents used in adsorption, zeolites are one of the most promising because they are one of the most efficient materials with high adsorption capacity due to their unique properties. However, despite the promising performance, the adsorbents need studies that enable a lower cost, more efficient, and selective control to better understand and validate utilization as a material for flue gas CO_2 capture.
Keywords: Post-Combustion. Zeolites. Separation Methods. Adsorption. Selectivity.

Introduction

The impacts caused by the greenhouse effect have environmental and health problems that directly impact the global economy, directly affecting the world GDP by about 5% to 20% due to this phenomenon [1]. Gases such as carbon dioxide (CO_2) represent about 74% of polluting gases in the atmosphere, in addition to methane (CH_4) and nitrous oxide (N_2O), which represent 17% and 6.2%, respectively, of the total emissions produced by man. Emissions of greenhouse gases that trap heat from the sun are constantly increasing, leading to global warming and climate change. According to the United Nations, such effects are linked to fossil-based energy generation, deforestation, industrial and manufacturing flue gas emissions, transportation, and food production [2].

Despite all the incentives and technological advances, the global energy matrix still depends on the use of fossil fuels. According to the International Energy Agency (IEA), more than 80% of the world's electricity production is made up of fossil fuels, emphasizing the panorama of dependence on sources that generate more significant emissions of greenhouse gases. In addition, the context of technological development grows and generates an ever-increasing energy demand, which leads to a vicious cycle of greenhouse gas generation [3]. Thus, several capture processes are being developed to treat gases in the industry, such as pre-combustion, oxy-combustion, and post-combustion. These methods are studied and applied to separate and recover polluting gases, mainly carbon dioxide. However, the financial infeasibility, reduced performance of thermoelectric plants, and other factors make applying these practices difficult. In this context, there is a clear need to study techniques to mitigate carbon dioxide emission and reduce its concentration in the atmosphere. Therefore, the objective of this article is to understand the adsorption technology used to capture carbon from post-combustion gases and to conduct a comparative study of the primary adsorbent materials.

Materials and Methods

A technological prospection of the leading carbon capture processes was initially carried out to achieve the proposed objective. After studies on the technical feasibility of carbon capture technologies for the various gas generation processes (pre-combustion, oxy-combustion, and post-combustion), the application of carbon capture technologies in the post-combustion process was selected because it is a process, relatively

Received on 15 October 2022; revised 26 January 2023.
Address for correspondence: Lucas Meireles Fontes. Avenida Orlando Gomes, Piatã. Zipcode: 41650-010. Salvador, Bahia, Brazil. E-mail: lucas.fontes@ba.estudante.senai.br.DOI 10.34178/jbth.v6i1.283.

J Bioeng. Tech. Health 2023;6(1):76-82

easier to implement and with less intervention in the existing industrial layout. Furthermore, it is possible to implement different carbon capture technologies in post-combustion processes. This work selected the adsorption method due to its very high efficiency, primarily through microporous materials. There are several adsorbent materials under study and others with high technological maturity. Zeolites is an established material on the market, however, needs to be better studied and compared due to their properties, such as high selectivity and versatility. Figure 1 shows the method sequence used in this work, ranging from the study of technological prospecting of the various carbon capture technologies to the use of zeolites as adsorbent materials in capturing carbon from post-combustion gases.

Results and Discussion

Carbon capture technologies can be implemented at different stages of an industrial process. However, the simplest way, with fewer structural modifications of an industrial plant already in operation, is the implementation of carbon capture technologies in the post-combustion process. In this process, channeling the flue gases to a carbon capture unit is sufficient. In this unit, different carbon capture technologies can be used.

Carbon Capture Methods

Among the CO_2 capture methods, the most relevant and economically viable technologies for separating carbon dioxide from the flue gas are chemical absorption, adsorption, cryogenics, and membrane separation. Table 1 shows these methods' main differences and characteristics that separate carbon dioxide from flue gases [4].

Of the methods showed in Table 1, the adsorption method was one of the most efficient, cheap, and currently used, easy to handle, with less environmental risks, and requires less energy to regenerate adsorbent materials [1].

Adsorption

It is the physicochemical process where atoms are retained on the surface of a given material and can vary between chemical adsorption (chemisorption) or physical adsorption (physisorption). The first refers to the interaction between the molecules and the solid adsorbent material, which rearrange themselves and change the shape of the electronic orbit, even partially. It is an almost always exothermic process and similar to a chemical reaction. The second occurs through interactions through weak and long-range Van der Waals forces that are physically attached to the adsorbent, and this process is always exothermic and reversible. [8] Figure 2 shows a schematic of a fixed bed adsorption process. The flue gas enters through the lower part of the adsorption tower at 25oC and 0.0059 atm, where adsorption occurs in the porous adsorbent material. The flue gas that contains CO_2 interacts with the adsorbent material while the other flue gas components permeate through the bed and exit the process through the top of the tower.

Figure 1. Flowchart of the method used in this study.

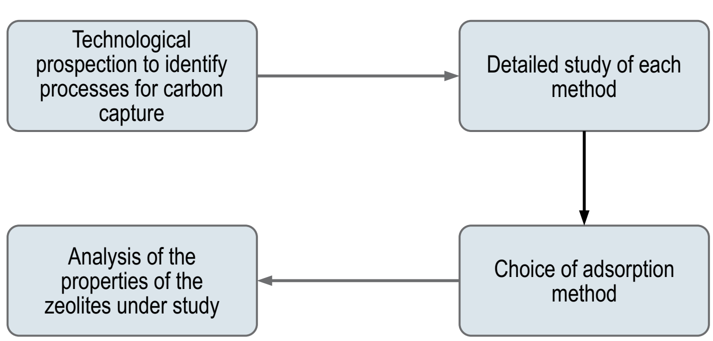

Table 1. Separation methods.

Separation Methods	Features	Process Conditions	Ref.
Adsorption	It is the physicochemical process where atoms are retained on the surface of adsorbent material. This method is very efficient and is one of the most used for CO_2 capture, especially with zeolites. Usually, for CO_2 capture, the adsorption technology is typically used with amine solvents to optimize the process.	Adsorption process: P = 0.04-1.97 atm; T=25°C-30°C Desorption Process: P= 0.001-0.008 atm; T= 40°C -60°C	[1] [4] [5]
Absorption	A physical or chemical process in which molecules are introduced into another component's medium and fixed. It is one of the most promising methods to capture CO_2 due to its ease of application, efficiency, and low operating cost, and CO_2 adsorption is usually used with amines.	Absorber: P= 2.24 atm T= 38°C-50°C; Regenerator: P=1 atm; T=100°C-121°C.	[1] [4] [6]
Cryogenic	The technique that causes CO_2 to be desublimated from the process stream through refrigeration and/or expansion of this gas. CO_2 can be recovered with 99% purity despite the high energy consumption associated with cooling the flue gases by refrigeration.	Vapor-liquid phase change: T=217 K-304 K; P=630 kPa- 7396 kPa	[1] [4]
Membranes	The physical barrier of ceramics or polymers through which the CO_2-rich gas is forced by the partial pressure difference at the entrance and exit of the permeable and selective membrane, its main problems are selectivity, permeability, and regeneration energy. Calcium oxide (CaO) membranes stand out for their crystalline structure and high porosity.	Permeate relative pressure: 0.928-11.23 bar; Input current pressure: 28 to 111 bar; T: 40°C -60°C	[1] [4] [7]

Therefore, only carbon dioxide is adsorbed due to the selectivity of the adsorbent material. This adsorbent material, after its saturation, will leave the base of the adsorption tower to the desorption tower under a temperature of 40°C and a pressure of 0.0013 atm. However, this process may vary according to the adsorbent material used. After this step, the CO_2 will be desorbed so that the CO_2 can be recovered at the top of the desorption/regeneration tower, and the adsorbent material can be reused [5].

The adsorption process is considered one of the cleanest methods for capturing CO_2. It has

Figure 2. Adsorption tower [5].

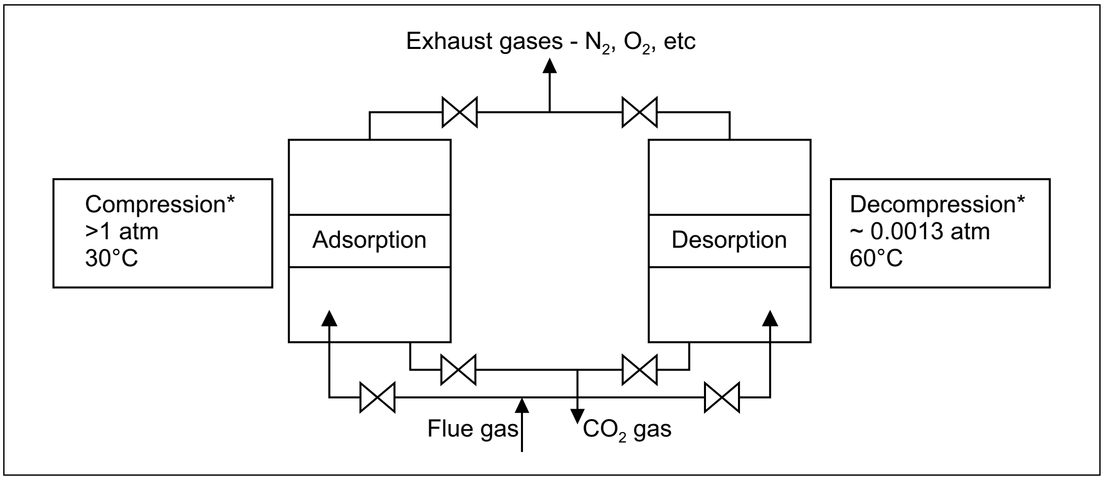

advantages over the absorption process, such as energy efficiency and regeneration, that can be easily manipulated through pressure and temperature changes. Furthermore, this method generates less toxic residue than the absorption process that typically generates alkanolamines, whose disadvantages are the toxicity and environmental damage of the solvent degradation compounds (nitrosamines) [9].

Zeolites

In 1756, the first mineral zeolite (stilbite) was discovered by Baron Cronstedt in Sweden; however, it was only in 1926 that its adsorbent characteristics came to be widely discussed due to its microporous internal structure that allows selective adsorption [10]. Its application for several processes has been carried out; in industry, zeolites have been used mainly as adsorbents for gas purification and as ion exchangers in detergents, but they are extremely useful as catalysts in petroleum refining, petrochemistry, and synthesis. of organic products whose molecules have a kinetic diameter of less than 10 Å [11]. These zeolites are natural and/or synthetic minerals, usually microporous with three-dimensional crystal lattice structures. Their vertices are joined by an oxygen atom and form a TO4 tetrahedron (T = Si, Al, B, Ge, Fe, P, Co...). Its structure is like a molecular sieve, and its microporous properties allow selectivity and high adsorption capacity with the transfer of matter between intracrystalline spaces that are limited by the diameter of the pores [12]. In addition to the properties mentioned above, it has a high specific surface area and the ability to model the electronic properties of active sites and pre-activate molecules within the pores, thanks to high electric fields and molecular confinement. Finally, it has acidic and basic properties widely used in most hydrocarbon and organic compounds reactions [13].

According to the IUPAC, zeolites are classified by ring diameter as small (less than 4 Â), medium (from 4 to 6 Â), significant (from 6 to 8 Â), and very large (from 8 to 20 Â) [14]. Regarding pressure, zeolites, generally used with amines, adsorb better at high pressures above 2 bar without water vapor and low temperatures below 30°C [15]. Among the zeolites most used in the industry, type X (faujasite) and type A stand out due to their stable crystalline structures and large pore volumes [16]. The zeolites used in this article are A, X, Y, and ZSM-5 types because of the more than 150 zeolites that have been synthesized. The most common in commercials are them because of their unique adsorption, ion exchange, molecular sieve, and catalytic properties [17]. Figure 3 (i) represents the structures of the zeolites discussed, respectively: (a) zeolite A, (b)

Figure 3. Structures of zeolites (i) and zeolites in CO_2 adsorption(ii) [18,19].

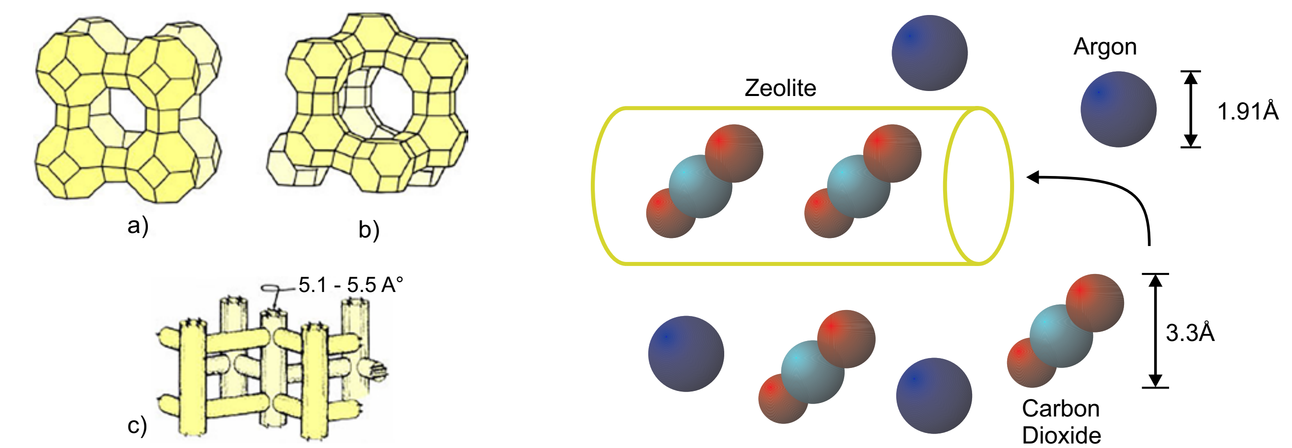

zeolite type X, Y, and (c) zeolite ZSM-5. In (ii), the entry of CO_2 into a zeolite is represented due to the reduced diameter.

It is evident the excellent adsorption capacity that allows the capture of CO_2, a molecule that, having 3.3 Å in diameter, allows mobility between the CO_2 molecules that will be trapped inside the zeolites that have a larger diameter, 5 Å for the 5A zeolite and 7.8Å for 13X zeolite, Ar whose molecule has a diameter of 1.91 Å, on the other hand, is not captured.[20] Table 2 shows the characteristics of the leading commercial zeolites.

Conclusion

After the analysis of several methods, post-combustion proved to be cheaper and easier to access the technology in order to be the most applied and developed in the industry. Among the post-combustion processes, adsorption is evident due to studies that point out that solid adsorbents potentially offer a greater capacity for capturing and separating gases in a reduced space with energy efficiency and low cost compared to other technologies. However, there is still a need to improve performance, in addition to being easy to handle and low environmental risk. Among the adsorbent materials, zeolites are most used due to their microporous structure, which has a very high effectiveness in CO_2 selectivity and requires studies that enable applications aimed at mitigating carbon dioxide emission in the atmosphere.

Acknowledgments

The authors thank PRH 27.1, ANP/FINEP, and SENAI/CIMATEC for the financial support and the research incentives.

Table 2. Characteristics of the main commercial zeolites.

Zeolites	Structure	Pore diameter(Å)/ Micropore size	Description	Application	Adsorption capacity (120oC and 1 ATM)	Silica/ Alumina ratio	Structural symbol/ Dimensionality	Ref.
A	$Na_{12}[(AlO_2)_{12}(SiO_2)_{12}] \bullet 27H_2O$ (Type 5A)	4.1 / Small	They are formed by a simple cubic arrangement with the union of two rings of four tetrahedra and the other by a truncated octahedron combining 24 tetrahedra, called cavity ß or sodalite cavity. They filter branched structures passing linear molecules, and types 3A, 4A, and 5A are defined by the position of the cations in the zeolitic structure; the effective pore diameter can vary depending on the compensating cation.	Detergent manufacturing and water hardness removal	~0.38 mol/kg	2–5	LTA / 3	[15] [11] [10] [21]
X, Y	$Na_{86}[(AlO_2)_{86}(SiO_2)_{106}] \bullet H_2O$ (Type 13X)	7.4 / Big	Type X and Y zeolites belong to the Faujasites group and have a topologically similar structure. Its unit cells have cubic structures with a dimension of about 25 Å, containing 192 tetrahedrons of (Si, Al) O_4. It is compatible with many industry reagents because it has the largest pore diameter among microporous sieves, making it a significant research focus.	Catalytic cracking and hydrocracking	~0.70 mol/kg	3–6	FAU / 3	[22] [11] [10] [21]
ZSM-5	$Na_nAl_nSi_{96-n}O_{192} \cdot 16H_2O$	5.2×5.8 / Medium	ZSM-5 zeolite is synthetic and is a suitable adsorbent for CO_2 adsorption due to its high surface area and thermal and mechanical stability. In addition, it has a high Si/Al ratio that generates format selectivity, high thermal stability, and acidity, as well as moderate hydrophilicity and high hydrophobicity.	Xylene isomerization, benzene alkylation, catalytic cracking, catalyst dewaxing, and methanol conversion	~0.38 mol/kg	30–200	MFI / 3	[23] [11] [10] [24]

References

1. Wallace B. Análise e levantamento das principais técnicas Para. 2018:1–10.
2. Nações Unidas. Causas e efeitos das mudanças climáticas | Nações Unidas. https://www.un.org/pt/climatechange/science/causes-effects-climate-change. Accessed on Jul 15, 2022.
3. International Energy Agency. Explore energy data by category, indicator, country or region. 2019. https://www.iea.org/data-and-statistics/data-browser?country=WORLD&fuel=Energy supply&indicator=TESbySource.
4. Lessa MDO. Avaliação da capacidade de adsorção do CO_2 em zeólita 13X com gases sintéticos e originados da pirólise do lodo de esgoto. 2012:93. [Online]. Available: https://repositorio.ufrn.br/jspui/bitstream/123456789/15836/1/MayaraOL_DISSERT.pdf.
5. Aaron D, Tsouris C. Separation of CO_2 from flue gas: A review," Sep Sci Technol 2005;40(1–3):321–348. Doi: 10.1081/SS-200042244.
6. Ruzaik F. Model based control of absorption tower for CO_2 capturing. 管理现代化 2008:61–64.
7. Asmara R. Modelagem matemática e simulação de um permeador de gases para separação de CO_2 de gás natural. Rev Bras Ergon 2016;3(2):80–91. [Online]. Available: https://www.infodesign.org.br/infodesign/article/view/355%0Ahttp://www.abergo.org.br/revista/index.php/ae/article/view/731%0Ahttp://www.abergo.org.br/revista/index.php/ae/article/view/269%0Ahttp://www.abergo.org.br/revista/index.php/ae/article/view/106.
8. Letterman S. 4 Adsorção 4.1. 1999:43–58.
9. Dantas TLP. Separação de dióxido de carbono por adsorção a partir de misturas sintéticas do tipo gás de exaustão. Univ Fed St Catarina 2009:172.
10. Silvestre Á, Vieira E, Barreto L. Importância das zeólitas na indústria do petróleo e no craqueamento em leito fluidizado (fcc). Bols Valor Rev Divulg do Proj Univ Petrobras e IF Flum 2012;2(1):63–75.
11. Luna FJ, Schuchardt U. Modificação de zeólitas para uso em catálise. Quim Nova 2001;24(6):885–892. Doi: 10.1590/S0100-40422001000600027.
12. Souza JVT, Massocatto CL, Diniz KM, Tarley CRT, Caetano J, Dragunski DC. Adsorção de cromo (III) por resíduos de laranja in natura e quimicamente modificados 2012;33(1).
13. Grecco STF, Rangel MC, Urquieta-González EA. Zeólitas hierarquicamente estruturadas. Quim Nova 2013; 36(1):131–142. Doi: 10.1590/S0100-40422013000100023.
14. Netto D. Utilização de zeolitas como adsorvente no tratamento terciário de efluentes líquidos provenientes de indústrias de processamento de leite. 2011:50.
15. Aquino. Remoção de CO_2 em argilas bentoníticas e zeólitas ZSM-5 modificadas com aminas. 2021:6.
16. Sherman JD. Synthetic zeolites and other microporous oxide molecular sieves. 1999. https://www.pnas.org/doi/10.1073/pnas.96.7.3471.
17. National Minerals Information Center. Zeolites Statistics and Information." https://www.usgs.gov/centers/national-minerals-information-center/zeolites-statistics-and-information#:~:text=About 40 natural zeolites have,laumontite%2C mordenite%2C and phillipsite.
18. Bonenfant D, Kharoune M, Niquette P, Mimeault M, Hausler R. Advances in principal factors influencing carbon dioxide adsorption on zeolites. Sci Technol Adv Mater 2008;9(1). Doi: 10.1088/1468-6996/9/1/013007.
19. Diego A, Lisboa O, Fagundes RC, Lima YS. Avaliação da capacidade de adsorção de CO_2 em zeólitas 13X e 5A através do Método Gravimétrico. Seminário Estudantilde Produção Acadêmica 2007;10(1).
20. Figueiredo C, Neves C, Abreu M, Schvartzman M. Separación de CO_2 por medio de tecnología PSA. 2005;28(4):622–628.
21. Magee HM, Sullivan MNS. Nitrogen gas adsorption in zeolites 13X and 5A. Adsorption 2010;24:2563–5698.
22. Vicente JGP. Síntese e propriedades da zeólita faujasita nanométrica aplicada à catálise básica. Mestrado Mestrado em Engenharia Qímica, Universidade de São Carlos,São Paulo 2015:150.
23. Frantz TS. Síntese e caracterização de zeólitas do tipo Zsm-5 para a adsorção de CO_2.Dissertação.Mestrado em Engenharia Qímica, Universidade Federal do Rio Grande do Sul 2015.
24. World of Chemicals. ZSM-5 Properties. 2022. https://www.worldofchemicals.com/chemicals/chemical-properties/zsm-5.html.

Graphene-Based Polymer Nanocomposites Preparation and Their Advantages

Felipe Valente Santos Fiscina[1*], Ricardo de Ferreira Cavalcanti de Albuquerque[1], Lilian Lefol Nani Guarieiro[1]
[1]SENAI CIMATEC Uiversity Center; Salvador, Bahia, Brazil

Graphene and its derivatives have attracted the attention of researchers since its discovery due to its surprising properties. Since then, scientists have been trying to improve the processes that allow the incorporation of this material into polymeric matrices, to improve them, through the development of graphene-based polymeric nanocomposites. This review study reviewed these methods meticulously. Furthermore, it has already been cataloged that adding small amounts of graphene nano-fillers tends to improve the polymers' mechanical, electrical, and thermal properties.
Keywords: Graphene. Nanocomposites. Polymers. Preparation Methods.

Introduction

Approximately 70 years ago, studies on graphene began, so-called then as "2D graphite". This name was given because its fine two-dimensional structure, resembling a honeycomb, which serves as a basis for other materials composed of graphite [1]. Nevertheless, what drew the most attention to this one, so far, new material, was its exceptional properties. With a specific strength of 48,000 kN m kg^{-1}, a characteristic suitable for improving the mechanical properties of polymers, together with Young's modulus of 1 TPa and fracture resistance of 130 GPa, graphene is considered one of the most robust material today [2].

Graphene oxide (GO), a product of the chemical oxidation and exfoliation of graphite, has, unlike graphene, hydroxy, and epoxy groups, which allows GO to have excellent solubility in water [3,4]. Furthermore, among the graphene derivatives (GO and rGO), graphene oxide has the highest interaction energy with polar polymer matrices, which makes it the most suitable polymer of this classification (Figure 1) [5].

Received on 18 November 2022; revised 22 February 2023.
Address for correspondence: Felipe Valente Santos Fiscina. Avenida Orlando Gomes,1845, Piatã. Salvador, Bahia, Brazil. Zipcode: 42701-310. E-mail: felipe.fiscina@aln.senaicimatec.edu.br.
DOI 10.34178/jbth.v6i1.284.

J Bioeng. Tech. Health 2023;6(1):83-86

Presenting intermediate properties to graphene and GO, such as good thermal and chemical stability and excellent electrical conductivity [6,7], reduced graphene oxide (rGO) comes from the reduction of oxygen in graphene oxide through a chemical or thermal process [5].

In order to improve the bond between the polymer and the graphene-based filler, the material is subjected to some processes, which allow graphene oxide to improve the properties of the polymer matrix, depending on the desired result with the mixture [5,8]. This surface functionalization process can be characterized into 2 types: covalent and non-covalent functionalization.

Because of the hydrophilic character of GO, due to the hydroxy and epoxy groups on its surface, small functional groups are covalently bonded to it, allowing the use of graphene oxide as a nanofiller [5]. This bond can usually be made by an aqueous solution [9]. In turn, the methods of covalent functionalization can be divided into 2 groups concerning how the covalent molecules will be integrated into the final compound.

The polymeric chains can be sintered before and then grafted onto graphene oxide through radical addition, nitrene chemistry, and amidation reaction, along with others [5]. It can also occur through the ATRP and RAFT methods, where macroinitiators are positioned on the surface, initiating the polymerization of the monomers (Figure 2) [5].

Unlike covalent functionalization, the non-covalent method has certain advantages regarding

Figure 1. Process of transforming graphene into GO and rGO [5].

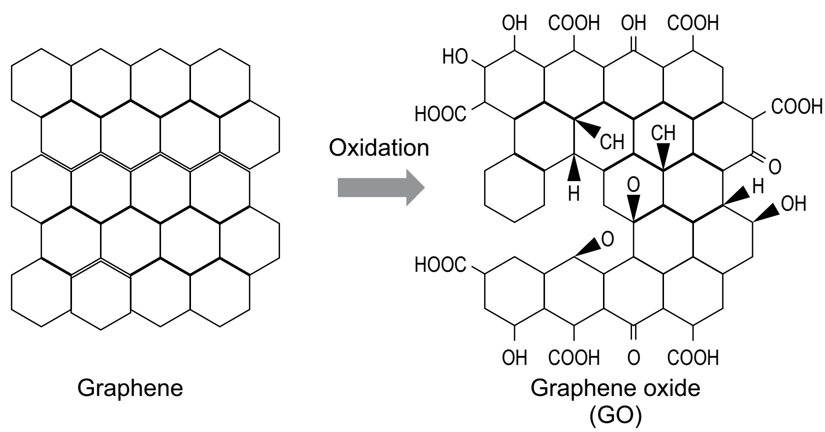

Figure 2. Classification of surface functionalization [5].

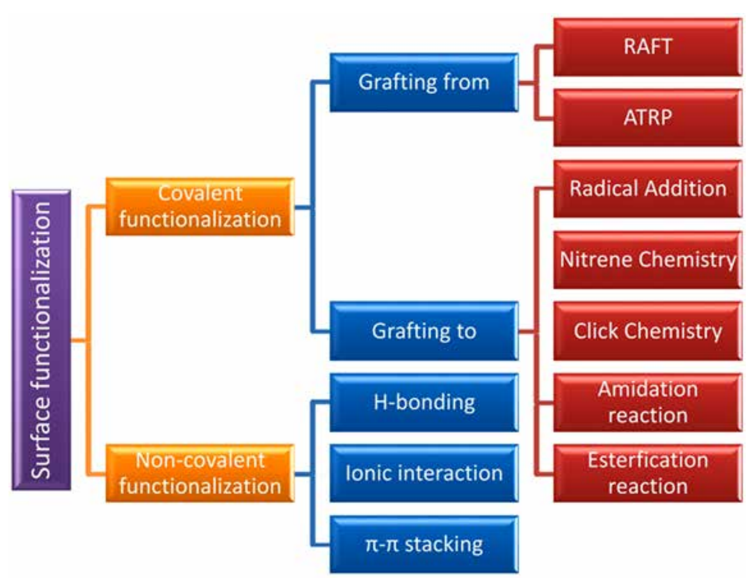

material properties, as it preserves the π-conjugation and the electronic characteristics of graphene oxide [5,9]. Furthermore, because it can be carried out in aqueous solutions at a temperature environment (mild conditions), the structure of the aromatic ring is preserved, in addition to preserving the GO nanosheets [9]. Non-covalent functionalization can occur through π-π interactions, ionic interactions, and hydrogen bonds [5].

Because of the current importance of graphene's properties, this work reviews the development of graphene-based polymeric nanocomposites.

Materials and Methods

For the development of the article, the Science Direct and Google Scholar tools were widely used to contribute to the selection of data used in the current review. In order to present current data, articles were meticulously searched using the following filters: texts published between 2012 and 2022, texts in English and present in review articles, scientific journals, and research articles.

Results and Discussion

Some methods aim to enable the synthesis of graphene-based polymer nanocomposites. For them to happen correctly, it is expected that the dispersion of graphene in the composite is as homogeneous as possible [5]. Each processing route has advantages and often presents different characteristics in the final product. Table 1 presents the primary methods found in the literature.

Over the decades, there has been an advance in the methods of synthesizing graphene-based polymer nanocomposites in terms of technologies and processes.

Developing these composites presents excellent advantages for the scientific society as a whole, as it guarantees a possibility of significant improvement of materials such as polymers through small additions of graphene and its derivatives (Table 2).

Just as the addition of graphene changes the nanocomposite's properties, the method used for this mixture also plays an essential role in the final product (Table 3).

Due to the significant improvement in the mechanical properties of the material, in addition to the cost-effectiveness for mass production, the

Table 1. Processing route of graphene-based polymer nanocomposites.

Processing Route	Procedure	Ref.
Dip-coating	It occurs when the substrate is immersed in a precursor solution composed of the polymer in a liquid state with graphene. In this way, the solution's components adhere to the surface of the immersed substrate, forming thin layers.	[5,12]
Casting	Graphene nano-filler fills a mold, adding the polymer to the entire filler. Then, heat is added to start the polymerization process when a uniform mixture is obtained.	[5]
Melt mixing	This process is done by pouring the graphene nano-filler and molten state polymer into a mixer, causing both to be homogeneously incorporated, producing graphene-based nanocomposite polymers.	[13]

Table 2. Properties of graphene-based polymer nanocomposites.

Polymer	Graphene (wt%)	Results	Ref.
Epoxy resin	0.5	Young's modulus and tensile strength increased by 13% and 83%, respectively.	[10]
PVP	2.0	Decreased tensile strength and high increase in Young's modulus.	[11]
Silicone rubber (SR)	0.5	Tensile strength increased by 175%. Also, the melting point (Tm) decreased, and the glass transition temperature (Tg) increased.	[11]
Cyanate ester resin	1.0	Flexural and impact strength increased.	[11]
Unsaturated polyester resin	10	Stiffness enhanced and a 55% increase in flexural properties.	[11]

Table 3. Advantages of processing routes.

Processing Route	Advantages	Ref.
Dip-coating	Used for polymers in a liquid state, homogeneous results cheaply.	[5,12]
Casting	Simple and inexpensive method; good thermal and electrical properties.	[14]
Melt mixing	Advantageous for large-scale production; improvement in mechanical properties (Young's modulus, tensile strength, storage modulus).	[15]

melt mixing method is the one that presents the most advantages to the product consumer.

Conclusion

Technological advances made possible by implementing graphene and its derivatives in the composites industry are increasingly observed. After showing improvements from the initial to the end phase, graphene-based polymer nanocomposites have been well-seen as the future material due to their impressive properties in several aspects.

References

1. Geim AK, Novoselov KS. The rise of graphene. In: Rodgers P. (Ed.). Nanoscience and Technology. [s.l.] Co-Published with Macmillan Publishers Ltd, UK, 2009. p. 11–19.
2. Gahlot S, Kulshrestha V. Graphene-based polymer electrolyte membranes for electrochemical energy applications, International Journal of Hydrogen Energy. Available at: <https://doi.org/10.1016/j.ijhydene.2019.06.047>.
3. Ajala OJ, Tijani JO, Bankole MT, Abdulkareem AS. A critical review on graphene oxide nanostructured material: Properties, synthesis, characterization, and application in water and wastewater treatment. Environmental Nanotechnology, Monitoring & Management 2022;18.Availabe at: <https://doi.org/10.1016/j.enmm.2022.100673>.
4. Yu H, Zhang B, Bulin C et al. High-efficient synthesis of graphene oxide based on improved hummers method. Sci Rep 2016;6. Available at: <https://doi.org/10.1038/srep36143>. Acessed on Jul 28, 2022.
5. Trivedi DN, Rachchh NV. Graphene and its application in thermoplastic polymers as nano-filler- A review. Polymer 2022;240. Available at: <https://doi.org/10.1016/j.polymer.2021.124486>. Acessed on Jul 27, 2022.
6. Castillo J et al. Influence of graphene-based compounds on the mechanical toughness and thermal stability of polypropylene. Journal of Applied Polymer Science 2020;137(10):48258.
7. Yu H, Guo W, Lu X et al. Reduced graphene oxide nanocomposite based electrochemical biosensors for monitoring foodborne pathogenic bacteria: A review. Food Control 2021;127. Available at: <https://doi.org/10.1016/j.foodcont.2021.108117>.
8. Potts JR, Dreyer DR, Bielawski CW, Ruoff RS. Graphene-based polymer nanocomposites. Polymer 2011;52(1):5-25. Available at: <https://doi.org/10.1016/j.polymer.2010.11.042≥.
9. Sainz-Urruela C, Vera-López S, San Andrés MP, Díez-Pascual AM. Surface functionalization of graphene oxide with tannic acid: Covalent *vs*. non-covalent approaches. Journal of Molecular Liquids 2022;357. Available at: <https://doi.org/10.1016/j.molliq.2022.119104>.
10. Li Z, Wang R, Young RJ et al. Control of the functionality of graphene oxide for its application in epoxy nanocomposites, Polymer 2013;54(23):6437-6446Available at: <https://doi.org/10.1016/j.polymer.2013.09.054>.
11. Saleem H, Edathil A, Ncube T et al. Mechanical and thermal properties of termoset–graphene nanocomposites. Macromol Mater Eng 2022;301:231-259. Available at: <https://doi.org/10.1002/mame.201500335>.
12. Machuno LGB et al. Multilayer graphene films obtained by dip coating technique. Materials Research [online]. 2015;18(4): 775-780. Available at: <https://doi.org/10.1590/1516-1439.005415>.
13. Allahbakhsh A. PVC/rice straw/SDBS-modified graphene oxide sustainable Nanocomposites: Melt mixing process and electrical insulation characteristics. Composites Part A: Applied Science and Manufacturing 2020;134. Available at: <https://doi.org/10.1016/j.compositesa.2020.105902>.
14. Giuri A, Colella S, Listorti A et al. GO/glucose/PEDOT:PSS ternary nanocomposites for flexible supercapacitors, Composites Part B: Engineering 2018;148:149-155. Available at: <https://doi.org/10.1016/j.compositesb.2018.04.053>.
15. Yaragalla S, Zahid M, Panda JK et al. Comprehensive enhancement in thermomechanical performance of melt-extruded PEEK filaments by graphene incorporation. Polymers 2021;13:1425. Available at: <https://doi.org/10.3390/polym13091425>.

CO_2 Separation Process of NaturalGas Streams by Membrane Permeation: Technological and Operational Approach

Fernanda dos Santos Cardoso[1*], Gabriel de Veiga Cabral Malgaresi[1], Reinaldo Coelho Mirre[1]
[1]*SENAI CIMATEC University Center; Salvador, Bahia, Brazil*

The increase in clean energy's demand, and the new policies in mitigating gas emissions with greenhouse gas have reactivated the production and market of natural gas (NG). In the fields of Brazilian pre-salt, it is ordinary for natural gas to be produced with a high CO_2 content. Therefore, the CO_2 content present in natural gas shall be separated for marketing purposes. This study aimed to review the literature on the methods of CO_2 removal of NG currents, in which the membrane permeation method was evidenced. We concluded that membrane permeation is an efficient method for CO_2 separation in isolated processes and in hybrid processes, having a lower energy consumption and enabling a higher removal rate at a relatively lower cost.
Keywords: Permeation. Membrane. CO_2. Natural Gas.

Introduction

Natural gas has become a significant energy source and is less polluted for the environment. The production and commercialization of natural gas have been growing in the face of increased oil production, new greenhouse gas emission mitigation policies, and the panorama of the international energy reality. When we analyzed the possibilities for the energy future, natural gas is a strong trend for the next twenty to fifty years [1].

Natural gas can be used in many forms, such as: in thermoelectric plants, as fuel in cars and industries, and in producing fertilizers, along with others. However, in Brazil, the form most used by natural gas is as an energy source generator for the extraction platform itself or injected back into the reservoirs to increase the amount of oil produced [2,3].

It is necessary a pre-treatment of natural gas to be marketable since it is a mixture of gases, has contaminants, especially CO_2, which cause changes in its properties and loss of its energy power [4].

Received on 10 November 2022; revised 21 February 2023.
Address for correspondence: Fernanda dos Santos Cardoso. Av. Orlando Gomes, 1845 – Piatã, Salvador – BA, Brazil. CEP: 41650-010. Email: fernanda.cardoso@aln.senaicimatec.edu.br.
DOI 10.34178/jbth.v6i1.285.

J Bioeng. Tech. Health 2023;6(1):87-90

This study aims to review the literature to understand the current techniques of CO_2 separation of natural gas, emphasizing the study of the membrane permeation separation method.

Materials and Methods

This work presents a review of the literature to understand the techniques of separation of CO_2 from natural gas streams and to explore and analyze the collected informations. The study results from qualitative approaches based on a bibliographic survey of articles dating from 2006 to 2021, based on keywords such as separation, CO_2, natural gas, and technologies.

Therefore, we did a bibliographic research in which the processes of CO_2 separation, importance, and industrial applicability was studied. The purpose included a theoretical background to consolidate a more specific approach concerning separation technologies. Regarding applicability, we would incorporate this know-how into the CO_2 separation (PECO2) pilot plant, which will be installed at SENAI CIMATEC Park in Camaçari, Bahia.

Results and Discussion

The acquisition of natural gas has increased over the years, with the search for less polluting means of fuel production and the increase in oil production. In Brazil, the production of oil and natural gas in the coming years will be influenced by the production of pre-salt reservoirs, mainly in the Santos Basin, since the oil from these reservoirs has higher levels of CO_2 [5]. The pre-salt natural gas has been used in the reservoir as reinjection. This fact is due to the need for more infrastructure for the flow of natural gas production to avoid the emission of the CO_2 produced and increase the final recovery of oil. However, because natural gas has high levels of contaminants, it is necessary to treat it so that environmental standards consume it [5].

Considering that CO_2 is one of the contaminants that can modify the characteristics of natural gas to enable the transport and commercialization of NG, the allowed limit of CO_2 in its composition is 3% v/v.

Gas efficiency is improved, and treatment is carried out by means of CO_2 separation. There are several methods of separating CO_2 from natural gas, and the main methods are based on five techniques: (i) absorption (chemical and/or physical); (ii) adsorption on solids; (iii) cryogenic separation; (iv) membrane permeation; and (v) hybrid processes, which are processes that combine more than one separation technique [6,7].

We chose the membrane separation method to be studied since it will be the technology used in the pilot plant for CO_2 removal (PECO2), which is in the mobilizing process in Atalaia Experimental Nucleus (NEAT) in Aracaju (SE) to SENAI CIMATEC Park, in Camaçari (BA).

Membranes are semipermeable barriers that selectively separate undesirable compounds from a mixture of components. The separation occurs by the difference in selectivity, membrane permeability, size of molecules, and transmembrane pressure. Membrane structures can be spiral, hollow fiber, or envelope (Figure 1). The choice of the ideal membrane depends on the components to be separated and the interaction of these components with the membrane material [8].

In the spiral membrane and the envelope type, there is a central perforated tube called the collection tube. Around this tube, layers of membrane sheets are built, composed of two membranes with a spacer between them. For the separation, the mixture of gases is injected into the space between the membranes in a horizontal direction, preventing the formation of incrustations on the membrane surface. Then, through the positive pressure generated, the gases smaller than the membrane's porosity move in the counter-current direction from the feed to the collection tube, forming the permeate. On the other hand, gases that are larger than the pore size cannot pass through and remain in what is called retentate [10].

The hollow fiber type membrane is constructed by long tubes of small diameter. For industrial applications, hundreds of thousands of these fibers are arranged in a bundle, with their ends connected to a "mirror", similar to those used in heat exchangers. They are inserted into a hull, which, unlike a spiral membrane, is generally installed upright. For separation, a mixture of gases is inserted over the outside of the fibers. Thus, gases that interact with the membrane material or that are smaller than the membrane's porosity permeate to the fiber's interior, flowing to the ends of the module and forming total permeate currents. Then, the stream that did not permeate flows to the central tube of the permeator, where it is collected in the waste stream [10].

In addition to selecting the ideal membrane structure for the process, the membrane material must be chosen correctly. This material can be divided into three types: (i) ceramic membrane (inorganic), (ii) polymeric membrane (organic), and (iii) hybrid membrane. Ceramic membranes operate in a temperature range greater than 150°C to 400°C, for a pH range of 0 to 14. They have good mechanical resistance, have a useful life of up to 10 years, and are usually used to separate gas mixtures with permanent vapors, or water with organic products. Polymeric membranes, on the other hand, operate in a temperature range of 40°C to 90°C, have a pH range of 2 to 12, have medium to poor mechanical strength, have a shelf life of up to 5 years, and are generally used to separate contaminants. Concerning the diameter of the pores

Figure 1. Structures of the different types of membranes [9]: (a) spiral-type membrane; (b) hollow fiber--type membrane; and (c) envelope-type membrane

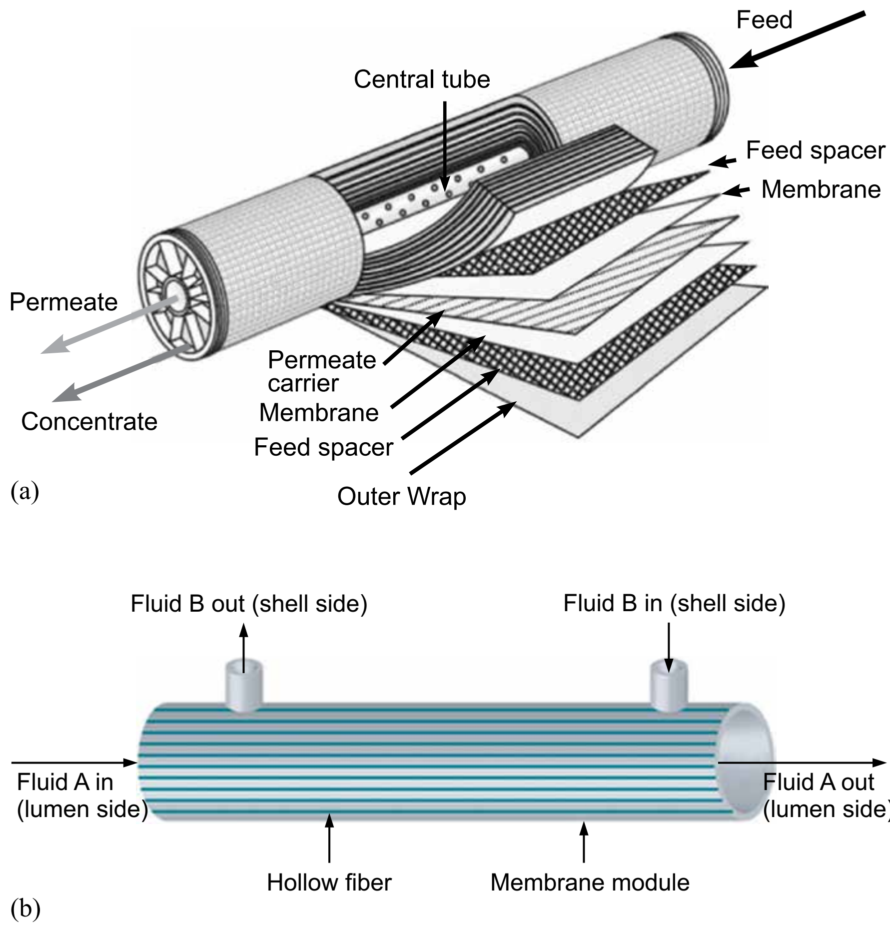

used in water treatment, industrial and domestic effluent treatment, along with others [11].

After selecting the membrane structure and material, the next step is to obtain the operational parameters, which can cause changes in membrane efficiency. The main parameters observed are: component partial pressure, stream inlet pressure, the molar fraction of the inlet gas, and the difference between the chemical potentials of the permeate and the retentate, among other factors (Table 1) [11].

Thus, to select and design a membrane, it is necessary to study several points, ranging from the operational conditions to the material chosen to manufacture the membrane. However, compared to other separation methods, membranes are a potential technology to reduce capture costs [12].

Currently, membranes are not used for industrial use, as it is desirable for this use that the separation factor is sufficiently high. Therefore, studies are being conducted to minimize process limitations and increase separation performance [12].

Conclusion

This study aimed to conduct a technical approach involving CO_2 separation technologies from natural gas streams. From the literature study, technical information was sought to support the implementation of the permeation technique in membranes as a promising method for CO_2 separation. Compared to the other methods, this one has greater energy efficiency, lower energy consumption, and simplicity in operation, in addition to good results when

Table 1. Operational parameters that affect the efficiency of the membrane separation process [11].

Variation	Effect
Increase in ΔP	Increase in permeate flow; decrease in the concentration of the most permeable component (generally CO_2) in the permeate
Increase in feed flow	Decreases the percentage of CO_2 recovery as permeate and decreases retentate purity despite increasing permeate purity
Decreased feed flow	Decreases separation efficiency (below a critical value)
Temperature rise	Increases most permeabilities around 10-15%/10°C
Increase in permeation area	Increase in retentate purity
Decrease in permeation area	Increase in permeate purity

subjected to a hybrid process, reaching expected values and helping to reduce the cost of the process. It is expected that this work, still in its preliminary phase, can lead to a study of the technical and economic feasibility of a process of separation of CO_2 in natural gas streams, supporting the technological model to be implemented in SENAI CIMATEC Park from the Atalaia Experimental Nucleus (NEAT).

Acknowledgments

We thank the Human Resources Program of the National Agency for Petroleum, Natural Gas, and Biofuels, particularly PRH 27.1 ANP/FINEP/SENAI CIMATEC, for the scholarship opportunity for this project.

References

1. Santos EM et al. Gás natural: a construção de uma nova civilização, 2007.
2. Exploração e Produção de Petróleo e Gás. Available at: <https://petrobras.com.br/pt/nossas-atividades/areas-deatuacao/exploracao-e-producao-de-petroleo-e-gas/>. Accessed on Jun 24, 2022.
3. Gás Natural. Available at: <https://petrobras.com.br/pt/nossas-atividades/areas-de-atuacao/gas-natural/>. Accessed on Jun 24, 2022.
4. Goldenstein M,Azevedo RLS. Combustíveis alternativos e inovações no setor automotivo: será o fim da“ era do petróleo“? Rio de Janeiro -RJ, 2006.
5. Estudo sobre o Aproveitamento do Gás Natural do Pré-Sal. Available at: <https://www.presalpetroleo.gov.br/ppsa/conteudo/aproveitamento-gn-pre-sal.pdf>. Accessed on Jun 26, 2022.
6. Araújo OQF, Medeiros JL. Análise de tecnologias para separação de CO_2 em plataformas offshore: absorção física por líquidos iônicos, absorção química por aminas e permeação por membranas. Rio de Janeiro - RJ, 2018.
7. Gadelha TS. Análise das tecnologias de remoção de CO_2 do gás natural: uma comparação técnico-econômica de absorção, membranas e híbridos. Rio de Janeiro - RJ 2013:156.
8. Nascimento JT. Avaliação técnico-econômica de ultracentrífugas a gás para remoção de CO_2 em poços do pré-sal. Rio de Janeiro - RJ, 2012.
9. Wang Y et al. A Review of Post-combustion CO_2 Capture Technologies from Coal-fired Power Plants. Energy Procedia. Aachen – Germany 2017:650-665.
10. Crivellari GP. Modelagem matemática e simulação de um permeador de gases para separação de CO_2 de gás natural. São Paulo - SP, 2016.
11. Maleski TPS, Ritter CT. Tecnologias para separação de dióxido de carbono do gás natural associado ao petróleo. Revista Conectus Caxias do Sul -RS 2021:1-23.
12. Wiesberg IL et al. Economic evaluation of CO_2 capture from flue gas by membrane permeation. 14 AIChe Annual Meeting 2014.

A Literature Review of Additive Manufacturing in the Fabrication of Soft Robots: Main Techniques, Applications, and Related Industrial-Sized Machines

Rafael Santana Queiroz[1*], Lucas Marins Batista[1], Miguel Felipe Nery Vieira[1], Lucas Cruz da Silva[1], Bruno Caetano dos Santos Silva[1], Rodrigo Santiago Coelho[1]
[1]SENAI CIMATEC University Center; Salvador, Bahia, Brazil

Soft robots have been receiving unprecedented attention in recent years for being able to be used side-by-side with humans, exploring dangerous environments and confined spaces, moving across uneven terrain, and solving problems that rigid robots cannot solve. The wide range of additive manufacturing techniques has also boosted research in the area. This work summarizes the characteristics of the five most relevant techniques – FDM, DIW, SLS, Inkjet, and SLA – for fabricating soft robots together with case studies. A summary contains models of industrial-sized additive manufacturing machines that can compose a facility for fabricating large-scale soft robots.
Keywords: Additive Manufacturing. 3D Printing. BiLi Method. Manufacturing Techniques. Soft Robots.

Introduction

Traditional robotics uses hard materials that allow robots to be precise but limit their ability to deform elastically and closely interact with the environment. Soft robots are the next generation of robots – made of soft and deformable materials – capable of safely cooperating with humans, steering through narrow spaces, and performing tasks that complex robots cannot do [1].

Several methods have been used to manufacture soft robots, but additive manufacturing (AM) stands out due to its versatility, especially regarding materials and techniques. AM can act on three levels in a soft robot project: rapid mold fabrication, hybrid approach, and total additive manufacturing. The latter is, however, the only one that takes full advantage of AM capabilities [2].

Fused deposition modeling, direct ink writing, selective laser sintering, inkjet printing, and stereolithography are the main techniques covered by the AM reviews aimed at soft robot fabrication [1-5]. However, to our knowledge, no review depicts the techniques and models of industrial-sized commercial 3D printing machines and their corresponding capacities, such as printable materials and build volume. Thus, this paper also aims to bring this information to the literature.

We organized this documents in sections: Introduction, Materials Methods, which presents the method used to gather and extract information of the main works on the theme; the Additive Manufacturing in Soft Robots that details the characteristics of each manufacturing technique, along with examples in soft robots and commercial machine models, and the Conclusion that closes this study.

Materials and Methods

The review was based on three steps: mining scientific articles, identifying the main AM techniques applied in soft robots, and surveying related industrial machinery.

The BiLi method [6] was used in the first step for collecting and mining scientific articles. The method requires iterative search strings to filter relevant candidate works for evaluation. As a result, it allowed a significant reduction in the number of documents for reading and analysis in this review - from 1,136 to 28.

The second step consisted of parsing the collection of works to map the main AM techniques used for soft robot fabrication according to the following criteria:

Received on 29 October 2022; revised 18 February 2022.
Address for correspondence: Rafael Santana Queiroz. Travessa Luis Anselmo, No. 43, Ap. 403, Ed. Beethoven, Salvador, Bahia, Brazil. Zipcode: 40.270-030.E-mail: rafael.queiroz@fieb.org.br. DOI 10.34178/jbth.v6i1.286.

J Bioeng. Tech. Health 2023;6(1):91-97

- Application in soft robot fabrication.
- Occurrences within the scientific works.

The last step consisted of listing industrial-sized AM machines corresponding to all techniques summarized in the previous step. The research sources for these machines comprised articles, manufacturer websites, and magazines. The selection used the following criteria:

- Large building volume.
- High market price.
- Consolidation of the manufacturer in the market (qualitatively assessed).

Figure 1 summarizes the method used in the study.

Additive Manufacturing in Soft Robots

The concept map shown in Figure 2 depicts the main ideas related to the theme "additive manufacturing in soft robots," as provided by the research conducted in Materials and Methdos Section. It showed that manufacturing in soft robots has four main fronts: role (rapid mold fabrication, hybrid approach, or total additive manufacturing), purpose (actuation or sensing), materials, and manufacturing techniques. The latter is the focus of this work, so the following subsections present the concepts of the main techniques, their applications in soft robots, and corresponding models of industrial-sized commercial machines.

Figure 1. Summary of the used method.

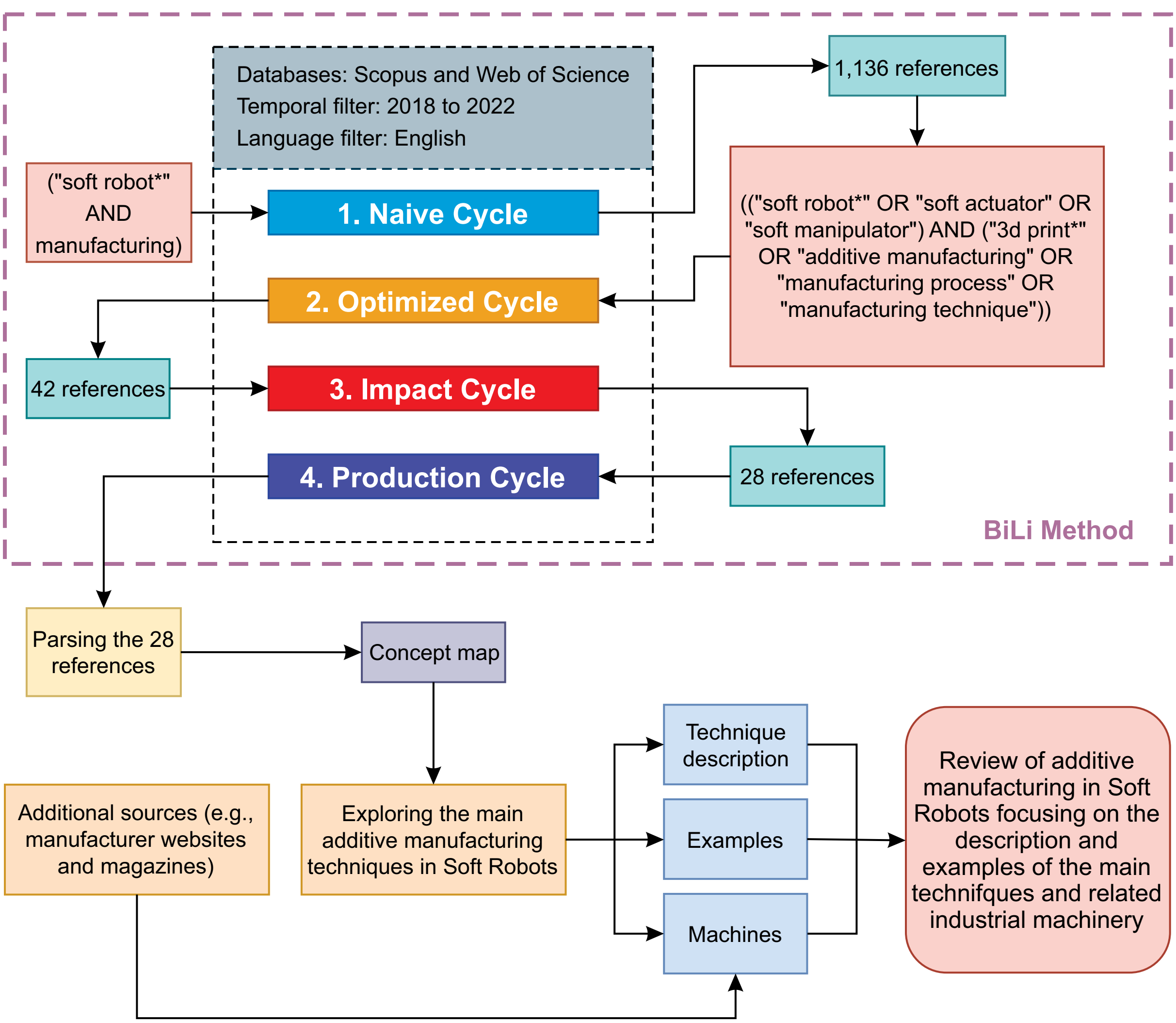

Figure 2. Concept map regarding additive manufacturing in soft robots

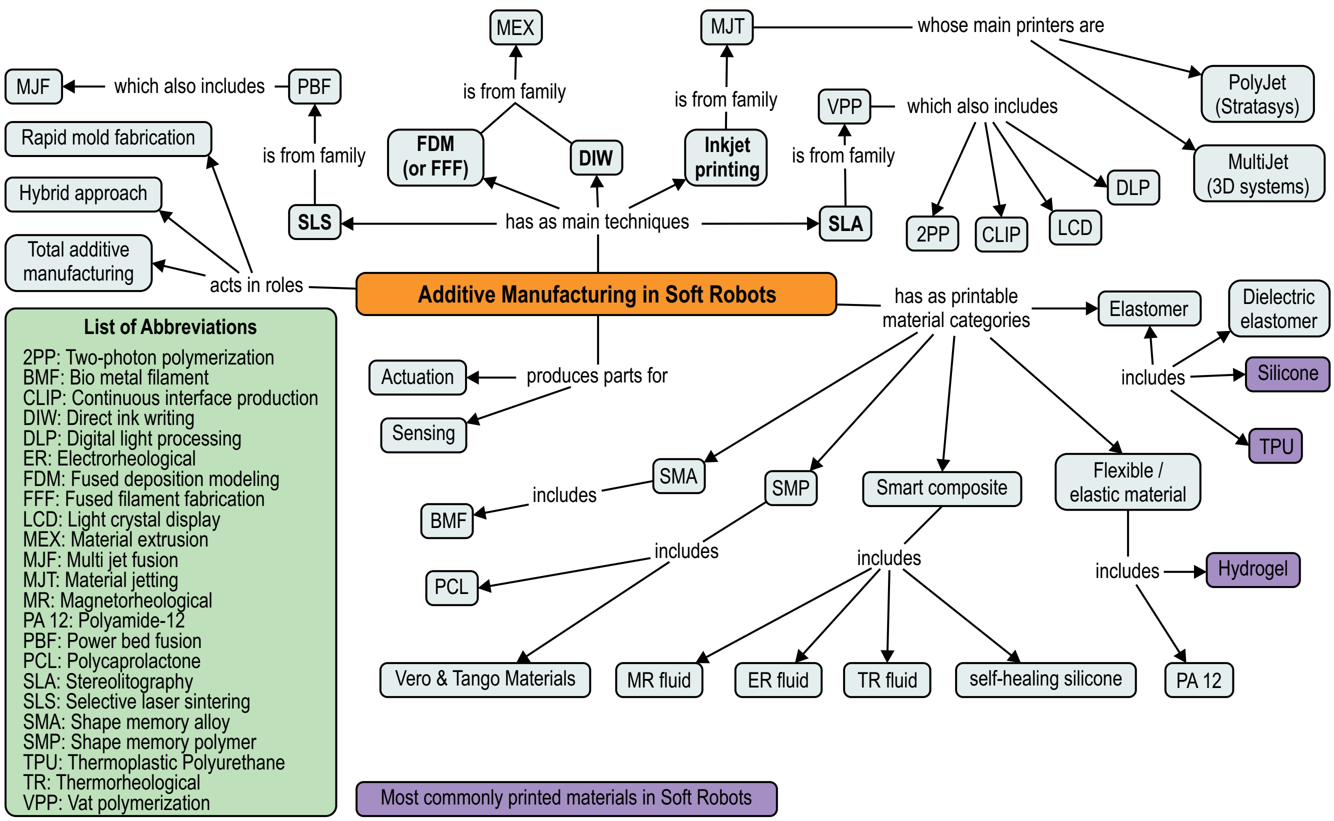

FDM

Fused deposition modeling (FDM) is one of the most common AM processes, with wide adoption, especially in research centers. The material – usually thermoplastic filament – is extruded layer by layer, being printed continuously. Materials often used in FDM machines are polycarbonate (PC), polylactic acid (PLA), nylon, and acrylonitrile butadiene styrene (ABS). This technology allows printing a wide range of geometries, and the principal advantages of this method are linked to its low cost and ease of use. However, FDM printers usually present low resolution, poor surface quality, and long printing times, depending on the material's filaments [4].

The literature reports some cases where FDM was used to print soft robots, like a soft-legged robot presented in Xia and colleagues [7]. It comprises a soft body with motor modules inside, soft legs, and electronics, each leg being independently actuated by a servo motor. The soft body and legs were printed using a desktop 3D printer (Troodon CoreXY printer, VIVEDINO) and a flexible thermoplastic polyurethane (TPU) filament.

Soft pneumatic actuators with complex geometry were printed in Yap and colleagues [8] using FDM technology and a commercially available filament, NinjaFlex TPU. Through a low-cost 3D printer (Geeetech Prusa Pro C), the authors printed four soft actuators and built a soft gripper that could grasp objects up to 5 kg. Similarly, in Curkovic and Cubric [9], the authors utilized a Prusa FDM printer with the same material to print soft fingers to form an anthropomorphic hand.

DIW

Direct ink writing (DIW) is an extrusion-based printing process where the ink is extruded, layer by layer, through a nozzle under controlled flow. Some additional steps may be required to solidify the printed object completely. DIW is one of the most flexible 3D technologies [10], and with simple adaptations, it is possible to have multi-material parts, switches, or mixing inks. The possibility of using conductive inks allows DIW 3D printers to create sensitive elements and actuator elements. DIW technique is compatible with many printable materials, including electrical, biological, and structural ones, e.g., colloidal suspension, hydrogel, and thermoset polymers. Besides, it enables the production of tiny patterns with high precision.

DIW technology was utilized to print multi-material pneumatic actuators made from a hybrid resin composed of silicon and epoxy [11]. The printing was conducted on a commercially available 3D printer System 30M, Hyrel INC. In Zhou and colleagues [12], the authors utilized DIW to print soft sensors and pneumatic-actuated artificial muscles. In addition, a multi-material ink composed of silicone and nanosilica (NS) was developed, and results indicate that adding NS increases the silicone ink's viscosity.

In Guan and colleagues [13], a new hybrid magnetorheological material was presented and fabricated using a custom-made printer in a soft gripper by DIW 3D technology. By adjusting the magnetic field, the gripper developed accurate grab and release tasks, indicating that the developed material is feasible for applications in soft robotics. A custom-made 3D DIW printer was also used in [14], where the authors printed a soft pneumatic manipulator made of carbon gel.

<u>SLS</u>

Selective laser sintering (SLS) is a powder bed fusion (PBF) technique applicable to metals and polymers that uses a rastering laser to fuse solid grains of powder in a powder bed [1,5]. Once the irradiation stops, the material cools and fuses. Then, a new powder layer is deposited on the bed, repeated until the part is built [3]. In the process, the non-fused powders act as support material, being reused after fabrication to reduce material consumption [1]. SLS is very similar to multi-jet fusion (MJF), whose principle is also based on powder fusion. The main difference is the heat source. In SLS, a laser is used to scan and sinter across each cross-section, while in MJF, an ink (fusing agent) is dispensed on the powder to absorb infrared light, which fuses the inked areas [15].

The main advantages of SLS are the possibility of material reuse and the achievement of isotropic mechanical proprieties in the printed object. However, among the disadvantages stands out the constraints regarding material compatibility and the need for precise temperature control to maintain an appropriately sized melt pool to fuse the material without distorting it [3,20].

Researchers have used SLS to fabricate soft robots. For instance, in Rost and Schädle [17], a silicone robotic hand was printed with four fingers and twelve degrees of freedom using bellow actuators to perform complex tasks like lifting, rotating, and precisely positioning a ball made of polystyrene. In Roppenecker and colleagues [18], a multi-arm snake-like robot was printed with PA 12 to manipulate instruments at the tip of a flexible endoscope.

<u>Inkjet</u>

Another option for printing soft robots is inkjet, an AM technique that uses several nozzles to jet droplets of different liquid or molten materials on a platform, which become solid by the vitrification process, evaporation, or polymerization. The droplets can also use components sensitive to UV light to solidify the material in a rapid and controlled process that accumulates the material in 2D layers to form high-precision 3D objects directly [3].

In Drotmand and colleagues [19], the materials were combined through selective deposition of different materials to build a pneumatic actuator for a legged robot capable of navigating over unstructured terrain. Using the same printer – Objet500 Connex3 PolyJet –, the authors in Zatopa and colleagues [20] developed a soft robot with integrated fluidic circuitry. Finally, in Shorthouse and colleagues [21], a soft actuator capable of bending bi-directional motions was printed with the Stratasys J735 printer with multiple materials.

SLA

The stereolithography (SLA) technique uses a container with photopolymer resin and a laser or ultraviolet light source to solidify a defined area through polymerization. Then, a layer is printed by moving the laser beams on the material's surface layer by layer to form a complete and unique object [3].

Different light sources and materials can be used to form structures and maintain a high resolution, being a commercially attractive technique for soft robots with microscale characteristics and complex geometry. The materials usually applied for this method are poly(ethylene glycol), diacrylate (PEGDA), acrylic-PEG-collagen mixtures, elastomeric precursor, and Spot-E, Spot-A resins [1]. For instance, one application developed a miniaturized walking biological machine with an actuation module for movement with PEGDA hydrogel and the SLA 250/50 printer from 3D Systems [22]. Another example was the building of Tango Plus elastomer test samples using a Stratasys Objet260 Connex 3D printer [23].

Industrial-Sized Commercial Machinery Models

Among the models of AM machines available on the market, some stand out for their applicability in the industrial environment, productive capacity, printing volume, manufacturing quality, and manufacturer consolidation. Table 1 shows machine models of the techniques mentioned above, which have the potential to constitute an AM facility focused on the manufacture of big soft robots. Models were selected from the literature [21,24], a manufacturer's website [25], and a digital magazine [26,27].

The best option for printing large-volume parts is the Tractus 3D T3500, with a building volume of 1.65 m^3 and a maximum height (z) of more than 2 m. According to Wallin and colleagues [3], the best options in terms of productivity are SLS and SLA, with an approximate deposition rate of 106 mm^3/h, while DIW and SLA are the best regarding resolution, reaching up to 1 µm. These values cannot be generalized to the machines in Table 1, making it necessary to consult the technical datasheet for each equipment.

Conclusion

We showed a compilation of AM techniques aimed at fabricating soft robots – FDM, DIW, SLS,

Table 1. Examples of industrial-sized commercial additive manufacturing machines.

	Printer Model	Building Volume (mm)	Printable Materials
FDM	Tractus 3D T3500	Ø 1000 x 2100	PLA, PETG, ABS, TPU, TPE
	Stratasys F900	914 x 609 x 914	ASA, ABS, PC, Ultem, Nylon
	Roboze 1000	1000 x 1000 x 1000	PLA, ABS, PC, Nylon, Peek, Ultem
DIW	Lynxter S600D	Ø 390 x 600	Silicone (with toolhead LIQ21)
	Delta Tower Fluid MT	Ø 420 x 400	Almost all fluid and pastes
	InnovatiQ LiQ 320	250 x 200 x 150	Silicone
SLS	EOS FORMIGA P 110 Velocis	200 x 250 x 330	Alumide, PA 1101, PA 1102 black, PA 2200, PA 2201, PA 3200 glass filled, PrimeCast 101, PA 2105
	Nexa3D QLS 820	350 x 350 x 400	PA 11, PA 12, PBT, PP, aluminum, glass and fiber-filled
	Sindoh S100	510 x 510 x 500	PA 11, PA 12, TPU, PP
Inkjet	Stratasys Objet500 Connex3	490 x 390 x 200	Resin, ABS
	Stratasys J750	490 x 390 x 200	
	Stratasys J4100	1000 x 800 x 500	
SLA	Stratasys Neo800	800 x 800 x 600	Open resin system*
	3D Systems ProJet 7000 HD	380 x 380 x 250	VisiJet SL Flex, Tough, Clear, Black
	3D Systems ProX 950	1500 x 750 x 550	Thermally resistant plastic, polypropylene, ABS, Accura resin

* Compatible with commercially available 355 nm stereolithography resins.

Inkjet, and SLA – by relevant works in the area, mined by the BiLi method. Finally, we presented a summary containing options of industrial-sized machines with the potential to compose a facility for soft robot manufacturing.

Acknowledgments

This research was executed in partnership between SENAI CIMATEC and Shell Brasil. The authors would like to acknowledge Shell Brasil Petróleo LTDA, the Brazilian Company for Industrial Research and Innovation (EMBRAPII), and Brazilian National Agency for Petroleum, Natural Gas and Biofuels (ANP) for the support and investments in RD&I.

References

1. Gul JZ et al. 3D printing for soft robotics - a review. Science and Technology of Advanced Materials 2018;19(1):243–262.
2. Stano G, Percoco G. Additive manufacturing aimed to soft robots fabrication: A review. Extreme Mechanics Letters 2021;42:101079.
3. Wallin TJ, Pikul J, Shepherd RF. 3D printing of soft robotic systems. Nature Reviews Materials 2018;3(6):84–100.
4. Schmitt F et al. Soft robots manufacturing: A review. Frontiers Robotics AI 2018;5(Jun).
5. Yap YL, Sing SL, Yeong WY. A review of 3D printing processes and materials for soft robotics. Rapid Prototyping Journal 2020;26(8):1345–1361.
6. Reis M, Vale A. Método BiLi - Uma otimização para revisão bibliográfica. Available at: <https://github.com/Brazilian-Institute-of-Robotics/bir-mini_bili-method>. Accessed on: 31 mai. 2022.

7. Xia B et al. A Legged soft robot platform for dynamic locomotion. Proceedings - IEEE International Conference on Robotics and Automation 2021;May:11812–11819.
8. Yap HK, Ng HY, Yeow CH. High-force soft printable pneumatics for soft robotic applications. Soft Robotics 2016;3(3):144–158.
9. Curkovic P, Cubric G. Fused deposition modeling for 3d printing of soft anthropomorphic actuators. International Journal of Simulation Modelling 2021;20(2):303–314.
10. Zhan S et al. 3D printing soft matters and applications: A review. International Journal of Molecular Sciences 2022;23(7).
11. Joseph VS et al. Silicone/epoxy hybrid resins with tunable mechanical and interfacial properties for additive manufacture of soft robots. Applied Materials Today 2021;22.
12. Zhou LY et al. Multimaterial 3D printing of highly stretchable silicone elastomers. ACS Applied Materials and Interfaces 2019;11(26):23573–23583.
13. Guan R et al. DIW 3D printing of hybrid magnetorheological materials for application in soft robotic grippers. Composites Science and Technology 2022;223(January):109409.
14. Wang Z et al. Freeform fabrication of pneumatic soft robots via multi-material jointed direct ink writing. Macromolecular Materials and Engineering 2022.
15. Hubs. What is the difference between Selective Laser Sintering (SLS) and Multi Jet Fusion (MJF) 3D printing? Available at: <https://www.hubs.com/knowledge-base/hp-mjf-vs-sls-3d-printing-technology-comparison/>. Accessed on: Jul 11, 2022.
16. Zhou X, Lee PS. Three-dimensional printing of tactile sensors for soft robotics. MRS Bulletin 2021;46(4): 330–336.
17. Rost A, Schädle S. The SLS-generated soft robotic hand - An integrated approach using additive manufacturing and reinforcement learning. Proceedings - 2013 12th International Conference on Machine Learning and Applications - ICMLA 2013;1:215–220.
18 Roppenecker DB et al. Multi arm snake-like robot kinematics. IEEE International Conference on Intelligent Robots and Systems 2013:5040–5045.
19. Drotman D et al. 3D printed soft actuators for a legged robot capable of navigating unstructured terrain. 2017 IEEE International Conference on Robotics and Automation (ICRA) 2017.
20. Zatopa A, Walker S, Menguc Y. Fully soft 3D-printed electroactive fluidic valve for soft hydraulic robots. Soft Robotics 2018;5(3):258–271.
21. Shorthose O et al. Design of a multimaterial 3D-printed soft actuator with bi-directional variable stiffness. In: Lecture Notes in Computer Science 2021:238–248.
22 Chan V et al. Development of miniaturized walking biological machines. Scientific Reports 2012;2.
23. Patel DK et al. Highly stretchable and UV curable elastomers for digital light processing based 3D printing. Advanced Materials 2017;29(15):1–7.
24. Weigang F et al. Toward industrial silicone 3D printing of soft robots. 2021 IEEE 4th International Conference on Soft Robotics, RoboSoft 2021:523–526.
25. Stratasys. Stratasys Website. Available at: <https://www.stratasys.com/en>. Accessed on Jul 20, 2022.
26. Kauppila I. The Best SLS 3D Printers of 2022. Available at: <https://all3dp.com/1/best-sls-3d-printer-desktop-industrial/>. Accessed on Jul 11, 2022.
27. ALL3DP. The Best Industrial FDM 3D Printers of 2022. Available at: <https://all3dp.com/1/best-industrial-fdm-3d-printers-2021/>. Accessed on Jul 13, 2022.

Knowledge Management: A Case Study in a Construction Company

Mário Joel Ramos Júnior[1*], Priscila Coutinho Miranda[1,2], Eric Vostal Hausner[1], Renelson Ribeiro Sampaio[1]
[1]SENAI CIMATEC University Center; [2]Federal Institute of Education, Science and Technoology; Salvador, Bahia, Brazil

Knowledge management and innovation are important for organizational environments, acting as a strategy to maintain and improve competitiveness. This article evaluates, in an exploratory study, knowledge management in a medium-sized company. To this end, a systematic literature review and a qualitative interview with fourteen employees of a medium-sized company in the construction industry were conducted. The questionnaires were applied remotely to employees with leadership positions and direct labor from the company. The results showed that, although it was evident that the company follows management principles that tangent dimensions of the SECI Model, there is an opportunity for improvement in the internalization and combination dimensions.
Keywords: Organizations. Medium-Sized Company. Explicit. Tacit.

Introduction

Nonaka and Takeuchi [1] described knowledge as a potential source of advantage and ongoing competitiveness in economies permeated by change and uncertainty. The authors also point out two types of knowledge: tacit and explicit. Tacit knowledge is personal, specific to the context, and difficult to be formulated and communicate. Explicit or codified knowledge, on the other hand, refers to knowledge that can be transmitted in formal and systematic languages. There are two dimensions of this knowledge: the technical and the cognitive. The latter relates to values, beliefs, and ability to perform, which the individual cannot demonstrate. Therefore, organizations must take advantage of this inherent knowledge and transform it into organizational knowledge, which is a knowledge that adds value.

The need for companies to remain competitive in the market has favored management practices that aim to create and share knowledge. Studies show that using knowledge management practices provides process optimization and error reduction, which contributes to more assertive decision-making by managers [2].

According to Corrêa [3], several theoretical and practical approaches have been developed throughout the development of studies related to Knowledge Management (KM). There are types of theoretical knowledge that can be managed, such as declarative, procedural, cause, relational, basic, advanced, and innovative [4], tacit and explicit [1], and implicit [5, 6].

Personal knowledge emerges from information, interpretation, reflection, and experience in a particular situation. The personal knowledge (explicit and tacit) must be externalized to create organizational knowledge [7]. Knowledge creation is a synthesizing process by which individuals interact with each other in the organization (internal), external individuals, and the environment (external) to transcend emerging contradictions that the organization faces [8].

According to Nonaka and Takeuchi [1], there are four patterns of knowledge conversion: socialization, externalization, combination, and internalization. Knowledge expands in an increasing spiral as it moves from the levels of the individual to that of the organization. Therefore, the set of these forms is called the knowledge spiral.

Knowledge management is creating and disseminating knowledge in the organization and its incorporation into many services [1]. In addition, its main objective is to favor the best use

Received on 20 November 2022; revised 15 February 2023.
Address for correspondence: Mário Joel Ramos Júnior. Travessa Luis Anselmo, No. 43, Ap. 403, Ed. Beethoven, Salvador, Bahia, Brazil. Zipcode: 40.270-030. E-mail: ramosjuniormariojoel@gmail.com. DOI 10.34178/jbth.v6i1.287.

J Bioeng. Tech. Health 2023;6(1):98-103

of the information [9]. According to Nonaka and Takeuchi [1], the present work addresses the use of knowledge creation in a medium-sized company in the construction industry.

Materials and Methods

The guiding question of this study was: How is the knowledge accumulated over the years shared in a medium-sized construction company? Therefore, the present research was conducted to guide and determine the variables and define the sample to be researched.

The database used to search was Scielo. The descriptors used were: Knowledge Management and Companies.

We found 56 relevant studiesabout the subject, however, 10 studies were selected as relevant to compose this systematic review.

We used the classification of the Brazilian Service of Support to Micro and Small Enterprises to find the company [10].This database include in industrial and construction companies that are classified according to the number of employees, namely microenterprise (up to 19 people employed), small enterprise (from 20 to 99 people employed), medium-sized enterprise (from 100 to 499 people employed), and comprehensive enterprise (500 people employed or more)

We also used the classification of the National Bank for Economic and Social Development [11], which applies to industry, commerce, and services and is defined according to the annual turnover of the company or the economic group to which the company belongs, specifically: micro-enterprise (up to R$ 2.4 million), a small company (above R$ 2.4 million up to R$ 16 million), medium company (above R$ 16 million up to R$ 90 million), medium-large company (above R$ 90 million up to R$ 300 million) and large company (above R$ 300 million).

The evaluated company, herein named "X", was classified using the abovementioned criteria: number of employees and annual turnover. The company offers services in the areas of specialized boiler making, industrial fabrication, welding, spot services, refurbishments, and maintenance. The company name has been omitted for confidentiality reasons.

We did 12 questions: 4 related to general data and 8 related to the SECI dimensions based on the study by Arantes and colleagues and Gonzalez and colleagues [7,12]. In addition, the questions were reworded to make them easier to understand for all company's employees, who had different levels of education.

Socialization Dimension

Does the company offer courses/lectures to employees to improve their competencies? Do the employees recognize the importance of their work in the company's strategy?

Externalization Dimension

Does the company have practices encouraging experienced employees to transfer their knowledge to new or less experienced professionals? After the training sessions, do employees interact with the acquired knowledge?

Combination Dimension

Is there in the company the sharing of knowledge from a database with regular updates, best work practices, lessons learned, and guidance from experts (for consultation)? Is there access to a computer network where specific knowledge related to the work is stored?

Internalization Dimension

Does the company offer training outside the workplace (e.g., knowledge fairs, workshops, along with others) to its professionals? Does it disseminate the organizational culture?

The questionnaires were applied remotely, using the Google Forms platform, to fourteen company employees with leadership positions (coordinator and foreman) and direct labor (painter, mason, boilermaker, welder, and construction helper, along with others).

Results and Discussion

Table 1 summarizes how knowledge sharing accumulated over the years occurs in medium-sized companies, according to the studies evaluated).

Regarding the general data from the questionnaire, the results showed that 93% of the interviewees have more than five years of experience in the construction industry, and 71.4% have worked less than five years in the same company. As for the respondents' level of education, 71.4% have completed high school. Regarding the four ways of creating knowledge (Socialization, Externalization, Combination, and Internalization), according to Nonaka and Takeuchi (1997) [1], the results of the questionnaires showed the following:

1. Socialization Dimension: All interviewees informed that they participated in courses and lectures offered by their company in the last 12 months, as well as recognizing their importance for achieving the corporate goals of their company.

2. Externalization Dimension: All respondents answered that they received and/or shared knowledge with other employees (new and experienced) of the company in the last 12 months and interacted on the topics discussed with other employees.

3. Combination Dimension: One employee reported that he or she does not have access to the organization's operational procedures with the best practices to perform daily tasks, and five reported that they do not have access to training and corporate procedures via computer tablet, cell phone on topics related to their work.

4. Internalization Dimension: Internalization Dimension: ten employees answered that they did not participate in training outside the work environment. They also did not participate in any event related to disseminating the company's organizational culture (Figure 1).

The result of the questionnaire was discussed with the manager of the company studied. This collaborator informed that the contracting company (which has as its main activity the storage of flammable products) requires that all workers who performed activities in the company must previously undergo training as established in the Regulatory Norm (NR-20). This norm establishes minimum requirements for managing safety and health at work against risk factors of accidents arising from extraction, production, storage, transfer, handling, and manipulation of flammables and combustible liquids. In addition, the company's manager also informed us that recycling training is carried out for employees every 12 months.

The manager understands that the internalization of explicit knowledge into tacit knowledge is an opportunity for improvement within the organization after being explained that training outside the workplace will allow his employees to interact with people from other corporate environments and that developing the absorption capacity of workers in such training and internalization in the company's environment can culminate in improvements in the firm's organizational performance and become a competitive differential [3,12] since innovative companies develop a training policy that encompasses technical, managerial and creative skills, where multidisciplinary teams play an essential role in innovation [19] and that knowledge assets (in this case people) have a positive influence on organizational performance [17].

As for disseminating the organizational culture, the manager informed that when they join the company, the employees go through a stage called integration. At this stage, the company is presented, the projects already carried out, and the benefits, among other relevant aspects of the company. However, since 2015, due to several crises that the country has been going through, there has been a significant oscillation in the company's staff,

Table 1. Guiding questioNnaire of the study.

References	Guiding Question: How is the Knowledge Accumulated Over the Years Shared in Medium-Sized Companies?
[3]	Holistic knowledge management is a proposal that aims to approach the parts by the whole, considering that these parts should not be analyzed in isolation because there is an interconnection between them and, therefore, results in contextualizing these parts in a mold that contemplates the whole.
[7]	As for the degree of maturity of knowledge management, the results showed that companies spend more effort on the variables connected to the socialization and externalization dimensions and less on internalization and combination.
[12]	Five organizational constructs related to knowledge management: human resources, teamwork, organizational culture and structure, and knowledge development and absorption.
[13]	Management can contribute as a company differential concerning its competitors, providing a competitive advantage. These two aspects are essential elements for the performance of organizations.
[14]	Significant relationships between the dimensions of absorptive capacity and organizational performance are translated by adaptive capacity. Firms must be able to use their knowledge capacity fully and to transfer and disseminate such information to other relevant people.
[15]	Through the application of benchmarking of tacit knowledge that is in the minds of employees and can be transmitted through informal conversations, as well as the search for information that allows bringing and storing mostly tacit knowledge not only from competitors but also from suppliers and the customers themselves.
[16]	All the knowledge acquired by the companies was documented, and all the files about the simulation project were stored on the company's computers and had free access to manage them: conceptual model in image format, Excel spreadsheets, versions of the computer model in simulator-specific format, project reports in document format, and videos.
[17]	Identified the relationship that positively influences organizational performance: knowledge assets, organizational learning, knowledge process capability, business process capability, and organizational performance.
[18]	In reality, as experienced by SMEs, knowledge management still presents itself as a goal to be reached that might be achieved through a better understanding and conception of the practice of information management and the use of IT is still essentially operative and aimed at organizing, systematizing, and making efficient the daily activities, being far from knowledge management.
[19]	Group of facilitators of innovation in construction companies: external collaboration, innovation culture, top management support, and knowledge management, with leadership being an essential aspect of promoting systematic innovation.

Figure 1. Result of the internalization dimension in the evaluated company.

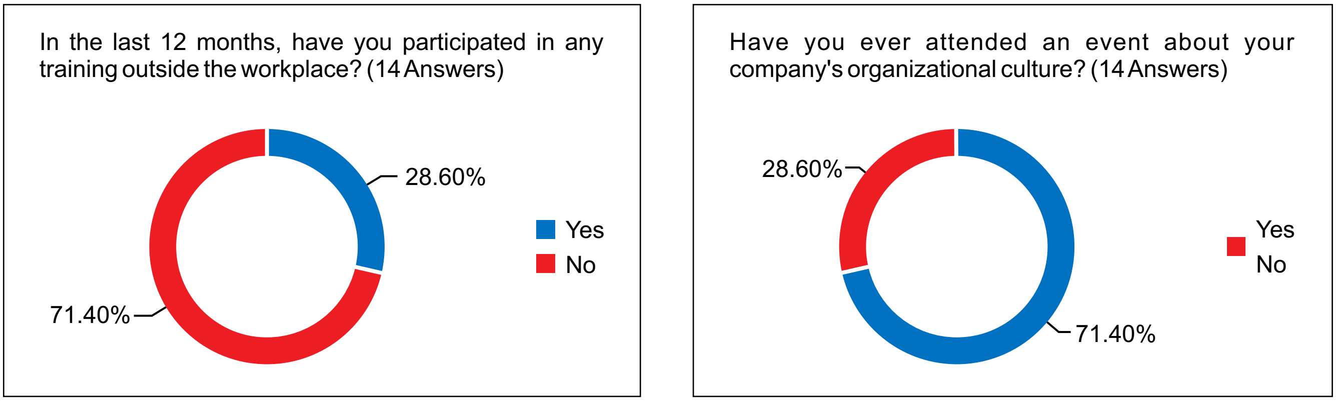

which can be reflected in the years of service per employee ratio. It is observed that strengthening the organizational culture with employees is an opportunity for company X to build employee loyalty, as well as achieve better financial results, especially in challenging scenarios [14,15].

Conclusion

The knowledge creation process in the company studied relates to tacit and explicit knowledge. Regarding the unfolding of the four ways of creating knowledge (Socialization, Externalization, Combination, and Internalization), we could observe that knowledge is acquired through employee training with the participation of employees in courses and lectures (conversion of explicit knowledge into Tacit knowledge) besides the interaction between people in the workplace, so that there is the conversion of tacit knowledge into other tacit knowledge, in the process of socialization.

We observed through the SECI spiral of continuous knowledge creation and used that tacit and explicit knowledge expands, in an unstructured way, from the individual to the group and then to the organizational level in the company studied. There are opportunities for improvement in knowledge management at company X, especially in the internalization and combination dimensions.

References

1. Nonaka I, Takeuchi H. Criação de conhecimento na empresa. 1a edição. Rio de Janeiro: Elsevier, 1997.
2. Menezes CRC, Olave MEL. Práticas de gestão do conhecimento em micro e pequenas empresas de Sergipe. Gestão & Regionalidade 2016;32(94)31 Mar. Doi: 10.13037/gr.vol32n94.2698. Disponível em: http://seer.uscs.edu.br/index.php/revista_gestao/article/view/2698. Accessed on Jul 2, 2022.
3. Corrêa F. A gestão do conhecimento holística: delineamento teórico conceitual. Perspect Ciênc Inf 2019;24(1):122–146. https://doi.org/10.1590/1981-5344/3542.
4. Zack MH. Developing a knowledge strategy. California Management Review 1999;41(3):125–145. https://doi.org/10.2307/41166000.
5. Grant KA. Tacit knowledge revisited – We can still learn from Polanyi. Research Gate 2007;5(2):9. Available at www.ejkm.com
6. Nickols F. The knowledge in knowledge management. Distance Consulting LLC. 2000;9.
7. Arantes LS, Martinelli Jr.,O, Viegas TOC, Rohenkoh JE. Maturity and level of knowledge management in the company: an application of Nonaka and Takeuchi model and Fuzzy Logic. Gestão & Produção 2021;28(2):e5305, 2021. https://doi.org/10.1590/1806-9649-2020v28e5305.
8. Nonaka I, Toyama R. The Knowledge-creating Theory Revisited: Knowledge Creation as a Synthesizing Process. In: Edwards, J.S. (eds) The Essentials of Knowledge Management. OR Essentials Series. Palgrave Macmillan, London. 2015. https://doi.org/10.1057/9781137552105_4.
9. Alvarenga Neto RCD. Gestão do conhecimento em organizações: proposta de mapeamento conceitual integrativo. Perspect Ciênc Inf, Belo Horizonte, 2006;11(1):146-147.

10. SEBRAE. Anuário do Trabalho nos Pequenos Negócios. 2018:327.
11. BNDES. Cartilha MPME 2015. Brasília: Banco Nacional de Desenvolvimento, 2015. Disponível em: https://web.bndes.gov.br/bib/jspui/bitstream/1408/4261/1/Cartilha%20MPME%202015.pdf. Accessed on Jun 20, 2022.
12. Gonzalez VD, Martins MF, Melo TM. Gestão do conhecimento: tipologia a partir dos fatores contextuais da organização. Transformação 2018;30(2):249–266, ago. 2018. https://doi.org/10.1590/2318-08892018000200009.
13. Tomomitsu HTA, Carvalho MM, Moraes RO. A evolução da relação entre a gestão de projetos e a gestão do conhecimento: um estudo bibliométrico. Gest Prod 2018;25(2):354–369. https://doi.org/10.1590/0104-530x3150-16.
14. Cardozo CT, Kronmeyer Filho, OR, Vaccaro GLR. Keep innovating: Absorptive capacity and the performance of Brazilian information technology companies. Rev Adm Contemp 2019;23(4):499–519. https://doi.org/10.1590/1982-7849rac2019180221.
15. Davila G, Varvakis G, North K. Influence of strategic knowledge management on firm innovativeness and performance. Braz Bus Rev 2019;16(3):239–254. https://doi.org/10.15728/bbr.2019.16.3.3.
16. Pereira TF, Montevechi JAB, Leal F, Miranda RC. A gestão do conhecimento na condução de projetos de simulação: um estudo de caso em empresas de consultoria. Gest Prod 2019;26(1). Doi: 10.1590/0104-530x2211-19. Disponível em: http://www.scielo.br/scielo.php?script=sci_arttext&pid=S0104-530X2019000100204&lang=pt.
17. Ziviani F, Amarante EP, França RS, Isnard P. O impacto das práticas de gestão do conhecimento no desempenho organizacional: um estudo em empresas de base tecnológica. Perspect Ciênc Inf 2019;24(1):61–83. https://doi.org/10.1590/1981-5344/3468.
18. Fell AFA, Dornelas JS. Gestão do conhecimento, tecnologia da informação e pequenas e médias empresas de serviços: um estudo de casos múltiplos na Região Metropolitana do Recife. Perspect Ciênc Inf 2020;25(2):29–55. https://doi.org/10.1590/1981-5344/3781.
19. Duarte CMM, Picchi FA. Key elements to enable systemic innovation in construction firms. Ambiente Construído 2021;21(4):385–405. https://doi.org/10.1590/s1678-86212021000400575.

Project Management Best Practices in the Implementation of a Quality Management System (QMS) in an Environmental Analysis Laboratory

Valesca Eda Oliveira de Souza[1*], Rosana Vieira Albuquerque[1,2]
[1]SENAI CIMATEC University Center, MBA in Project Management; [2]SENAI Innovation Institute for Logistics; Salvador, Bahia, Brazil

This article proposes a study on the best project management practices for implementing a Quality Management System (QMS) in a Laboratory of Environmental Analysis in a shorter period and with the expected quality. In 2020 it was established as a guideline for the self-sustainability of the laboratory, obtained through revenues generated from the provision of services. For its insertion in the market of analysis, implementing a QMS was essential. This study is a case report of an exploratory, bibliographical nature. Tools and project management techniques were applied for its development, such as using PMCanvas, which corroborated fulfilling the established deadline with the expected quality.
Keywords: Project Management. Environmental Analysis Laboratory. Quality Management System. PMBOK.

Introduction

The intersection of particular attributes with the degree of conformity to an established standard characterizes quality. The junction of globalization and technology causes these standards to be constantly changed, and to adhere to this scenario, organizations continually seek improvement through a Quality System.

A Quality Management System (QMS) is composed of activities that determine processes and resources necessary to achieve objectives, add value to stakeholders through the interaction of these processes and resources, enable optimization of resources, and determine the means to plan actions that address intended or unintended consequences in the provision of products and services [1].

A QMS, besides providing quality improvement in processes and products, by meeting the specifications required in the certification standards, also generates credibility for the organization and helps fulfill objectives [2].

Received on 6 December 2022; revised 20 February 2023.
Address for correspondence: Valesca Eda Oliveira de Souza. Rua da Gratidão, 291D - Ap 706 – Piatã - Salvador - BA, Brazil | Zipcode: 41650-195. E-mail: valesca.eda@gmail.com. DOI 10.34178/jbth.v6i1.288.

J Bioeng. Tech. Health 2023;6(1):104-111

For laboratories, the expectation of QMS implementation is the improvements in processes for diagnostic testing [3], which ensures high levels of efficiency in reproducible and accurate results.

Implementing a Quality Management System (QMS) is temporary and has a specific result, indicating its project nature. The PMBOK (2018, 6ª ed., p. 10) elucidates project management as "*the application of knowledge, skills, tools, and techniques to project activities to meet project requirements* [...]". The guide clusters 47 management processes into 5 groups: Initiation, Planning, Execution, Monitoring and Control, and Closing [4].

A study conducted by Helgi (2015) [5] analyzed project management practices in implementing quality management: the degree to which project management was applied, what tools and techniques were used, and the most crucial success factors in its implementation were considered.

Quality managers from 21 different types of ISO 9001-certified organizations in Iceland were interviewed during the survey. However, of the 21 organizations analyzed, only 5 applied essential project management tools, such as initial and closing meetings, formal project description, Work Breakdown Structure (WBS), scope definition, and performed internal costing, as time spent by employees for implementation. As a result, the average implementation time for these organizations was 13 months as planned, unlike the other 16, which had an average time above the expected 24 months [5].

The research concluded that the direct participation of management and employees and including time and spending on these resources in the plan are critical factors for project success. Therefore, implementing a QMS as a project can reduce essential resources such as time and costs.

Research Question

The Laboratory of Environmental Analysis (LAA), allocated at the University of Salvador, originated as a place of research and university extension, aiming to assist in undergraduate and graduate education investigations. However, in 2020 the direction of the university established new guidelines for the laboratory, the main one being its self-sustainability obtained through revenues developed from service provision.

The educational institution's market research in Salvador and the Metropolitan Region indicated that the central environmental analysis laboratories have the Quality Management System (QMS). Furthermore, the research results contributed to the elaboration of the LAA's Strategic Planning (SP), which indicated the need to implement a QMS to make the laboratory competitive in the analysis market and establish a deadline for the implementation (Table 1).

The period of 180 days, 6 months, set in the SP, is below the average in his study in Iceland. He presented the average period of 13 months for companies that implemented QMS using project management tools [5].

In the article, we will answer the following question: How can a Quality Management System implementation project in an environmental analysis laboratory be best managed to achieve compliance in a shorter period with expected quality?

Research Objective

The principal objective of this work was to propose the best project management practices for implementing a Quality Management System in an environmental analysis laboratory in a shorter-than-average timeframe.

The specific objective was to analyze the Project Plan for implementing the QMS in the environmental analysis laboratory, which was used as the basis for developing this work, and to identify the optimum management practices that meet the specificity of the project.

Table 1. Strategic planning mapped activities for LAA.

Mapped Activities	Actions	Deadline
Plankton Analysis	Hiring a mid-level technician	Immediate
Developing research in Biology and Chemistry (1st Environmental Monitoring)	Atomic Absorption equipment in operation	45 days after the operation
Commercialization of environmental analyses	Implementation of the Quality Management System	180 days
Support for physicochemical assay certifications	Hiring a consultant (financial resources); Laboratory structure	240 days
Partnership with the Bahia Network of Atlantic Forest Seeds.	Refrigerated Chamber in Operation	Immediate
Research development - water analysis (physicochemical)	Spectrophotometer in operation and a scientific initiation student	30 days
Analysis of organic compounds.	Gas Chromatography equipment in operation and 20h contract	Immediate

Source: Authors, 2022.

Expected Results

We expected to elucidate best practices of project management in 180 days that meet the project's specificity, QMS implementation in a small environmental analysis laboratory, originally constituted to meet academic demands.

Materials and Methods

This study is characterized as an exploratory case study of a bibliographical nature, applying project management best practices.

Aiming to reactivate the competitiveness of the environmental analysis laboratory for the external market, the Rectory of the University where the laboratory is located established new guidelines. Based on market research, it was defined that implementing the Quality Management System (QMS) is fundamental for the commercialization of the analyses.

In 2021 began, the preparation of the Project Plan; the plan had the Project Management Body of Knowledge (PMBOK Guide) as a reference, built-in detail with 10 knowledge areas.

This case study was developed from February to June 2021 at a university in Salvador – Bahia – Brazil, where we collected the data. This data comprised the project documents for the laboratory's implementation, the laboratory's internal quality policy, and the university's strategic plan. In addition, we did local visits accompanied by the team responsible for the laboratory. After the document analysis, we identified many points of project management practices' application. A new project plan proposal was elaborated based on the QMS structuring phase and the standards, and the PMBOK Guide. In this international pattern of project management, tools and techniques used in the knowledge areas were analyzed and compared with other case studies, which generated the mapping of best management practices that helped to comply with the guideline. Besides these standards, the Project Model Canvas method was also used to structure a systemic vision of the project. Finally, the new proposal was presented to the university chancellor along with the benefits to be gained.

Results and Discussion

Based on the demand indicated by the Environmental Analysis Laboratory's Strategic Planning, we prepared a complete Project Plan with the 10 knowledge areas (Integration, Scope, Time, Costs, Quality, Human Resources, Communication, Risks, Procurement, and Stakeholders) listed by the PMBOK Guide.

In the integration area, the Project Model Canvas methodology was used (Figure 1), which allowed collaborative planning, with the participation of the main stakeholders (Sponsor, LAA Employees, Potential Customers, and Project Manager and Team)6. Essential project information, such as the objective, requirements, assumptions, constraints, team, delivery group, risks, and cost, was grouped and consolidated.

The PM Canvas enabled the project team to take ownership of the plan because it was easy to visualize and understand. In addition, it is a tool that strengthens communication.

The project's initial references defined in the PM Canvas brought an overview of the project that served as the basis for the construction of the scope, which creates 7 phases, 2 managerial (Project Management and Closing) and 5 operational (Hiring, Informational Project, QMS Structuring, Assisted Operation, and Improvement) (Figure 2).

The definition of the packages in the scope of the QMS implementation was based on the ISO 9001 Quality Management System - requirements and ISO 9000 - fundamentals and vocabulary, in case the laboratory was interested in obtaining the certification later. In addition, these packages provided the basis for estimating costs, human resources, and time and making results specific and measurable.

During the project, 11 key deliverables were defined, constituting the milestones, which go from the managerial to the operational packages, and

Figure 1.PM Canvas.

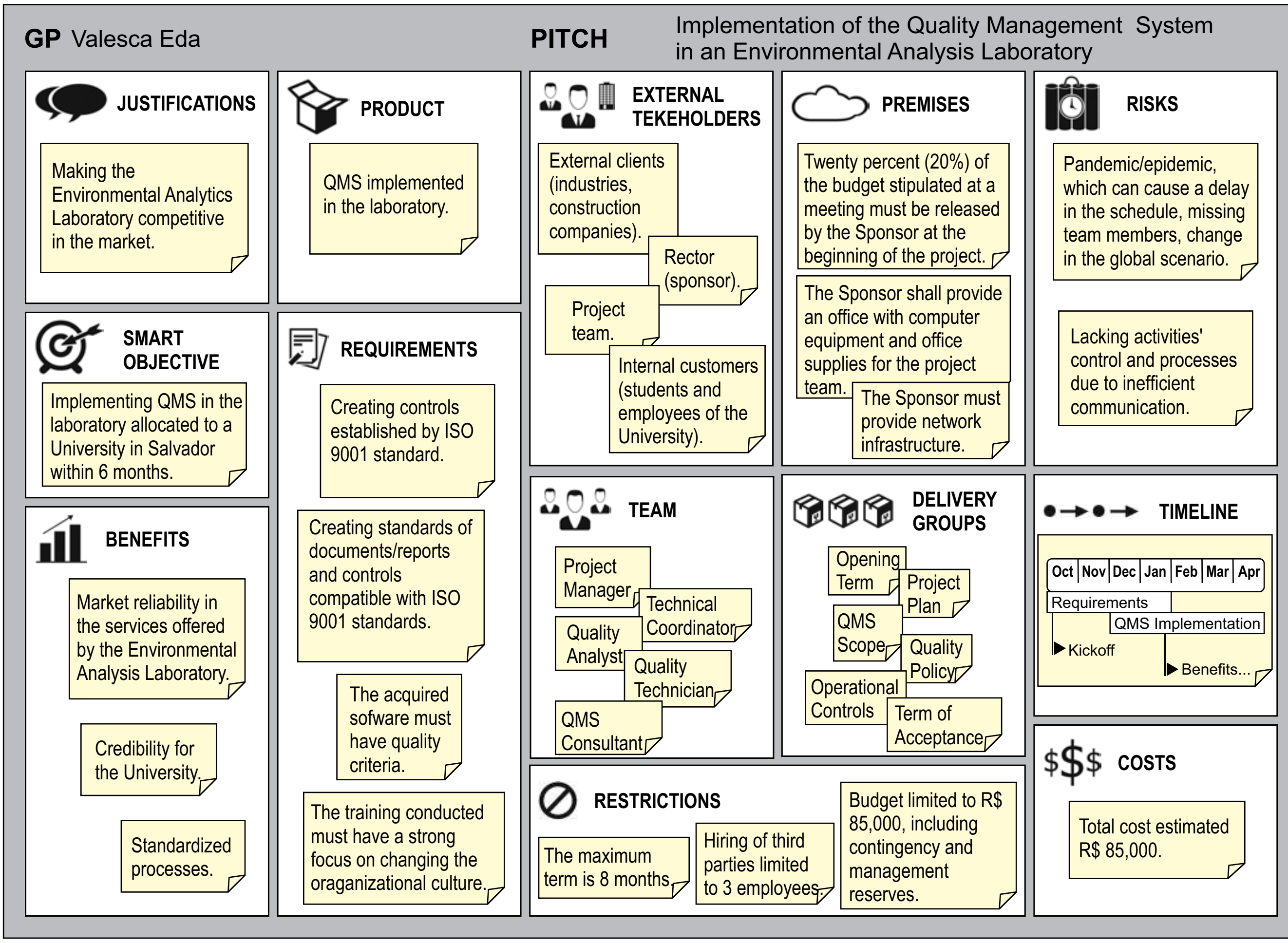

Source: Authors, 2022.

conclude with the implementation of the Quality Management System:

1. Approved opening term;
2. Approved plan;
3. Quality Policy Developed;
4. Document with the objectives and actions elaborated;
5. Change document validated;
6. Software installed;
7. Employees trained;
8. Standards for Updating/Control of Documented Information developed;
9. Manual for Communication with the Client and Control of Requirements Related to Internal and External Products and Services developed;
10. Continuous Improvement Pilot Completed;
11. SGQ Implanted.

The quality management of the project was based on the internal quality policy of the laboratory, elaborated from the QMS Structuring phase and the standards:

a. ABNT NBR ISO 9000:2015 - QMS - fundamentals and vocabulary;
b. ABNT NBR ISO 9001:2015 - QMS - requirements;
c. ABNT NBR ISO/IEC 17025:2017 - General requirements for the competence of testing and calibration laboratories;
d. PMBOK® Guide 6th edition.

Figure 2. Graphical WBS.

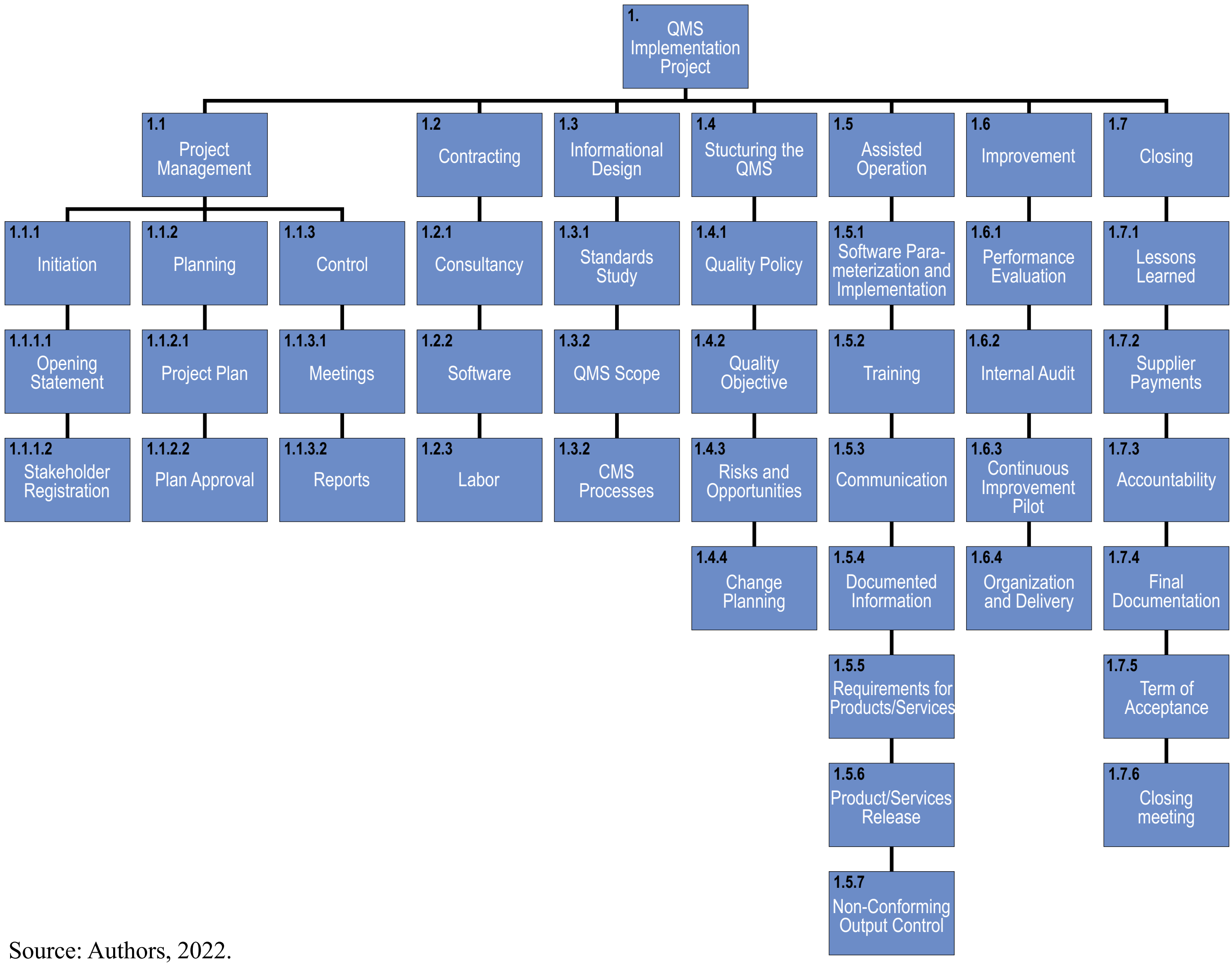

Source: Authors, 2022.

We associate the quality standards with the products/services and list their requirements to make the project's quality management more efficient (Table 2).

The project's risk management was formatted by the following processes: planning, identification, qualitative and quantitative analysis, response planning, and risk control. For each risk pointed out, a response and the person responsible for meeting the demand were defined. Verify evaluation details in Table 3.

The risk response plan enabled the project's strategic vision by planning to diminish or mitigate threats and visualize opportunities.

Conclusion

The PM Canvas methodology generated a framework of easy understanding and visualization, with the consolidation of the essential information for the development of the plan and consequently of the project, which enabled not only the participation of stakeholders in the first moment and the monitoring of the elements throughout the project.

If PM Canvas serves as a guide for the project, the Work Breakdown Structure (WBS) is the map that guided us throughout the process. The detailing and logical grouping of the phases, such

Table 2. Quality requirements and minimum criteria.

Product/ Service or Aspect Evaluated	Requirement	Standard / Acceptance Criterion	Verification Method
Project Management	Control of the project management plan.	Follow 100% of the requirements of NBR ISO 9001 and NBR ISO 9000 and 90% of the PMBOK® Guide.	Perform inspection on the execution of the plan.
Quality Management System	All processes are in quality standard.	Follow 100% of the requirements of NBR ISO 9001, NBR ISO 9000, and 60% of NBR ISO/IEC 17025.	Inspection with Checklist.
Training	Laboratory personnel qualified in quality.	Follow 100% of the requirements of NBR ISO 9001, NBR ISO 9000, and the laboratory's quality policy.	Perform internal audit after implementation.
Software	Software for Quality Management System.	Follow 100% of the requirements of NBR ISO 9001, NBR ISO 9000, and the laboratory's quality policy.	Performance evaluation.
Continuous Improvement Pilot	Critical analysis of the Quality Management System	Follow 100% of the requirements of the standards NBR ISO 9001 and NBR ISO 9000 and 40% of the standard NBR ISO/IEC 17025.	Simulation of system use and Checklist.

Source: Authors, 2022.

as the hiring phase being operationally first, made it possible for us to reduce time with bureaucratic processes and allocate human resources when needed, reducing financial resources.

The definition of milestones in the project schedule was created based on the main deliverables that could compromise the project's progress.

To maintain the quality of the project, we also follow international quality standards, besides providing guidelines, aligning our expectations with the market, and generating the possibility for the laboratory to obtain certification later on.

The mapping of risks was one of the main factors in „controlling" future situations, identifying possible factors that could intervene in the project, and establishing and directing actions. In this way, the project plan was followed as planned.

The fulfillment of the 180-day deadline set by the University Rector's Office, the implementation of the QMS in the Environmental Analysis Laboratory was only possible due to the planning, the involvement of the interested parties, including the top management, and the understanding of tools that would have a significant impact on the project.

The limitations of the research are, at the same time, opportunities for future development. The research was limited to a small environmental analysis laboratory. The tools and techniques used in this study, PM Canvas, WBS, Milestone, Quality Requirements, Minimum Criteria, and Planned Risk Responses, would have to be validated in other laboratory profiles. Comparative studies of the performance of projects implemented with and without these are also recommended to demonstrate best project management practices.

Table 3. Planned responses to risks

Item	Risk	Probability	Gravity Index	Exposure	Answer	Description
1.1	A pandemic/epidemic can cause a delay in the schedule, missing team members, and change in the global scenario.	Low	High	High	Acceptance	Establish remote work strategies and maintain all project documentation in the cloud.
2.1	Lack of control of activities and processes due to inefficient communication.	Medium	Medium	Medium	Attenuation	Follow the communication techniques provided in the plan and hold all scheduled events/ meetings.
3.1	Hiring qualified employees due to bureaucratic processes generates delays and additional costs.	Medium	Medium	Medium	Mitigation	Conduct the selection process in advance and maintain an updated vacancy database.
4.1	Wrong mapping of the laboratory operational processes may cause distortions in the QMS.	Medium	High	High	Mitigation	Involve a consultant with QMS experience in laboratories and the Project Manager to analyze the mapping of the processes before implementing the QMS.
4.2	Lack of technical mastery of the Quality Management Software by the laboratory staff may cause delays and quality problems in the standards created.	Medium	Medium	Medium	Attenuation	Require software training (basic and advanced) for all employees.

Source: Authors, 2022.

References

1. Associação Brasileira de Normas Técnicas - ABNT. ABNT NBR ISO 9000:2015: Sistemas de gestão da qualidade - fundamentos e vocabulário. Rio de Janeiro, 2015a.
2. Melo RM, Silva AM. Uma abordagem multicritério para a seleção de serviços de consultoria e certificação de Sistemas de Gestão da Qualidade. Gestão e Produção, São Carlos, 2018;25(1):160-174.
3. Kachuwaire O et al. Quality management system implementation in human and animal laboratories. One Health 2021;13.
4. PMI. Um guia do conhecimento em gerenciamento de projetos – Guia PMBOK – 6ª ed., Newtown Square, Pennsylvania.: Project Management Institute, Inc., 2018.
5. Ingason H. Best project management practices in implementing an ISO 9001 quality management system. procedia. Social and Behavioral Sciences 2015;194:192-200.
6. PM Canvas. PMCanvas Project Management, 2017. Home Page. Available at: <https:// http://pmcanvas.com.br/>. Accessed on Jul 3, 2022.
7. Associação Brasileira de Normas Técnicas - ABNT. ABNT NBR ISO 9001:2015: Sistemas de gestão da qualidade - requisitos. Rio de Janeiro, 2015b.

Instructions for Authors

The Authors must indicate in a cover letter the address, telephone number and e-mail of the corresponding author. The corresponding author will be asked to make a statement confirming that the content of the manuscript represents the views of the co-authors, that neither the corresponding author nor the co-authors have submitted duplicate or overlapping manuscripts elsewhere, and that the items indicated as personal communications in the text are supported by the referenced person. Also, the protocol letter with the number should be included in the submission article, as well as the name of sponsors (if applicable).

Manuscripts may be submitted within designated categories of communication, including:

- Original basic or clinical investigation (original articles on topics of broad interest in the field of bioengineering and biotechnology applied to health). We particularly welcome papers that discuss epidemiological aspects of international health, clinical reports, clinical trials and reports of laboratory investigations.
- Case presentation and discussion (case reports must be carefully documented and must be of importance because they illustrate or describe unusual features or have important practice implications).
- Brief reports of new methods or observations (short communications brief reports of unusual or preliminary findings).
- State-of-the-art presentations (reviews on protocols of importance to readers in diverse geographic areas. These should be comprehensive and fully referenced).
- Review articles (reviews on topics of importance with a new approach in the discussion). However, review articles only will be accepted after an invitation of the Editors.
- Letters to the editor or editorials concerning previous publications (correspondence relating to papers recently published in the Journal, or containing brief reports of unusual or preliminary findings).
- Editor's corner, containing ideas, hypotheses and comments (papers that advance a hypothesis or represent an opinion relating to a topic of current interest).
- Innovative medical products (description of new biotechnology and innovative products applied to health).
- Health innovation initiatives articles (innovative articles of technological production in Brazil and worldwide, national policies and directives related to technology applied to health in our country and abroad).

The authors should checklist comparing the text with the template of the Journal.

Supplements to the JBTH include articles under a unifying theme, such as those summarizing presentations of symposia or focusing on a specific subject. These will be added to the regular publication of the Journal as appropriate, and will be peer reviewed in the same manner as submitted manuscripts.

Statement of Editorial Policy

The editors of the Journal reserve the right to edit manuscripts for clarity, grammar and style. Authors will have an opportunity to review these changes prior to creation of galley proofs. Changes in content after galley proofs will be sent for reviewing and could be required charges to the author. The JBTH does not accept articles which duplicate or overlap publications elsewhere.

Peer-Review Process

All manuscripts are assigned to an Associate Editor by the Editor-in-Chief and Deputy Editor, and sent to outside experts for peer review. The Associate Editor, aided by the reviewers' comments, makes a recommendation to the Editor-in-Chief regarding the merits of the manuscript. The Editor-in-Chief makes a final decision to accept, reject, or request revision of the manuscript. A request for revision does not guarantee ultimate acceptance of the revised manuscript.

Manuscripts may also be sent out for statistical review ou *ad hoc* reviewers. The average time from submission to first decision is three weeks.

Revisions

Manuscripts that are sent back to authors for revision must be returned to the editorial office by 15 days after the date of the revision request. Unless the decision letter specifically indicates otherwise, it is important not to increase the text length of the manuscript in responding to the comments. The cover letter must include a point-by-point response to the reviewers and Editors comments, and should indicate any additional changes made. Any alteration in authorship, including a change in order of authors, must be agreed upon by all authors, and a statement signed by all authors must be submitted to the editorial office.

Style

Manuscripts may be submitted only in electronic form by www.jbth.com.br. Each manuscript will be assigned a registration number, and the author notified that the manuscript is complete and appropriate to begin the review process. The submission file is in OpenOffice, Microsoft Word, or RTF document file format for texts and JPG (300dpi) for figures.

Authors must indicate in a cover letter the address, telephone number, fax number, and e-mail of the corresponding author. The corresponding author will be asked to make a statement confirming that the content of the manuscript represents the views of the co-authors, that neither the corresponding author nor the co-authors have submitted duplicate or overlapping manuscripts elsewhere, and that the items indicated as personal communications in the text are supported by the referenced person.

Manuscripts are to be typed as indicated in Guide for Authors, as well as text, tables, references, legends. All pages are to be numbered with the order of presentation as follows: title page, abstract, text, acknowledgements, references, tables, figure legends and figures. A running title of not more than 40 characters should be at the top of each page. References should be listed consecutively in the text and recorded as follows in the reference list, and must follow the format of the National Library of Medicine as in Index Medicus and "Uniform Requirements for Manuscripts Submitted to Biomedical Journals" or in "Vancouver Citation Style". Titles of journals not listed in Index Medicus should be spelled out in full.

Manuscript style will follow accepted standards. Please refer to the JBTH for guidance. The final style will be determined by the Editor-in-Chief as reviewed and accepted by the manuscript's corresponding author.

Approval of the Ethics Committee

The JBTH will only accept articles that are approved by the ethics committees of the respective institutions (protocol number and/or approval certification should be sent after the references). The protocol number should be included in the end of the Introduction section of the article.

Publication Ethics

Authors should observe high standards with respect to publication ethics as set out by the International Committee of Medical Journal Editors (ICMJE). Falsification or fabrication of data, plagiarism, including duplicate publication of the authors' own work without proper citation, and misappropriation of the work are all unacceptable practices. Any cases of ethical misconduct are treated very seriously and will be dealt with in accordance with the JBTH guidelines.

Conflicts of Interest

At the point of submission, each author should reveal any financial interests or connections, direct or indirect, or other situations that might raise the question of bias in the work reported or the conclusions, implications, or opinions stated - including pertinent commercial or other sources of funding for the individual author(s) or for the associated department(s) or organizations(s), and personal relationships. There is a potential conflict of interest when anyone involved in the publication process has a financial or other beneficial interest in the products or concepts mentioned in a submitted manuscript or in competing products that might bias his or her judgment.

Material Disclaimer

The opinions expressed in JBTH are those of the authors and contributors, and do not necessarily reflect those of the SENAI CIMATEC, the editors, the editorial board, or the organization with which the authors are affiliated.

Privacy Statement

The names and email addresses entered in this Journal site will be used exclusively for the stated purposes of this journal and will not be made available for any other purpose or to any other party.

Brief Policies of Style

Manuscript	Original	Review	Birief Comunication	Case Report	Editorial ; Letter to the Editor; Editor' s Corner	Innovative Medical Products	State-of-the-Art	Health Innovation Initiatives
Font Type	Times or Arial	Times or Arial	Times or Arial	Times or Arial	Times or Arial	Times or Arial	Times or Arial	Times or Arial
Number of Words – Title	120	90	95	85	70	60	120	90
Font Size/Space-Title	12; double space	12; double space	12; double space	12; double space	12; double space	12; double space	12; double space	12; double space
Font Size/Space-Abstracts/Key Words and Abbreviations	10; single space	10; single space	10; single space	10; single space	-	-	10; single space	10; single space
Number of Words – Abstracts/Key Words	300/5	300/5	200/5	250/5	-	-	300/5	300/5
Font Size/Space-Text	12; Double space	12; Double space	12; Double space	12; Double space	12; Double space	12; Double space	12; Double space	12; Double space
Number of Words – Text	5,000 including spaces	5,500 including spaces	2,500 including spaces	1,000 including spaces	1,000 including spaces	550 including spaces	5,000 including spaces	5,500 including spaces
Number of Figures	8 (title font size 12, double space)	3 (title font size 12, double space)	2 (title font size 12, double space)	2 (title font size 12, double space)	-	2 (title font size 12, double space)	8 (title font size 12, double space)	8 (title font size 12, double space)
Number of Tables/Graphic	7 title font size 12, double space	2 title font size 12, double space	2(title font size 12, double space)	1(title font size 12, double space)	-	-	7 title font size 12, double space	4 title font size 12, double space
Number of Authors and Co-authors*	15	10	5	10	3	3	15	10
References	20 (font size 10,single space	30(font size 10,single space	15 (font size 10,single space)	10 (font size 10,single space)	10 (font size 10,single space	5(font size 10,single space	20 (font size 10,single space	20

*First and last name with a sequencing overwritten number. Corresponding author(s) should be identified with an asterisk; Type 10, Times or Arial, single space. Running title of not more than 40 characters should be at the top of each page. References should be listed consecutively in the text. References must be cited on (not above) the line of text and in brackets instead of parentheses, e.g., [7,8]. References must be numbered in the order in which they appear in the text. References not cited in the text cannot appear in the reference section. References only or first cited in a table or figures are numbered according to where the table or figure is cited in the text. For instance, if a table is placed after reference 8, a new reference cited in table 1 would be reference 9.1 would be reference 9.

Checklist for Submitted Manuscripts

- ❑1. Please provide a cover letter with your submission specifying the corresponding author as well as an address, telephone number and e-mail.
- ❑2. Submit your paper using our website www.jbth.com.br. Use Word Perfect/Word for Windows, each with a complete set of original illustrations.
- ❑3. The entire manuscript (including tables and references) must be typed according to the guidelines instructions.
- ❑4. The order of appearance of material in all manuscripts should be as follows: title page, abstract, text, acknowledgements, references, tables, figures/graphics/diagrams with the respective legends.
- ❑5. The title page must include a title of not more than three printed lines (please check the guidelines of each specific manuscript), authors (no titles or degrees), institutional affiliations, a running headline of not more than 40 letters with spaces.
- ❑6. Acknowledgements of persons who assisted the authors should be included on the page preceding the references.
- ❑7. References must begin on a separate page.
- ❑8. References must be cited on (not above) the line of text and in brackets instead of parentheses, e.g., [7,8].
- ❑9. References must be numbered in the order in which they appear in the text. References not cited in the text cannot appear in the reference section. References only or first cited in a table or figures are numbered according to where the table or figure is cited in the text. For instance, if a table is placed after reference 8, a new reference cited in table 1 would be reference 9.
- ❑10. Reference citations must follow the format established by the "Uniform Requirements for Manuscripts Submitted to Biomedical Journals" or in "Vancouver Citation Style".
- ❑11. If you reference your own unpublished work (i.e., an "in press" article) in the manuscript that you are submitting, you must attach a file of the "in press" article and an acceptance letter from the journal.
- ❑12. If you cite unpublished data that are not your own, you must provide a letter of permission from the author of that publication.
- ❑13. Please provide each figure in high quality (minimum 300 dpi: JPG or TIF). Figure must be on a separate file.
- ❑14. If the study received a financial support, the name of the sponsors must be included in the cover letter and in the text, after the author's affiliations.
- ❑15. Provide the number of the Ethics Committees (please check the guidelines for authors).